Environment CANADA Environnement
10209261 VOL ISS 82 860400
EXC # 001
TD 171.5.C3 R46
REPORT EE

OOFF

PACK ICE IN CANADIAN WATERS:

DIMENSIONS AND DYNAMICS OF LEADS AND FLOES

EE-82

PACK ICE IN CANADIAN WATERS:
Dimensions and Dynamics of Leads and Floes

by

David Dickins
Anthony Dickinson
Blair Humphrey

DF Dickins Associates Ltd.
Vancouver, B.C.

This report has not undergone detailed technical review by the Environmental Protection Service and the content does not necessarily reflect the views and policies of Environment Canada. Mention of trade names or commercial products does not constitute endorsement for use.

This unedited version is undergoing a limited distribution to transfer the information to people working in related studies. This distribution is not intended to signify publication and, if the report is referenced, the author should cite it as an unpublished report of the Branch indicated below.

Any comments concerning its content should be directed to:

Environmental Emergencies Technology Division
Technical Services Branch
Environmental Protection Programs Directorate
Environmental Protection Service
Environment Canada
Ottawa, Ontario K1A 1C8

April 1986

ABSTRACT

Pack ice conditions are described in three Canadian offshore regions: the Beaufort Sea, Lancaster Sound and the Labrador Sea. The primary study objective was to provide statistics on lead and floe dimensions, ice concentrations, ice movements and new ice growth for future predictions and modelling of oil spill behaviour in pack ice. Data on 1245 floes and 255 leads was collected from satellite buoy tracks and side looking airborne radar imagery.

Results show distinct regional differences in pack ice characteristics. Leads are the dominant pack ice feature in the Beaufort Sea while individual floes are more common in the Labrador Sea.

Lead motion statistics show that the Beaufort Sea and Lancaster Sound can be characterized as expanding ice covers. Lead closures were observed on only 17% of the documented lead movement events. Average closure rates indicate that typical leads of approximately 30 m width, will take over an hour to fully close. Maximum measured ice contraction rates were 125 mh^{-1}.

Floe movements showed regional differences in both speed and direction. In the Beaufort Sea, fewer than 38% of floes moved at rates greater than 10 km day^{-1} compared to 45% in Lancaster Sound and 75% off Labrador. The most rapid floe movements were observed at the entrance to Lancaster Sound and at the entrance to Hudson Strait. Measured floe directions agreed with known trends of large scale ice motion in the three regions, i.e. west in the Beaufort Sea, east in Lancaster Sound and south in the Labrador Sea. There was no significant dependence of floe speed on either surrounding ice concentration or floe size. Intuitively, there is less opportunity for extreme rates of relative floe movement as ice concentrations increase above 7/10. The existing data base is not sufficient to confirm this.

Ice freeboard was evaluated as a separate parameter of interest for oil spill modelling work. A range of values are presented based on limited

measurements of offshore pack ice thickness in the Beaufort Sea, theoretical ice growth in Lancaster Sound and field measurements of floe geometry in the Labrador Sea. Typical mid-winter values of ice freeboard are 15, 11 and 100 cm in the respective regions. The high freeboard of Labrador Sea ice reflects the dynamic nature of floe interactions.

A correlation of offshore wind records with cloud cover indicated that ice movements derived from Landsat imagery could be 20% lower than actual values. With this correction factor, the average ratio of ice floe speed to wind speed in this study was about 2% in the Beaufort Sea and Lancaster Sound, increasing to 3% in the Labrador Sea.

There is almost no public data which reports ice speed on an hourly basis. The few records available indicate a dramatic rise in ice speed as the recordinterval decreases. It is not known whether short term motions on the scale of seconds will be sufficient to explain the phenomenon of "lead pumping". The pulsing ice motions necessary to cause "lead pumping" will more likely be associated with individual floes in an ocean swell, than with leads in an almost continuous ice cover.

In conclusion, this study provides a valuable data set on lead and floe dynamics in three different pack ice regimes. This work also provides the only known statistical description of lead opening and closing rates. Recommendations are made for further investigations of relative short time period displacements of small scale ice features.

CONTENTS

		Page
	ABSTRACT	i
1.0	INTRODUCTION	1
2.0	METHODOLOGY	4
	2.1 Literature Review	4
	2.2 Geographic Subdivisions	5
	2.3 Ice Statistics: Definitions and Sources	9
	2.3.1 Median Ice Cover	11
	2.3.2 Ice Velocities	11
	2.4 Wind Statistics	17
	2.4.1 Wind Speed Dependence on Cloud Cover	17
	2.4.2 Offshore Wind Statistics	18
	2.5 Refreezing of Pack Ice Leads	19
3.0	RESULTS AND DISCUSSION	26
	3.1 Summary of Regional Ice Conditions	26
	3.2 Leads	32
	3.2.1 Distribution of Data	32
	3.2.2 Lead Dimensions	37
	3.2.3 Lead Orientation	43
	3.2.4 Lead Opening and Closing Rates	44
	3.3 Floes	46
	3.3.1 Distribution of Floe Data Sets	52
	3.3.2 Floe Velocities	54
	3.3.3 Ice Floe Size	68
	3.4 Ice Freeboard	70
	3.5 Winds Effects on Ice Dynamics	73
	3.5.1 Modification of Measured Ice Speeds to Reflect Cloud Cover Wind Speed Bias	73
	3.5.2 Comparison of Average Winds and Ice Velocity	75
	3.6 Refreezing of Pack Ice Leads	76

CONTENTS

		Page
4.0	CONCLUSIONS AND RECOMMENDATIONS	83
	ACKNOWLEDGEMENTS	
	REFERENCES AND BIBLIOGRAPHY	
	APPENDICES	
A	Listing of Remote Sensing Data	
B	Examples of Floe Movement Tracks Mapped from Successive SLAR Images	
C	Monthly and Reginal Floe Speed Distributions	
D	Representative Profiles of Labrador Sea Ice Cakes	
E	Changing Lead and Fracture Systems Mapped from Aerial Photography of Winter Pack Ice in the Vicinity of 73°45'N, 130°15'W March 11 to 23, 1971	

FIGURES

		Page
Figure 1.1	Location Map Showing Study Areas	1
Figure 2.1	Beaufort Sea Location Map	7
Figure 2.2	Lancaster Sound Location Map	7
Figure 2.3	Labrador Coast Location Map	8
Figure 2.4	March Landsat Image Showing Pack Ice North of Cape Bathurst	12
Figure 2.5	July SLAR Image Showing Pack Ice in Lancaster Sound	13
Figure 2.6	Example Data Format for Floes and Leads	15
Figure 2.7	March Aerial Photograph of Pack Ice in the Labrador Sea	16
Figure 2.8	Lead Refreezing Processes	20
Figure 3.1	Median Bi-Weekly Ice Concentration - Beaufort Sea	27
Figure 3.2	Median Bi-Weekly Ice Concentration - Lancaster Sound	28
Figure 3.3	Median Bi-Weekly Ice Concentration - Labrador Sea	29
Figure 3.4	Distribution of Beaufort Sea Lead Statistics by Region	33
Figure 3.5	Distribution of Lancaster Sound Lead Statistics by Month	33
Figure 3.6	Overlay of Landsat Image, March 10, 1975	34
Figure 3.7	Landsat Image of Same Area as Figure 3.6	35
Figure 3.8	Comparison of Lead Appearance in Lancaster Sound	36
Figure 3.9	Distribution of Lead Widths Measured from Landsat Imagery	38
Figure 3.10	Distribution of Lead Widths in the Polar Pack	38
Figure 3.11	Cumulative Probability of Lead Density Derived from March Landsat Imagery	39

FIGURES

		Page
Figure 3.12	Aerial Photography of Pack Ice in the Vicinity of 73°45'N, 130°15'W, March 11, 1971	41
Figure 3.13	Example of Lead Closure Leading to a Pressure Ridge	42
Figure 3.14	Lead Orientation	43
Figure 3.15	Lead Opening and Closing Rates - Beaufort Sea	45
Figure 3.16	Lead Opening and Closing Rates - Lancaster Sound	45
Figure 3.17	Lancaster Sound Landsat Image, April 25, 1977	48
Figure 3.18	Landsat Images Showing 24 Hour Changes in Pack Ice Concentration in the Beaufort Sea	49
Figure 3.19	Landsat Image Showing Labrador Sea Pack Ice, February 22, 1979	50
Figure 3.20	Labrador Sea Pack Ice Conditions, April 1, 1979	51
Figure 3.21	Distribution of Floe Data According to Month	53
Figure 3.22	Distribution of Floe Data According to Ice Concentration	53
Figure 3.23	Distribution of Floe Data According to Floe Area	54
Figure 3.24	Geographic Differences in Floe Speed Distributions	55
Figure 3.25	Direction of Floe Movements	57
Figure 3.26	Variation in Ice Speed with Concentration	58
Figure 3.27	Variation in Ice Speed with Floe Area	60
Figure 3.28	Cumulative Probability of Ice Speed - Comparison of Dickins et al. (1985) with Schwab (1978)	61
Figure 3.29	Comparison of Monthly Average Floe Speeds from Different Sources	62
Figure 3.30	Comparison of Reported Ice Speed Distributions for the Beaufort and Labrador Seas	63
Figure 3.31	Comparison of Daily and Hourly Speed Distributions - Beaufort Sea Summer	64

FIGURES

		Page
Figure 3.32	Comparison of Six Hourly and Daily Speed Distributions - Beaufort Sea Winter	65
Figure 3.33	Comparison of 15 Minute and 60 Minute Ice Movements (Three Individual Floes in Open Water)	66
Figure 3.34	Comparison of Summer and Winter Ice Speeds in the Beaufort Sea	67
Figure 3.35	Beaufort Sea Floe Size Distribution from SLAR	68
Figure 3.36	Labrador Sea Floe Size Distribution from 1:20,000 Scale Photography	69
Figure 3.37	Labrador Sea Floe Size Distribution from 1:2,600 Scale Photography	69
Figure 3.38	Correlation of Cloud Cover with Wind Speed 1:2,600 Scale Photography	74

TABLES

		Page
Table 2.1	Data Collection and Entry Rules	10
Table 2.2	Data Base on Offshore Wind Statistics	18
Table 2.3	Annual Non-Uniformity of Offshore Wind Statistics	19
Table 3.1	Regional Comparison of Ice Regimes	30
Table 3.2	Regional Summary of Average Pack Ice Duration	31
Table 3.3	Icebreaker Track Closure Observations	46
Table 3.4	Representative Ice Freeboard	72
Table 3.5	Comparison of Relative Frequency of Wind Speeds in Cloud Cover <20% to all Cloud Covers	75
Table 3.6	Wind Speed/Ice Floe Speed Comparison	76
Table 3.7	Beaufort Sea Climate	77
Table 3.8	Lancaster Area Climate	78
Table 3.9	Labrador Area Climate	78
Table 3.10	Beaufort Sea Lead Refreezing	79
Table 3.11	Lancaster Sound Lead Refreezing	80
Table 3.12	Labrador Sea Refreezing Rates	80

1.0 INTRODUCTION

This study was initiated to produce a data base on pack ice dynamics necessary for modelling and predicting the behaviour of oil spilled in a broken ice environment.

The term 'pack ice' describes any ice cover which is not fast to shore, and has the potential for movement in response to local winds and currents. There are significant, temporal and spatial differences in pack ice environments encountered in Canadian offshore exploration areas (Figure 1.1). Major regional differences include the seasonal variation in ice concentration, areal distribution of leads, floe sizes, and rates of ice movement.

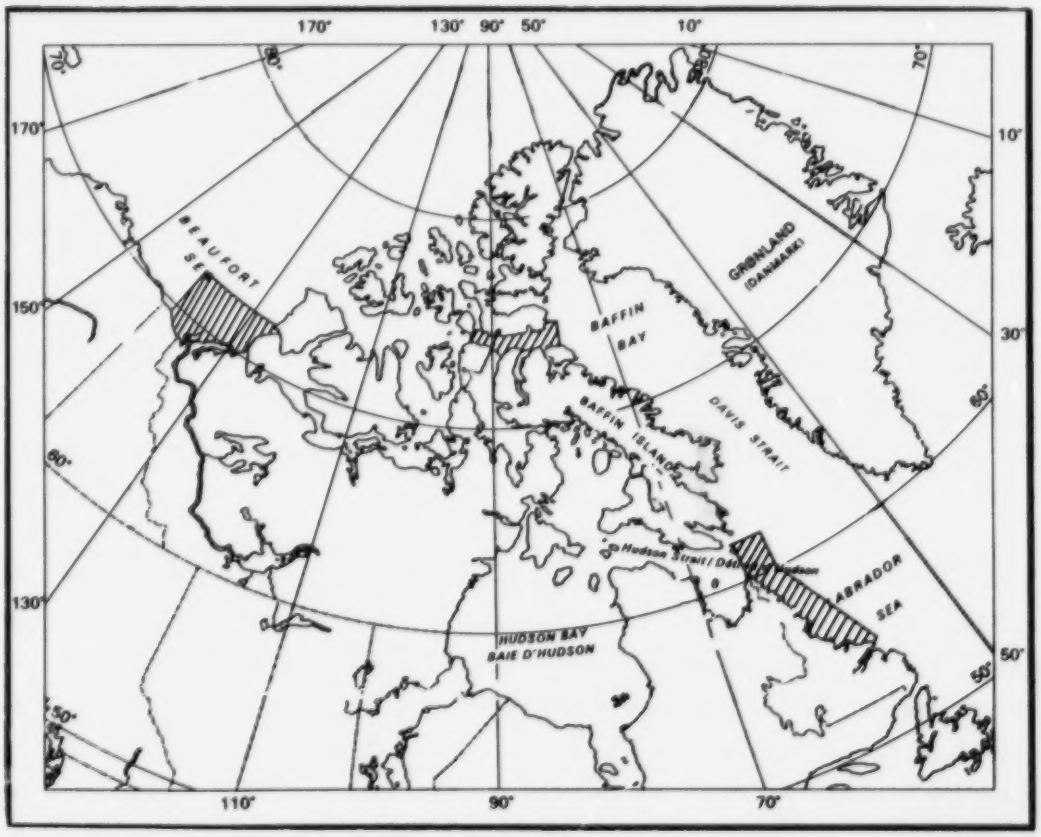

Figure 1.1 Location Map Showing Study Areas

The main objective of this study was to quantify the dynamics of different pack ice areas in terms of specific parameters of ice movement and geometry. Principal subject areas covered in this report include discussions of ice concentration, leads, and floes. Sub-categories treat specific characteristics such as lead opening and closing rates, lead refreezing and floe movements.

Three distinct regions, Beaufort Sea, Lancaster Sound, and Labrador Sea were selected as being of interest for hydrocarbon exploration and transportation and as having clearly defined differences in ice regimes. Hibernia was not included because pack ice is too infrequent to provide sufficient data.

The Beaufort Sea is characterized by an extensive seasonal pack ice cover bordered by the polar pack to the north and landfast ice to the south. North/south variations of hundreds of kilometres in the polar pack boundary lead to significant annual differences in ice dynamics within the predominantly first year pack covering offshore drilling locations between November and July.

The Lancaster Sound ice regime is largely controlled by the east/west location of the stable ice boundary which forms across Parry Channel between Resolute and Bylot Island. New ice is constantly being generated at this ice boundary and carried east into the vast expanse of the North Baffin pack by prevailing winds and currents. Ice influx from the Sound into Baffin Bay averaged 481 km^3/year from 1974 to 1978 (Dey, 1981).

The Labrador Sea is the third geographic region evaluated in this study. Here, the pack is comprised of individual floes driven compressed along the coast or dispersed several hundred kilometres offshore, according to the movements of low pressure storm systems. Ice thicknesses are extremely variable. Dynamic floe interactions lead to roughness features many times thicker than the maximum theoretical level ice thickness of about 1.4 m. The Labrador Sea pack is the most difficult area to categorize, due to the large variations in surface features, floe distributions, and areal extent.

Pack ice close to an open ocean margin such as occurs in the Labrador Sea, has properties very different from central arctic ice. The so-called marginal ice zone (MIZ) is strongly affected by the presence of an open ocean boundary. Ice in the MIZ is characterized by a number of peculiar processes related to a complex set of ice-ocean-atmosphere interactions. Examples are wave induced ice break-up, loss of ice across the ice edge (bands and clustering), warm water eddy effects, lateral melting of floes and wave induced melting (Wadhams, 1980). The MIZ is currently the subject of intense study on an international scale (see MIZ Bulletin Series produced by CRREL). This report does not deal specifically with the special case of the MIZ but concentrates on ice characteristics in the pack interior, removed from significant open ocean influences.

In summary, this study generates new ice statistics from publicly available remote sensing imagery, and reports on ice dynamics in three distinct regions with a diverse range of pack ice environments. The primary study objective was to provide quantitative data on pack ice dynamics. It was not the study intent to qualitatively describe the ice environment in detail. Many references provide overviews of the seasonal variation in ice conditions within the different regions (eg. Beaufort Sea - Markham, 1975, 1981; Lancaster Sound - Marko, 1982, Milne, 1978; Labrador Sea - Winsor and LeDrew, 1979; Wadhams, 1980).

2.0 METHODOLOGY

2.1 Literature Review

A literature search was conducted to obtain reference sources pertaining to the main subjects of ice movements, lead distributions and ice thickness (refreezing).

Ice drift information was first collected and reported by beset whaling vessels in the 1890's. One of the earliest programs to study ice dynamics in detail, with the benefit of modern electronics, was AIDJEX, conducted between 1970 and 1978. Five methods used by AIDJEX to measure ice drift included air photo analysis (Hartwell, 1972), satellite imagery (Hibler et al, 1976), ground surveys (Hibler et al, 1972) satellite navigation (Pritchard et al, 1977) and satellite located buoys (reported by Gulf Canada - McGonigal and Wright, 1975-1977).

Over six years of satellite buoy data is now available for the Beaufort Sea, including two years of more accurate French Argos system measurements reported by Murphy et al, 1981 and 1983. At their best, these newer buoys can provide daily positions of an ice floe to within ± 500 m. Earlier buoys known as RAMS, using the older U.S. Nimbus satellite, provided position accuracies in the range ± 1 to 2 km. Limited buoy data is available for Lancaster Sound as part of the Eastern Arctic Marine Environmental Studies (EAMES) program.

One other method for measuring ice movement nearshore has successfully used an anchored cable through a hole in the ice. Changes in the cable length were used to record small winter motions of the landfast ice relative to the seabed. This device has provided continuous ice movements in the Beaufort Sea shallow water areas (less than 50 ft of water) for the years 1972-78 (see Spedding - Imperial Oil Limited). The cable technique was used inadvertently at several sites too close to the moving shear zone and cable limits were quickly exceeded.

Other than the landfast ice movement records, there is almost no publicly available data on semi-instantaneous or hourly ice floe velocities. Dome Petroleum Limited has conducted several years of floe measurements at their drillsites using a microwave offshore positioning system. Limited release of this data in graphical form is presented in Marcellus and Morrison (1982).

Satellite imagery has proved to be the most popular, economical means of measuring ice floe displacements over periods of days. References include Markham, 1975; Marko 1976, 1982b; and Schwab, 1978.

Landsat with a scale of 1:1,000,000, and a resolution capability of 100 m, provides the most useful imagery for ice motion studies. There is minimal distortion between images, and slight orbital fluctuations maintain scale to within 10%. Unfortunately, Landsat is limited to daylight cloud free hours, a scarce commodity over much of the arctic offshore. The result is a total lack of imagery from early November until late February, and the loss of up to 85% of available images at other times due to excessive cloud. In spite of these problems sufficient overlapping daily images can be found to track individual floes for several days. Radar imagery (SAR and SLAR) allows accurate mapping of daily floe movements over longer time periods. Most of this data is proprietary to the oil industry. Two example plots of floe motions derived from SLAR imagery are included as Appendix B (AES 1979, 1980).

A major weakness of previous studies of interest to this study is the lack of any consistent record of ice concentrations associated with reported ice motions. Schwab (1978) provides a notable exception.

2.2 Geographic Subdivisions

Three Canadian offshore areas were selected for this study, the southeastern Beaufort Sea, Lancaster Sound and the Labrador Coast. These regions were selected because they may be affected

by future petroleum developments, and because they have very different ice climatologies. Each of the regions was further divided into sub-regions to identify spatial differences in the data. Every piece of data was grouped according to date and sub-region.

Figure 2.1 shows the Beaufort Sea study area and its sub-regions. The area is bounded by Cape Bathurst to the east, Herschel Island to the west; 71°N latitude to the north and the coastline to the south. Sub-regions were selected to separate shear zone ice and landfast ice.

Lancaster Sound was divided into three sub-regions (see Figure 2.2). The western sub-region (Zone A) is the smallest because it is usually covered by landfast ice in the spring. Zone B between Prince Leopold Island and Admiralty Inlet had the best data coverage. This was opportune as ice in Zone B was in motion during most years. The eastern mouth of Lancaster Sound is covered by Zone C. A number of authors have studied iceberg, floe, or buoy velocities in Zone C, but their data could only be included for comparison, as it lacked specific floe size and ice cover information.

The Labrador Coast area was divided into four equal width sub-regions parallel to the coastline (see Figure 2.3). A small landfast ice zone exists within each sub-zone, but all the data was collected from the larger offshore moving pack ice area. Measurements due east of Hudson Strait were identified in recognition of potential interference affects due to current outflow.

In general, the large quantity of data available for the Beaufort Sea allowed the selection of specific sub-regions which separated the shear zone, landfast ice, and Mackenzie delta regions. The choice of sub-regions in Lancaster Sound was governed by the location of inlets. Some authors have further subdivided the region into north and south halves of the channel according to known current loops. Selection of sub-regions along the Labrador Coast was more arbitrary, and was confined to the separation of north-south trends.

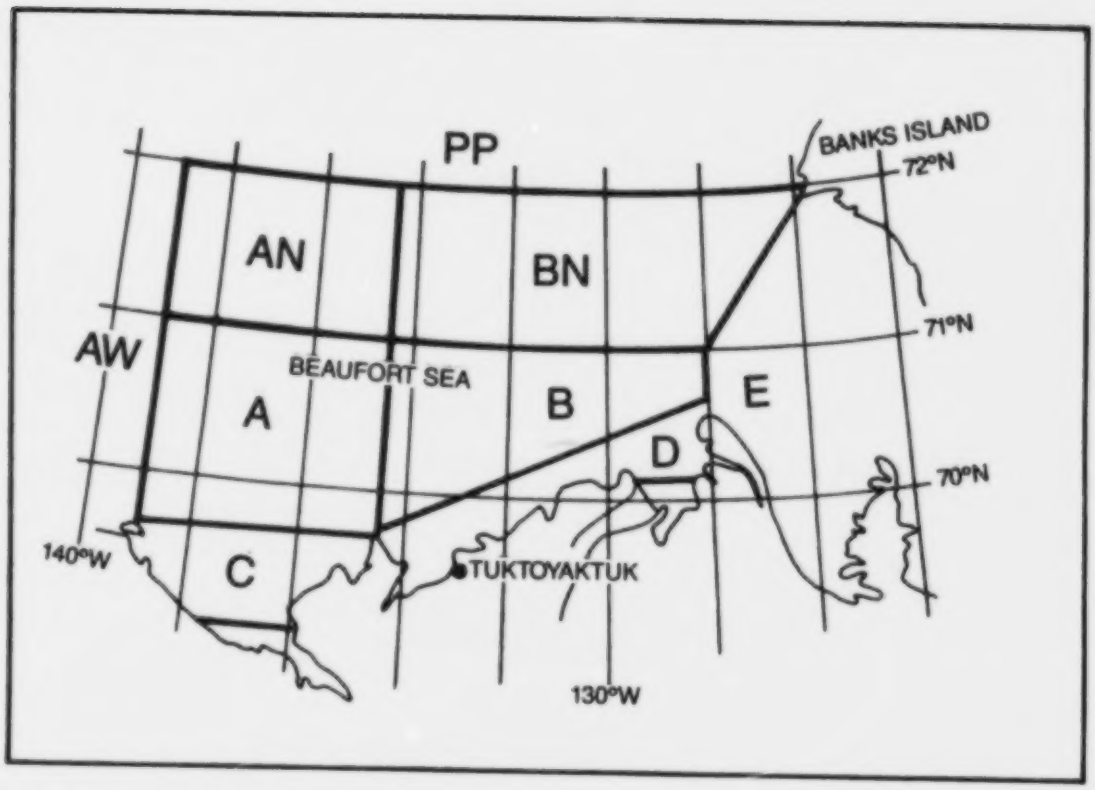

Figure 2.1 Beaufort Sea Location Map

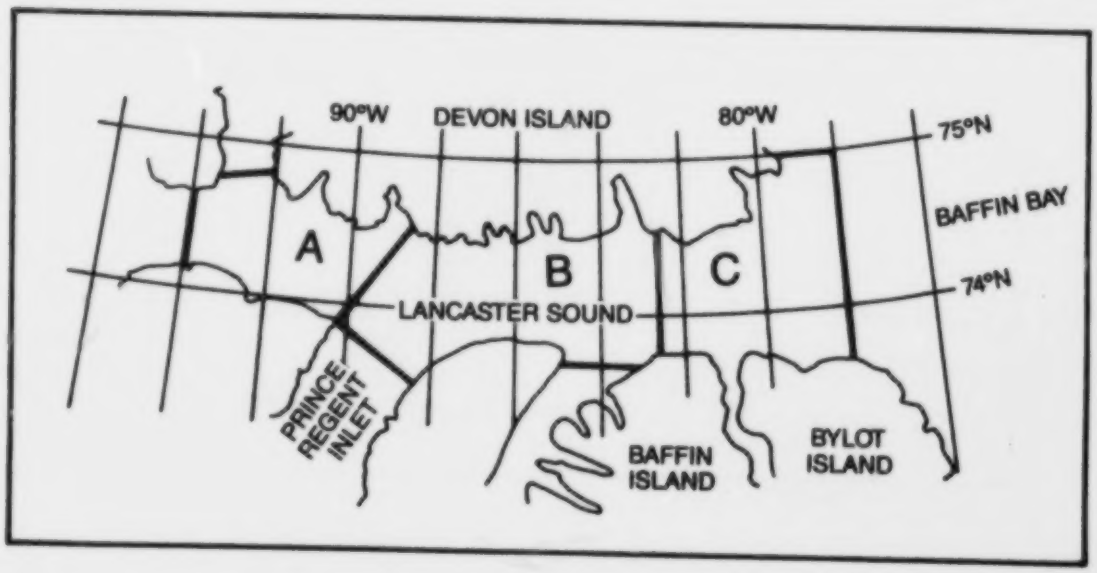

Figure 2.2 Lancaster Sound Location Map

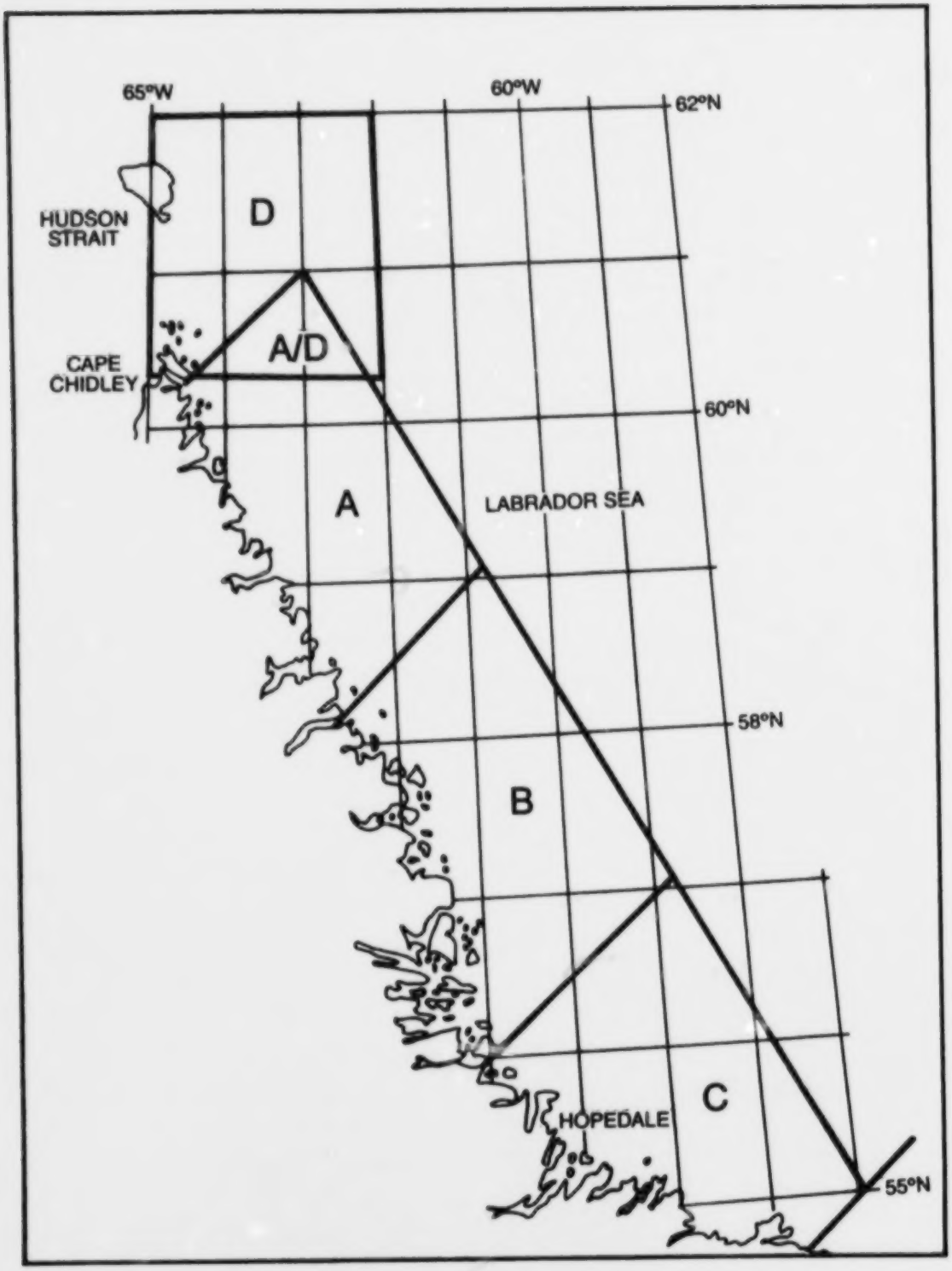

Figure 2.3 Labrador Coast Location Map

2.3 Ice Statistics: Definitions and Sources

Ice dynamics in the three geographic areas of this study were defined according to the following characteristics:

Floe Size
Ice Cover - Concentration in Tenths
Ice Displacement
Direction of Motion
Floe Rotation (only for Lancaster Sound Landsat Imagery)
Date
Lead Frequency (where possible)

Other data such as floe size distribution, and median ice cover were included to aid comparison with other studies, and to give a better understanding of the occurrence of extreme ice features. Where possible, data collected for this study was compared to information in the literature.

This study relied on the acquisition of remote sensing imagery, satellite and airborne, to study ice conditions between February and July, in the three regions of interest (Figures 2.1 to 2.3). Information from the imagery was augmented by a similar analysis completed by Schwab (1978) for the Beaufort Sea region.

The reliance on visible wave length imagery precluded the collection of winter data. Winter images are limited by the light conditions, and often suffer from poor contrast due to low light levels. The NOAA satellites can provide IR imagery during the dark period but the coarse resolution and small scale (typ 1:9,000,000) was not considered adequate for this study. Fall pack ice conditions were not documented because the new ice cover is extremely mobile. Floes and leads are not clearly defined, and the thin ice cover is constantly being broken, rafted and ridged. In addition, Landsat coverage of the Beaufort Sea ceases within three weeks of freeze-up offshore, severely restricting the number of available images.

Floe displacements were measured from remote sensing imagery by using the following definition: "A floe was defined as any planar area of ice surrounded by visible cracks or open water." The only exception to this definition occurred in determining the floe distributions for the Labrador Coast. Here, aerial photography was available at a scale of 1:6,000, which allowed a distinction to be made between the new ice and the thicker ice which had drifted south. The patches of thicker ice surrounded by thinner ice were counted as floes.

The definition of a lead was more difficult. During spring break-up, the ice reaches a state where it either has a lot of leads or a lot of floes. For this study, any distinct lineal, open water features bounded by ice on both sides and greater than 5 km in length, were counted as leads. Many leads were counted at the limits of image resolution. Large patches of open water adjacent to land were not included as leads.

A summary of rules used for collection and data entry on a computer is shown in Table 2.1.

Table 2.1 Data Collection and Entry Rules

1. If an ice floe crossed from pack ice to open water between images, the ice concentration was taken as 5/10.

2. If a lead crossed through more than one sub-region the region containing most of the lead was used to label the lead location.

3. A range of lead widths was recorded to show the maximum and minimum lead width.

4. If a shore lead was measured (open water between coast and pack ice in Lancaster Sound) the ice concentration was taken as 8/10.

5. Concentration of ice was taken as 9/10 for lead measurements unless rule 4 applied.

2.3.1 Median Ice Cover

Pack ice concentrations were tabulated from the AES ice charts. Total ice concentrations were tabulated in the groups 4/10 to 6/10 (loose pack), 7/10 to 8/10 (close pack) and 9/10 to 9+/10 (very close pack) ice cover. A single concentration value was extracted for each sub-region, year, and two week interval by area averaging the data (i.e. if 1/3 of the sub-region was covered by 3/10 ice cover and the other 2/3 by 9/10 ice cover, the area average = 1/3 * 3/10 + 2/3 * 9/10 = 7/10). Overall average concentrations for each sub-region and two week interval were derived from the average of 11 years of data (1975-1985).

2.3.2 Ice Velocities

The primary objective of this study was to determine ice displacement rates at various times of the year. Many authors report ice velocities, but very few consider floe size and ice cover. This study combined data from the analysis of 225 Landsat and 37 SLAR images with data reported by Schwab (1978), to provide a data base containing velocity, floe size, ice cover, and direction of motion information. Landsat and SLAR information was at a nominal scale of 1:1,000,000 (1 mm on image = 1 km full scale). Three pairs of SLAR imagery were obtained at a scale of 1:500,000, and one at 1:250,000 (Appendix A).

Estimates of daily ice motion were made by using images temporally separated by one, or in some cases, two days. A further screening of potential imagery selected images with 15% or less cloud cover. In some cases, images were used with greater than 15% cloud cover if they were viewed prior to purchase. (Note: Schwab used images with up to 50% cloud cover.)

In the case of the SLAR imagery, each potential pair was viewed before selection. Most of the SLAR images covered all

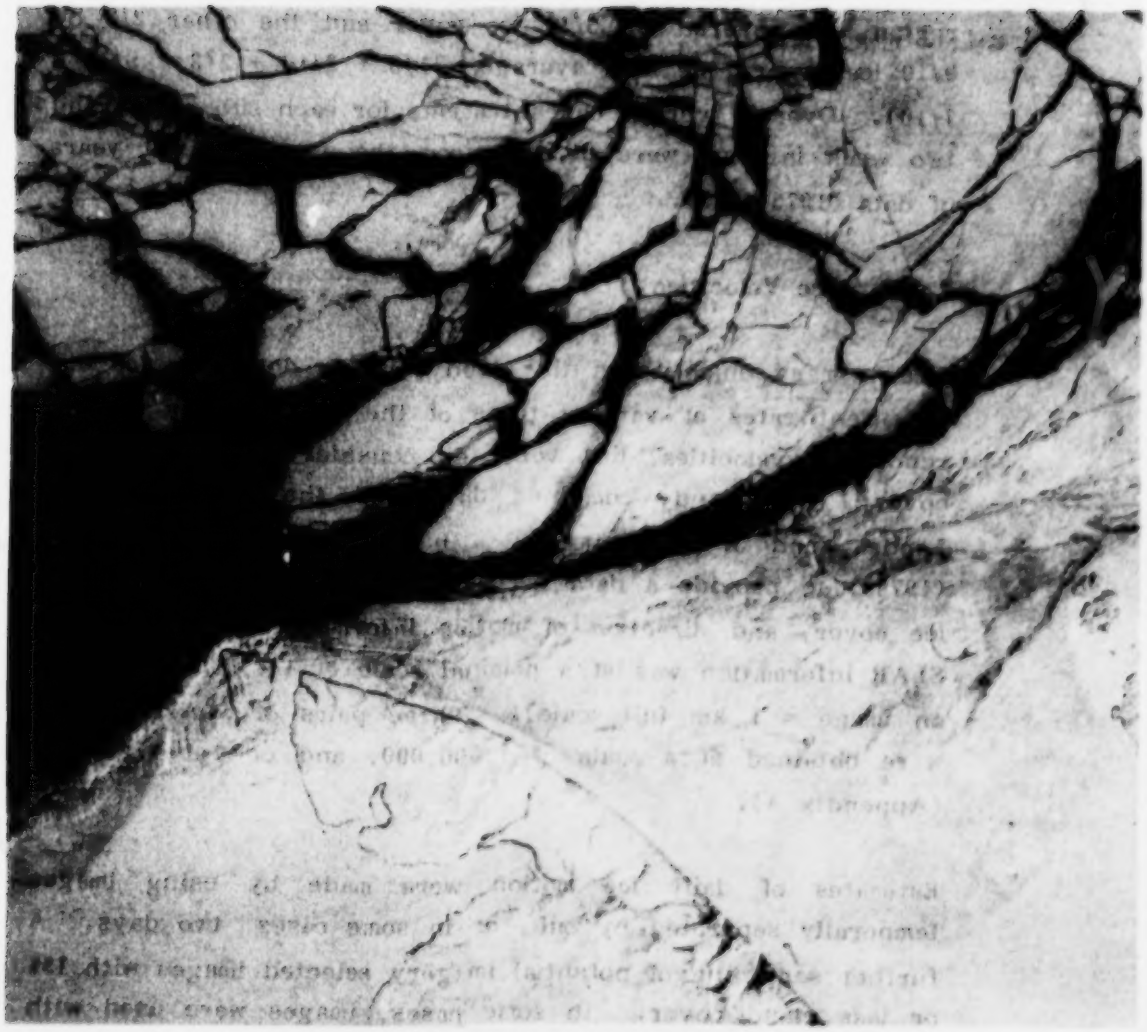

Figure 2.4 **March 21, 1981 Landsat Image Showing Pack Ice North of Cape Bathurst (Image Scale = 1:1,000,000)**

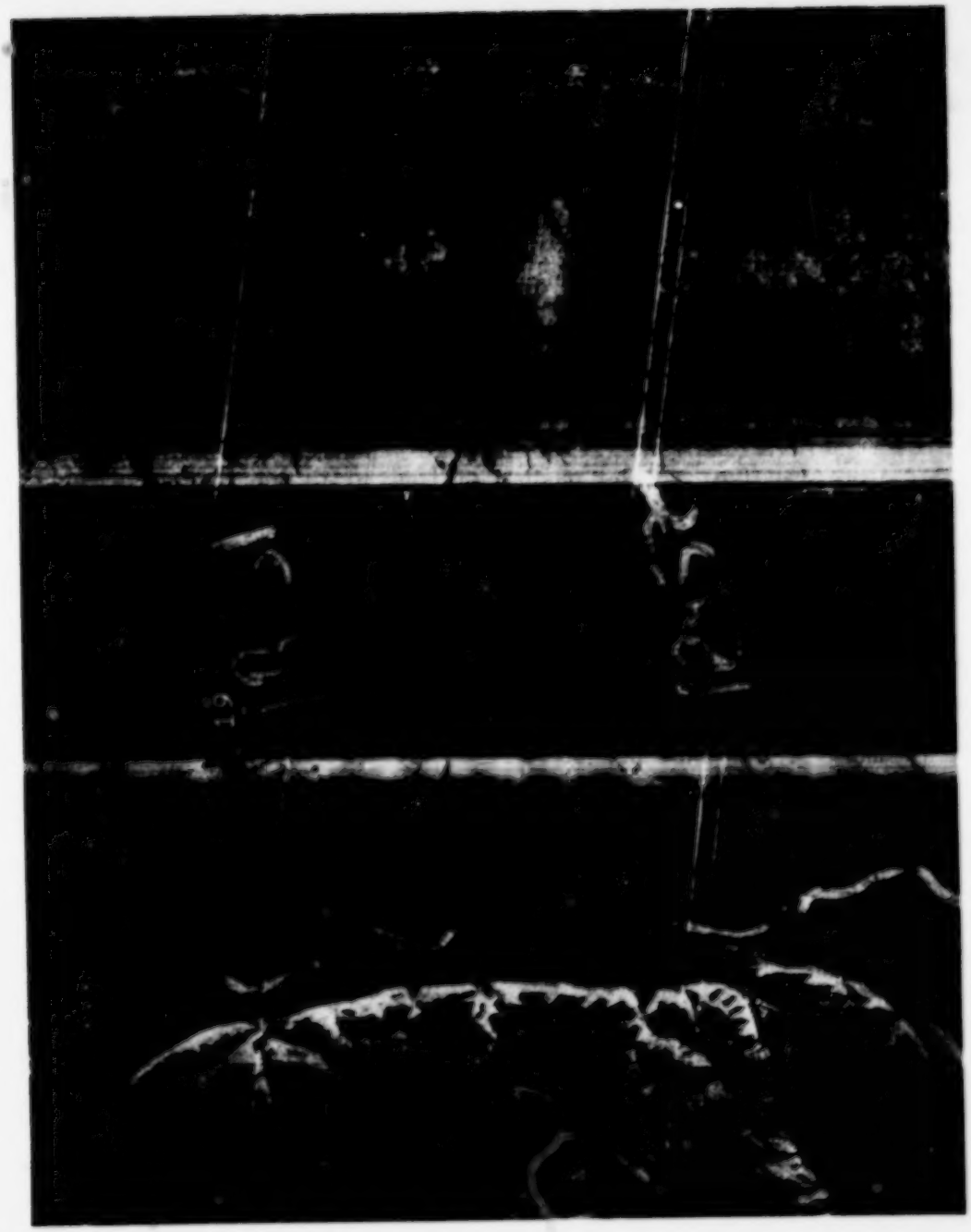

Figure 2.5 July 17, 1983 SLAR Image Showing Pack Ice in Lancaster Sound (Image Scale = 1:500,000)

of Lancaster Sound, so that each swath had a land reference. Figures 2.4 and 2.5 show examples of Landsat and SLAR imagery of Lancaster Sound. Appendix A contains a listing of Landsat and SLAR images used in this study.

Ice velocity was measured by determining the daily floe displacement relative to land, or the lead closure rate. An overlay technique was used to transfer information from one image to another. The reference coastline, each floe and each lead were traced onto a piece of vellum paper. The vellum was placed on top of the next day's image and the displacement of the floe or lead was measured. The geometric centre of a floe was used for displacement measurements. Lead measurements were relative, so the change of lead width was measured and not the movement of the lead relative to land. All displacements were measured relative to True North. The accuracy of the measurements depended on the scale of the image and the length of reference coastline in the image area. Ten floes and leads were sampled per image pair.

Most of the data has position accuracies of ± 1 km. Some of the Labrador coast measurements (sub-region D) may be in error by as much as ± 3 km due to the small lengths of available reference coastline. Figure 2.6 shows example data entries for a floe and for a lead.

REGION — LABEL */M/YR	BEAUFORT Δt (hours)	SEA a (km)	E b (km)	ΔN (km)	ΔE (km)	Δθ (deg)	CONC (Tenths)	BEARING (deg)
A/JUL/74	24.0	3.0	2.0	0.0	0.0	0.0	7	45
B	24.0	4.0	1.5	2.0	0.0	0.0	7	0
C	24.0	9.0	5.0	1.0	1.0	10.0	7	45
D	24.0	4.0	2.0	2.0	0.0	0.0	7	0
F	24.0	6.0	3.0	2.0	-1.0	0.0	7	333
C	24.0	9.0	5.0	0.0	3.0	10.0	7	90
D	24.0	4.0	2.0	4.0	4.0	5.0	7	45
F	24.0	6.0	3.0	3.0	3.0	5.0	7	45
P	24.0	6	5	1E-04	0	0	7	0
Q	24.0	14	11	1E-04	0	0	7	0
A/JUN/75	48.0	7.0	5.5	15.0	-40.0	-25.0	3	291
B	48.0	5.0	5.0	27.0	-30.0	55.0	1	312

Where:	*/M/YR = Floe label, Month, Year			Δt = time interval
	a, b = Major & Minor floe axes			& floe rotation
	ΔN, ΔE, Δθ = Change of floe position	to North	to East	
	Conc = Ice cover			

Figure 2.6 Example Data Format for Floes and Leads

As shown in Figure 2.6, the date of the image and the pack ice category (4-6/10, 7-8/10, 9-9+/10) were recorded. Ice cover was visually estimated. The date and time of each Landsat image was encoded within the Landsat image number. SLAR image dates and times available from flight logs and catalogues were provided by the Atmospheric Environment Service (AES).

Only one aerial photograph mosaic pair was found within the study areas. Most aerial photography either lacked a good coordinate fix, or was not taken on consecutive days. More images are known to exist, but are not available for public use. Aerial photography can provide very detailed informa tion, as shown in the 1:2,600 image in Figure 2.7.

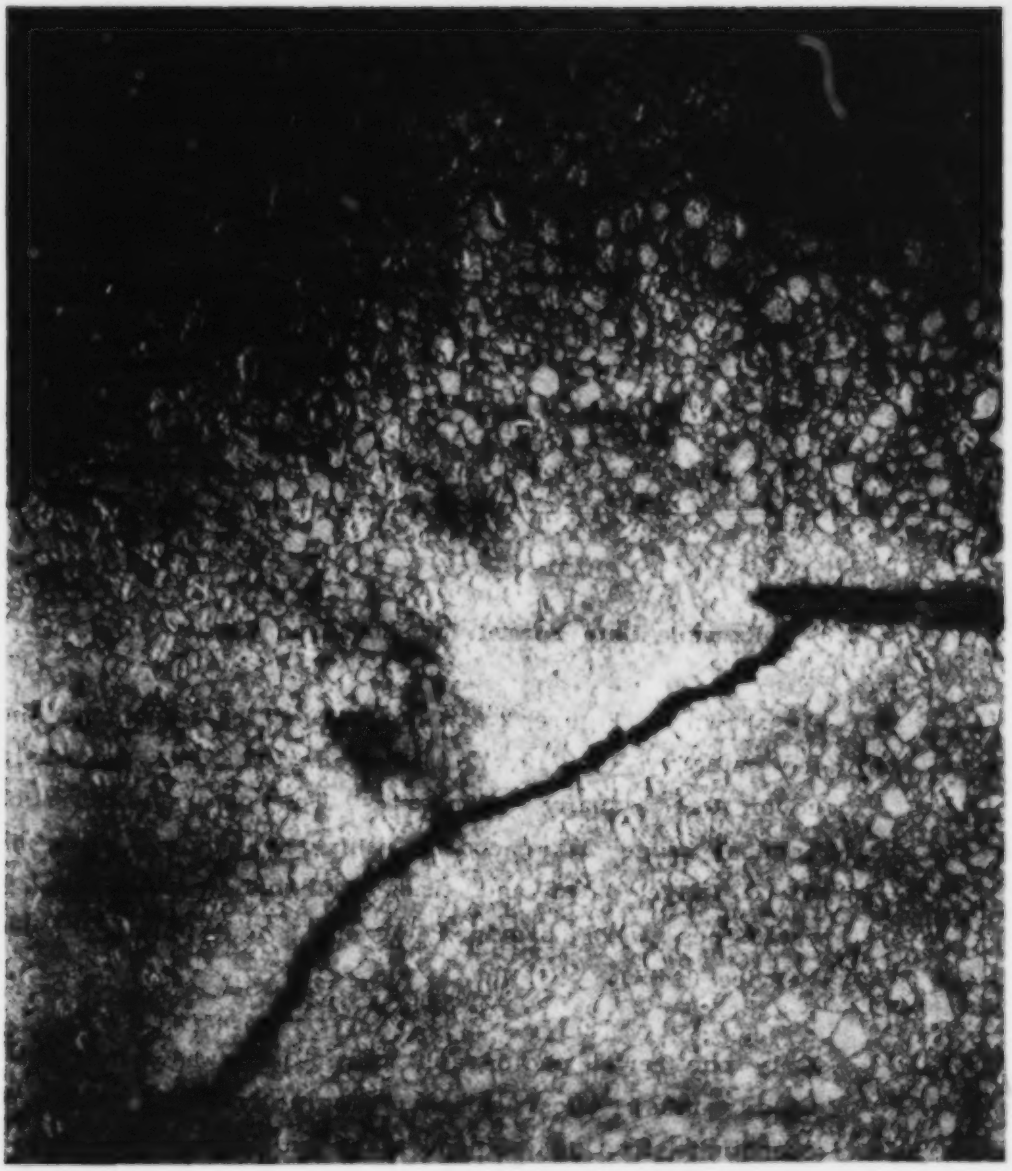

Figure 2.7 **March 24, 1982 Aerial Photograph Showing Pack Ice in the Labrador Sea (Image Scale = 1:2,600)**

Once all the ice data were recorded, they were entered into a spreadsheet type computer program (Microsoft Multiplan). Ice velocity, floe area and movement direction were calculated for each sub-region. The data was entered into a plotting program to allow a graphic representation of data.

Where possible, supporting data from the literature review was extracted for comparison with the data base generated for this study. Data included buoy, iceberg, and floe drift rates. In some cases, data outside the study area was shown as there was no other information. In all cases, data from the literature were distinguished, and notes on their sources included.

2.4 Wind Statistics

2.4.1 Wind Speed Dependence on Cloud Cover

New Landsat images were selected on the basis of 15% or less cloud cover. Previous images analyzed by Schwab (1978) had up to 50% cloud cover. Consequently, most of the ice movements are associated with winds occurring in conjunction with low cloud concentrations. The data set developed in this study may not contain the more extreme ice speeds concurrent with storm winds (and potentially overcast conditions). To test this hypothesis, wind speed and cloud cover statistics obtained from the Atmospheric Environment Service (AES) were analyzed in order to evaluate the concurrence of the two meteorological elements. For lack of offshore data, one onshore station with sufficient length of record was selected for each geographical area studied, as follows.

a) Beaufort Sea: Tuktoyaktuk, 1958-1983 (37,990 records);

b) Lancaster Sound: Resolute A, 1953-1983 (222,975 records);

c) Labrador Coast: Hopedale, 1953-1983 (206,939 records).

For each station, data were separated into two groups:

a) observations of wind speeds at 0 to 20% cloud cover, and

b) wind speeds at more than 20% cloud.

The percent frequency of the above two cloud cover groups within each wind speed interval was determined for the three onshore stations.

2.4.2 Offshore Wind Statistics

Data on frequency of wind speed and direction were also acquired from AES. Table 2.2 shows the distribution of observations by month at offshore sites falling within the study regions (Figures 2.1 to 2.3).

Table 2.2 Data Base on Offshore Wind Statistics

Area	Regions Lat	Regions Long	Period of Records	No. of Records Feb	Mar	Apr	May	Jun	Jul	Aug
Beaufort Sea	A,B,C,D (Figure 2.1)		1952-1979	*	*	*	*	*	850	2330
Lancaster Sound	as per Figure 2.2		1899-1979	*	*	*	58	43	481	3351
Labrador Coast	A/D,A,B,C (Figure 2.3)		1882-1979	35	206	218	31	223	2044	2862

*Number of records negligible or null.

It can be seen that the majority of the available offshore wind records fall in the summer months of July and August coincident with the frequency of vessel observations. Additional wind information was extracted for Hopedale on the Labrador coast, and Ocean Station Bravo to compare the differences between shore station and offshore data. In studying relationships between winds and ice dynamics, only those months and locations with reasonable data coverage were used. A

major difficulty with the offshore wind data is its non-uniformity between months and between years. Table 2.3 shows how over 2/3 of the offshore wind data set is concentrated in only one to three years of record.

Table 2.3 Annual Non-Uniformity of Offshore Wind Statistics

Area	Month	% of Record	Period
Beaufort Sea	July	62	1979
Lancaster Sound	May	97	1970, 1977
	June	73	1977
	July/August	77	1975-79
Labrador Coast	March	91	1965
	April	89	1965-67

For the selected months, the relative frequencies of speed and of direction of winds were tabulated and graphed for comparison with corresponding probability distributions of ice speed and direction of movement.

Even with the above selection procedure, some subsets of data are of questionable quality. For wind data, the spatial distribution of observations in each study area is not known, and the distribution of observations between years is in most cases highly non-uniform.

For ice movements, the distribution between subareas is also non-uniform. Owing to these limitations, the selected subsets of data were used with caution in making inferences on the wind-ice movement relationships. No attempt was made to provide a quantitative assessment of ice speed and wind speed distributions. Average values are compared and discussed in Section 3.5.2.

2.5 Refreezing of Pack Ice Leads

When a lead in the pack ice is open, the water surface is a heat source for colder air above the water. If the water is at or near

its freezing point, about -1.8°C for most sea water, the heat loss will result in formation of ice. If sufficient ice is produced, the lead will be covered in a new ice layer. The timing of this new ice formation will compete with the closure of the lead to determine which physical process will control the distribution of oil.

A number of processes are involved in the transfer of heat to and from the air-water interface, and the subsequent formation and behaviour of ice on the surface of the lead. Figure 2.8 depicts the many processes occurring while a lead is open. If there is no wind, heat will be lost from the water to the air, producing a skim of new ice. This ice will grow as fast as heat can be transferred from the water below to the air above, and depends on the air temperature and the thickness of the insulating ice layer. If there is a wind or a current, the ice being produced will be transported away, leaving open water for more ice production. Eventually, this ice will pile up against the boundary of the lead, and will expand to ultimately cover the lead.

As ice is produced at the water surface, the salt is generally excluded from the ice. This increase of salinity in the underlying water may cause a density instability to develop, and result in a turnover of the water column, bringing warmer deep water to the surface. This would act to slow the production of ice.

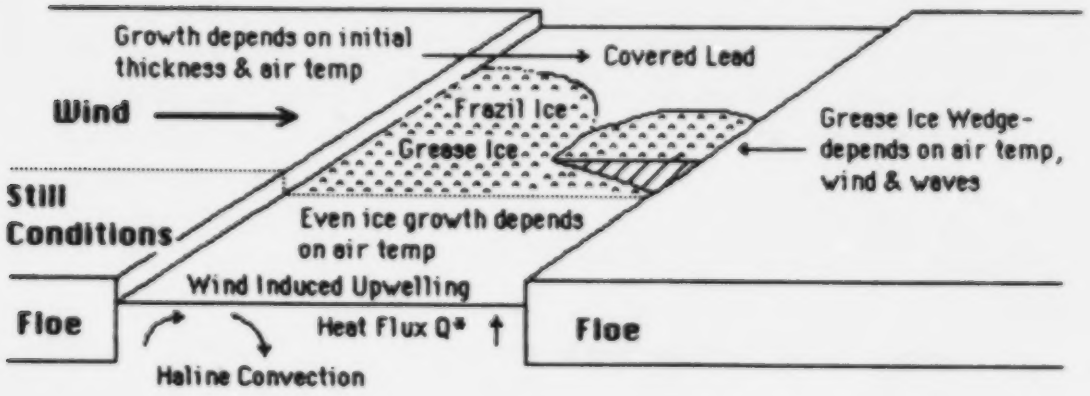

Figure 2.8 Lead Refreezing Processes

Each of the processes depicted have been studied and some have been modelled. No experimental study has been found in the literature which examines the problem of lead refreezing specifically, but an estimate of lead refreezing rates may be made using data from related studies.

The growth of ice has been generalized for Canadian waters by Burns (1974). Using the classical equation for ice growth, he relates the theoretical growth rates to measured growth rates, and provides a rough method for determining the thickness of ice given the temperature regime over time. The equation takes the following form:

$$D\ L_f\ dH = a\ K_i\ (T_w - T_a)/H_m/\ dt \qquad (1)$$

where

D = ice density (taken as 920 kg m^{-3})

a = constant correcting for included air (Burns suggests 0.94)

L_f = latent heat of fusion of water (taken as 320 kJ kg^{-1}, at -1.6°)

dH = change in ice thickness (metres)

K_i = thermal conductivity of ice (taken as 2.5 W $m^{-1}deg^{-1}$)

T_a, T_w = temperature of the air and water

H = ice thickness (metres)

dt = time interval (hours)

This equation is integrated to give the form:

$$H_{t2}^2 - H_{t1}^2 = 5.75 \times 10^{-5} \times \text{Freezing Degree Hours} \qquad (2)$$

This equation may be used to determine the growth of ice in an open lead under conditions with no wind or current. It is similar to the equation used by Bauer and Martin (1983) in their model treatment of ice growth.

If there is any wind, the ice will be transported away from the site of formation, leaving open water to produce more ice. This effect is well documented for polynyas and leads (Dunbar, 1981; Topham et al, 1983; Smith et al, 1983; den Hartog et al, 1983; Martin and

Kaufmann, 1981). Dunbar (1981) quotes Kupetski (1962) who determined that the open water of the North Water annually produced 4.5 times as much ice as adjacent ice covered areas.

Photographs of leads under windy conditions show grease ice formation, movement, and pile-up (Martin and Kaufmann, 1981). The formation of grease ice in leads has been modelled by Bauer and Martin (1983). Estimates of ice growth under wind conditions are all based on the determination of the heat flux to the air from the water, and are usually calculated assuming all the heat removed from the water is provided from the latent heat of vapourization, as the water will likely be at the freezing point. This assumption is acceptable as the latent heat of vapourization is much higher than the heat capacity of water and will be the major heat source. The heat flux consists of four components:

$$Q^* = Q_S + Q_L + Q_{lw} + Q_{sw} \qquad (3)$$

where

Q_S is the sensible heat flux
Q_L is the latent heat flux
Q_{lw} is the long wave radiation flux

and

Q_{sw} is the short wave radiation flux

Andreas et al (1979) measured the heat flux over small leads (6-10 m), and Bauer and Martin (1983) developed a model of heat flux over large leads (0.5 km). The environmental conditions of Andreas et al (1979) are mild, whereas those of Bauer and Martin (1983) are severe. The results of both workers may be simplified by plotting heat flux against a "wind chill" factor, $U\ (T_w - T_a)$, where U is wind speed in m s^{-1}. The flux equations may then be included in the equation for the production of ice, assuming all the heat is from the heat of fusion, to give two equations for ice production, one for small leads and mild wind chill, and the other for large leads and severe wind chill. Lo (1980) has pointed out that the heat flux may decrease in larger leads due to fog formation

above the leads, but no experimental data could be included in this analysis. The equations are:

$$P = 1.2 + 0.0312\ U\ (T_w - T_a) \quad (4)$$

and

$$P = 3.0 + 0.0204\ U\ (T_w - T_a) \quad (5)$$

P = Production Rate (kg $m^{-2}h^{-1}$)

U = Wind Speed (m sec^{-1})

Equation (4) will be used for mild conditions (wind chill less than 200 m sec^{-1} °C), equation (5) for severe conditions (wind chill greater than 200 m sec^{-1} °C).

The time required to cover a lead can be estimated by integrating the ice production rate over the dimensions of the lead as the lead becomes covered with ice. This integration is logarithmic, with the final stages of covering becoming infinitely slow, as the area for ice production approaches 0. By using 95% coverage and factoring it up to 100%, coverage times may be estimated according to equation (6) below:

$$t_c = 827\ P/H \quad (6)$$

where

H is the final covered ice thickness (m).

It should be noted that for leads wider than 50 m, coverage times are independent of lead width.

The results using this equation correspond closely to Bauer and Martin's (1983) results when their choice of ice thickness and environmental conditions are used. The weak point in this analysis is the estimation of the final ice thickness. Bauer and Martin (1983), developed a model based on wave action and wind induced current to determine the thickness of the grease ice wedge built up

at the end of the lead, and subsequently covering the lead. Their tank results have shown that the modelled thickness is typically only one-half of the observed thickness. By doubling their model results, and plotting against wind speed, an estimate of grease ice thickness of H = 0.06 U is arrived at for the present analysis.

The other factors depicted in Figure 2.8 have also been examined. The effect of haline convection in small (less than 1 m) leads was examined by Foster (1972). The circulation of water in a lead caused by the exclusion of salt during freezing, was modelled by Kozo (1983). His model broke down in a current of 5 cm s^{-1}, but showed significant circulation in quiet conditions. No attempt was made to include the introduction of warm, deep water in the present analysis, as the general oceanographic conditions for these areas are not well defined.

Some important factors should be considered. Schaas and Galt (1973) modelled heat flux as determined by water structure. They pointed out that any overturning of the water column will slow icing by introducing warmer deep water, and that any factors which reduce this turnover will encourage icing. A density or salinity discontinuity, such as occurs in the Beaufort Sea, insulates the upper layer from the deeper heat source. Horizontal currents have a similar but smaller effect. Buckley et al (1979) showed the presence of wind induced upwelling at pack ice edges. This effect may influence lead refreezing in the case of large leads.

Refreezing times for leads in the three regions studied are determined using the equation for calm conditions, equation (2), rearranged to give the time for production of 0.2 m of ice (selected as being a thickness which allows most forms of light transport). The times for coverage under mild and severe wind conditions will be determined using either equation (4) or (5), depending on the mean climatic conditions.

The climatic conditions used in each case are those provided by the "Canadian Climate Normals 1951-1982" for weather stations in each area. The Beaufort Sea area is represented by data from Nicholson

Peninsula and Tuktoyaktuk. The Lancaster Sound area is represented by data from Resolute Bay, and the Labrador area by data from Hopedale. The marine data collected for each area did not have sufficient data for the time periods of interest. The data used from each station are minimum, mean, and maximum monthly temperatures, and mean and maximum winds. The lead refreezing rates are presented in Section 3.6.

3.0 RESULTS AND DISCUSSION

3.1 Summary of Regional Ice Conditions

Figures 3.1 to 3.3 show median bi-weekly ice concentrations for the different regions. This information is an important indicator of the relative importance of a particular pack ice environment within the different offshore areas of interest for hydrocarbon exploration.

Ice concentration is considered the single most important pack ice descriptor. At low ice concentrations (less than 4/10) it seems unlikely that ice dynamics will play a major role in modifying or controlling oilspill behaviour. As concentrations reach 7/10, individual ice floes are contacting one another, and the potential exists for substantial ice/oil interaction. Eventually as the pack closes up and approaches a continuous sheet of ice, leads appear and become an important natural means for oil containment or spreading, depending on dynamics of the situation. Table 3.1 shows a simplified comparison of the most important characteristics of the ice regime in the three main areas.

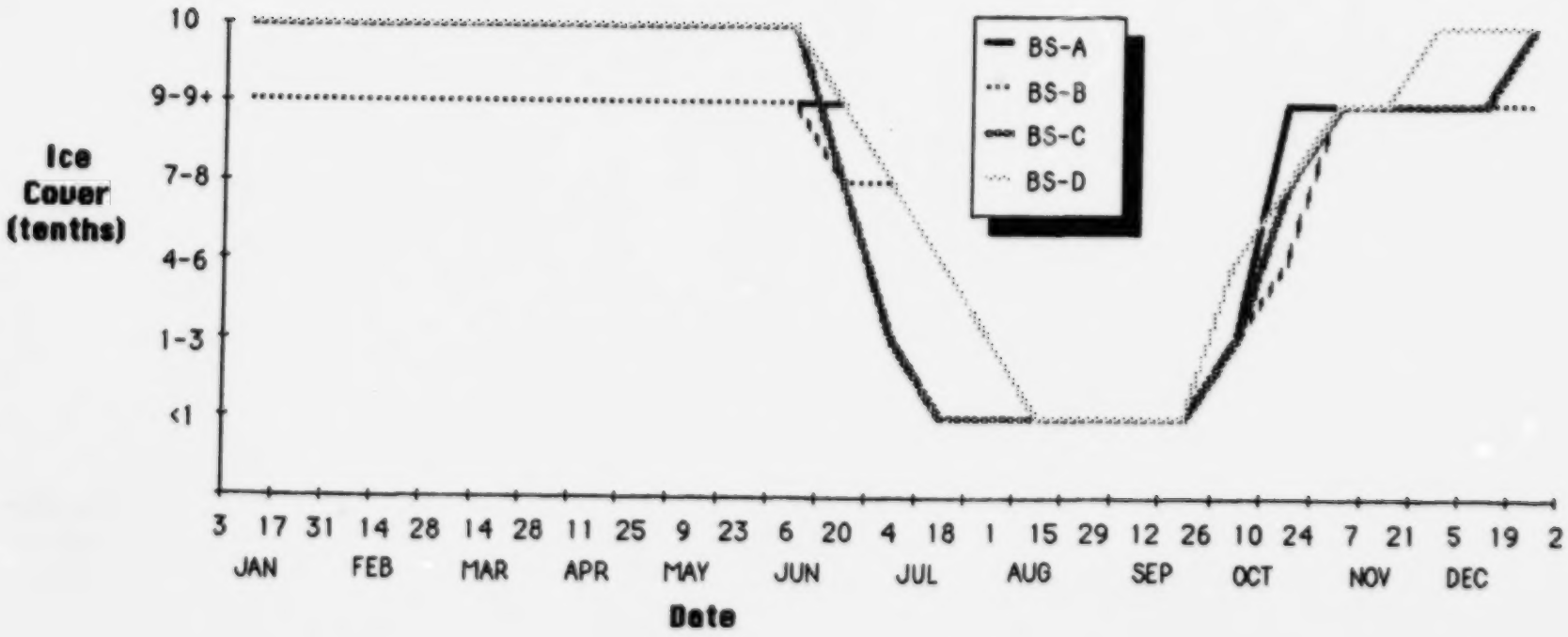

Figure 3.1 **Median Bi-Weekly Ice Concentration - Beaufort Sea**
(See Figure 2.1 for Locations of Sub-Regions Indicated in Legend)

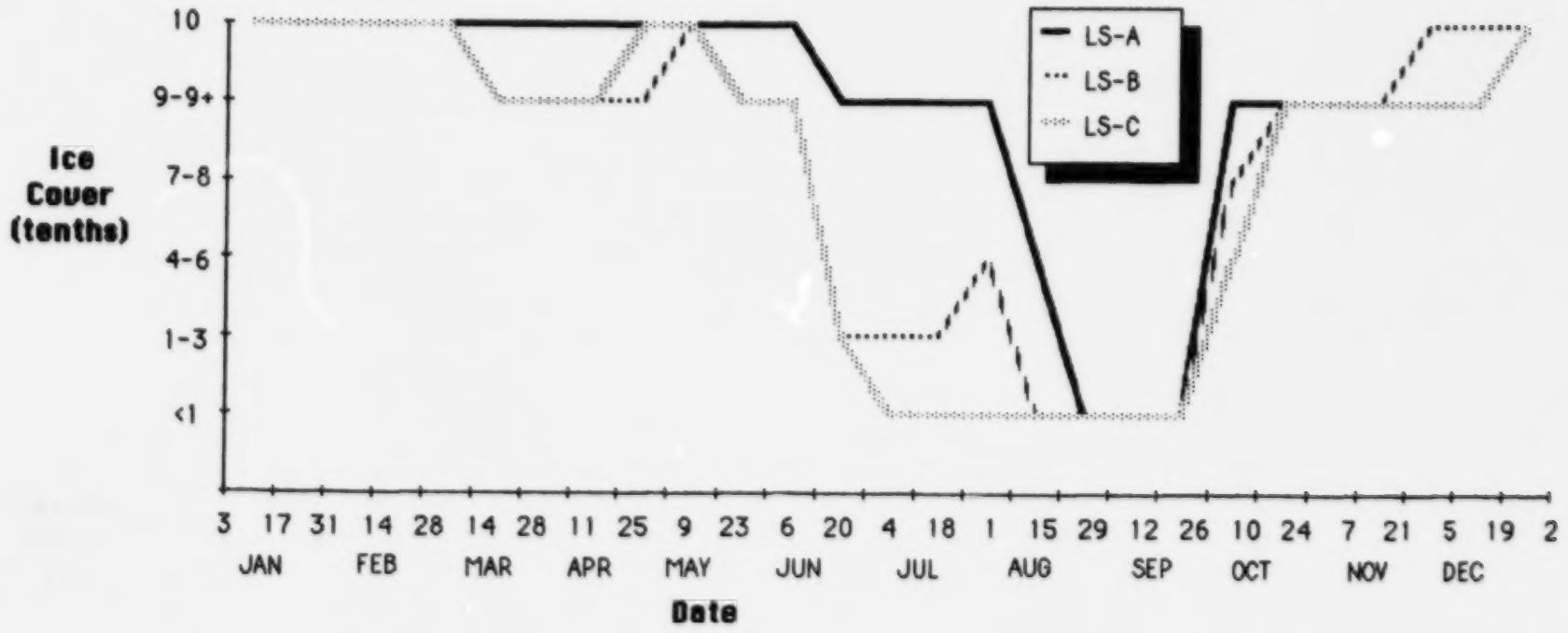
10
9-9+
7-8
4-6
1-3
<1
Ice Cover (tenths)
LS-A
LS-B
LS-C
3 17 31 14 28 14 28 11 25 9 23 6 20 4 18 1 15 29 12 26 10 24 7 21 5 19 2
JAN FEB MAR APR MAY JUN JUL AUG SEP OCT NOV DEC
Date

Figure 3.2 **Median Bi-Weekly Ice Concentration - Lancaster Sound**
(See Figure 2.2 for Locations of Sub-Regions Indicated in Legend)

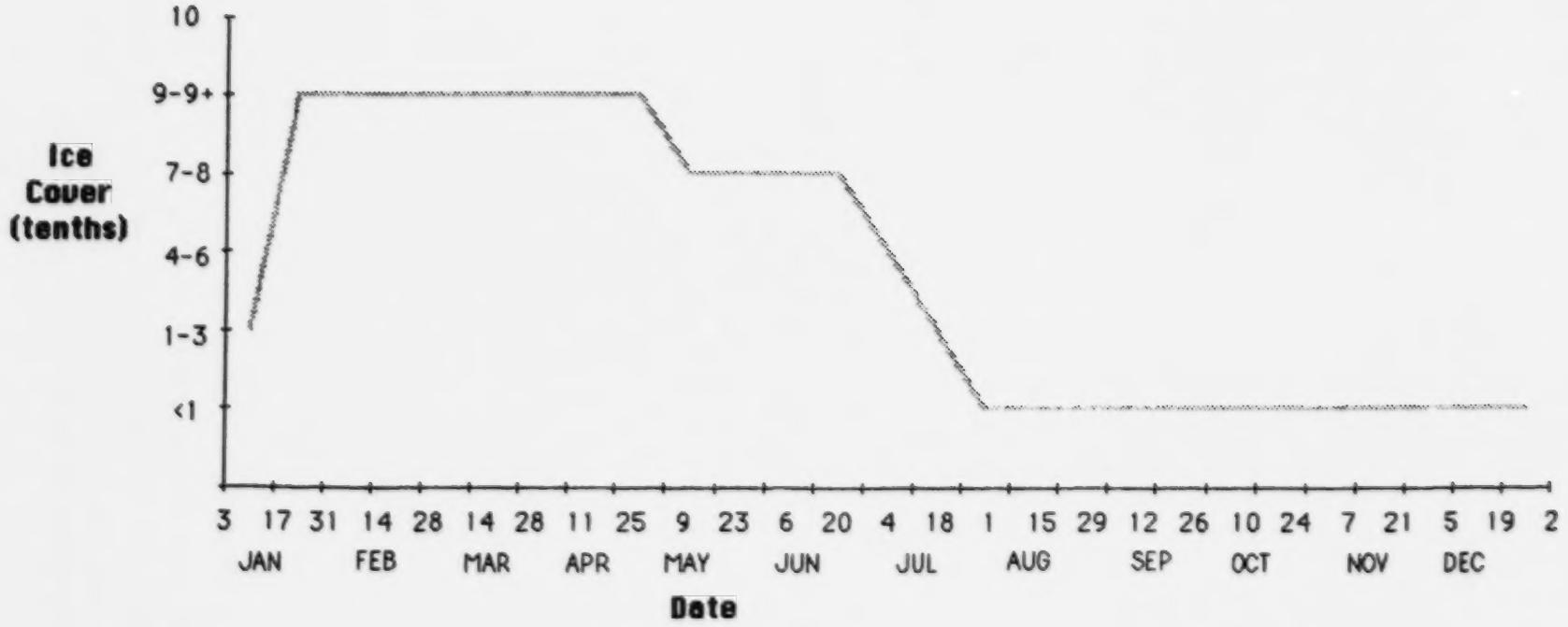

Figure 3.3 Median Bi-Weekly Ice Concentration - Labrador Sea

Table 3.1 Regional Comparison of Ice Regimes

	Beaufort Sea	Lancaster Sound	North Labrador Sea
Freeze-Up	Oct 5 ± 15 days	Oct 10 ± 10 days	Jan 10
Break-Up	July 16 ± 20 days	June 3 ± 40 days	June 20
Single Most Important Physical Control on the Ice Environment	Position of Polar Pack Relative to Shore	- East/West Location of Stable Ice Edge - Prevailing Winds	- Storm Tracks - Ocean Currents
Maximum Level Ice Thickness	1.8 m	1.9 m	1.4 m
Weeks of:			
7-8/10 Ice Floes	2 weeks	2 weeks	8 weeks
4-6/10 Floes	4	3	2
9-9+ Leads	34	30	16*
<4/10 Ice	12 weeks	17 weeks	26 weeks

*For Labrador Sea 9-9+/10 ice is still predominantly composed of individual floes. Lead patterns are transient and not well formed.

The Beaufort Sea region has the greatest number of weeks of 9/10 and greater ice cover (over twice as many weeks as the Labrador Sea).

Four to eight/tenths can be considered the maximum range of pack ice concentrations where the movement and interaction of individual floes will play a major role in affecting oil behaviour and fate. In lesser ice concentrations an oil spill can essentially be treated as an open water situation. In higher concentrations, individual floes gradually loose their identity, and linear openings in the cover known as leads become the major pack ice characteristic impacting oil distribution.

From Table 3.1, the three regions can be summarized as follows according to the proportion of the year when average pack ice conditions will impact an oil spill through a) individual floe dynamics and b) leads.

Table 3.2 Regional Summary of Average Pack Ice Duration

	% of Year by Region		
Pack Type	Beaufort Sea	Lancaster Sound	Labrador Sea
a) 4-9/10, Floes	11	10	50
b) 9/10+, Leads	65	58	Not Estimated

This simplified comparison indicates that in Lancaster Sound and the Beaufort Sea, open to close pack ice conditions persist on average for about 10% of the year, concentrated in a 5 to 6 week period preceding break-up. Both Arctic regions have almost complete ice cover for over half the year. During this period, leads and openings (polynyas) exist as evidence of continuing pack ice motion.

The Labrador Sea is not readily characterized in terms of a simple division between leads and floes. Instead of a rapid, predictable build-up and drop in ice concentrations characteristic of the arctic ice cycle, the marginal ice zone in the Labrador Sea tends to be much more variable both between years and within a single winter season. From previous descriptions and evaluation of remote sensing imagery in this study, floe interactions and new ice growth between floes are considered to be much more important than leads in potentially controlling oil behaviour and fate in the Labrador Sea. This hypothesis is borne out by recent experiences with an actual oil spill in east coast pack ice conditions (ESRF Study in progress - S.L. Ross Environmental Research Limited).

3.2 Leads

3.2.1 Distribution of Data

Figures 3.4 and 3.5 show the distribution of lead statistics collected in this study for the Beaufort Sea and Lancaster Sound.

In the Beaufort Sea, 85% of the remote sensing imagery suitable for the analysis of leads falls in the month of March, with the remainder in April. Sixty-two percent of the data was collected for Regions A and B of most interest for deep water offshore exploration (see Location Map, Figure 2.1).

In Lancaster Sound, the data is spread over the period March to August, with half of the measurements in April and July. The break-up of Lancaster Sound proceeds from east to west. Logically, most leads in April were in the central Region B (Figure 2.2), while July leads were concentrated in far western Region A, where the ice cover is last to clear.

Figures 3.6 to 3.8 show examples of lead dynamics in the Beaufort Sea and Lancaster Sound. Figures 3.6 and 3.7 show the closure of lead systems over a 24 hour period off the Tuktoyaktuk Peninsula. Figure 3.8 presents a pair of Landsat images showing the opening of lead systems in Lancaster Sound between March 30 and March 31, 1981.

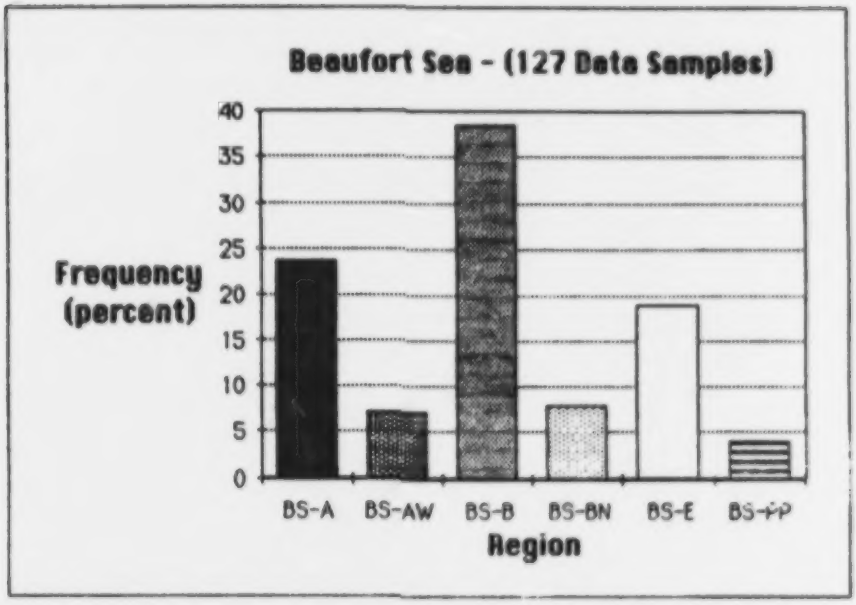

Figure 3.4 Distribution of Beaufort Sea Lead Statistics by Region

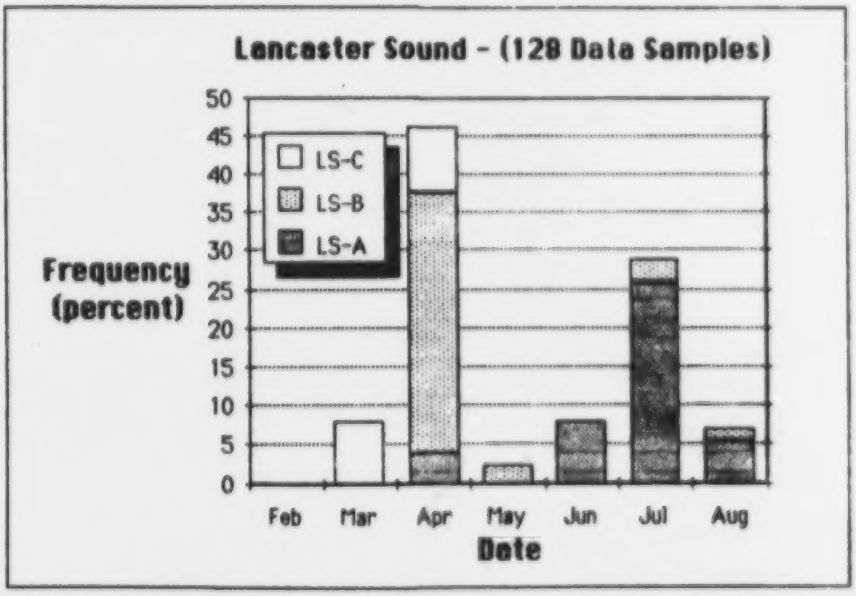

Figure 3.5 Distribution of Lancaster Sound Lead Statistics by Month

Scale 1:1,000,000

Figure 3.6 Overlay of Landsat Image, March 10, 1975 Showing Well Defined Lead Systems in the Beaufort Sea

Figure 3.7 Landsat Image of Same Area as Figure 3.6 Showing Compressed Pack Ice and Lead System Closure, on March 11, 1975

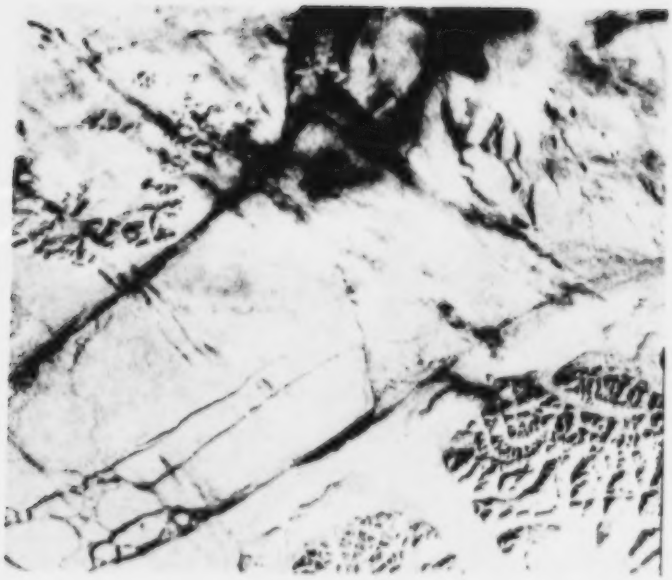

March 30, 1981, 1707 h

March 31, 1981, 1712 h

Figure 3.8 Comparison of Lead Appearance in Lancaster Sound Over 24 Hour Period

3.2.2 Lead Dimensions

Figure 3.9 shows the frequency distribution of lead widths measured from Landsat imagery for the Beaufort Sea and Lancaster Sound. With similar sized data sets (127 and 128 measurements respectively) these graphs show almost identical distributions, with over half the leads less than 500 m wide.

In summary, the lead width distributions appear to follow a negative exponential relationship within the range of values measureable off Landsat. It must be emphasized that for every lead large enough to appear on a satellite image (several hundred metres wide) there will be tens or hundreds of smaller leads and cracks which will also play a role in oil distribution within in a dynamic ice cover.

Some indication of the potential numbers of small leads which could contain oil is provided by Hall (1977). April 1972 aerial photography over the polar pack in the vicinity of the AIDJEX camp in the Alaskan Beaufort Sea was analyzed to determine the frequency distribution of lead widths in the range 0-800 m (Figure 3.10). In contrast, the Landsat analysis conducted in this study looked at leads from about 200 m to 10 km.

The AIDJEX research showed that for leads less than 100 m wide, 70% were less than 50 m width and 40% less than 20 m in width. Landsat analysis for the Beaufort Sea, shows 46% of all leads between 100 m and 1 km (Figure 3.9). Hall's analysis showed 26 leads between 100 and 800 m, vs 137 between 0 and 100 m. On this basis, there could be 137/26, or about 5 times more leads in the ice than can be documented from Landsat imagery. Interestingly, the 50 percentile lead width of about 30 m identified in Hall's analysis agrees with the values reported in the U.S. Navy Birdseye flights (from Wadhams, 1975).

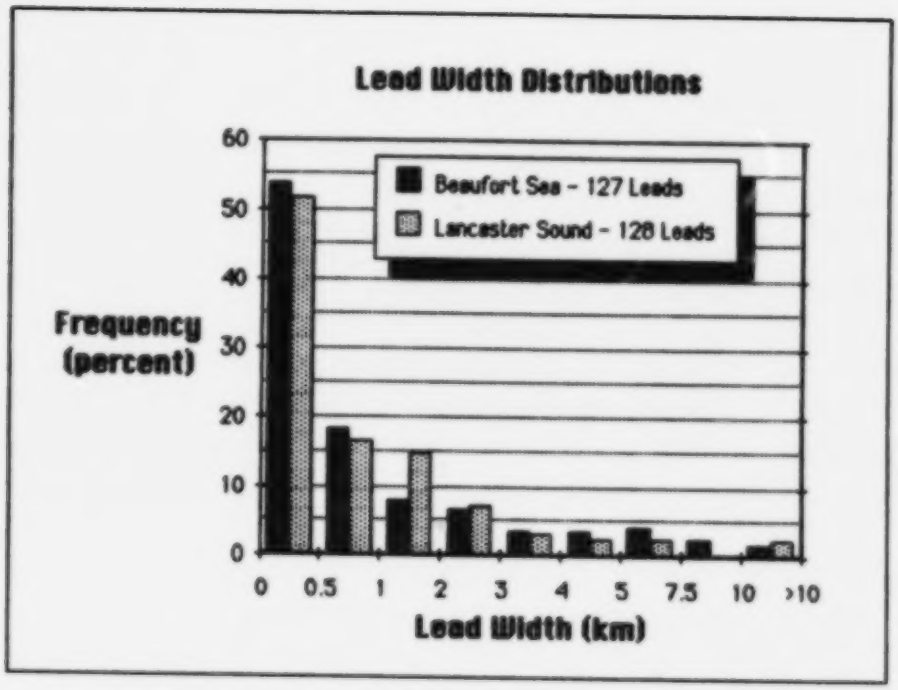

Figure 3.9 Distribution of Lead Widths Measured from Landsat Imagery

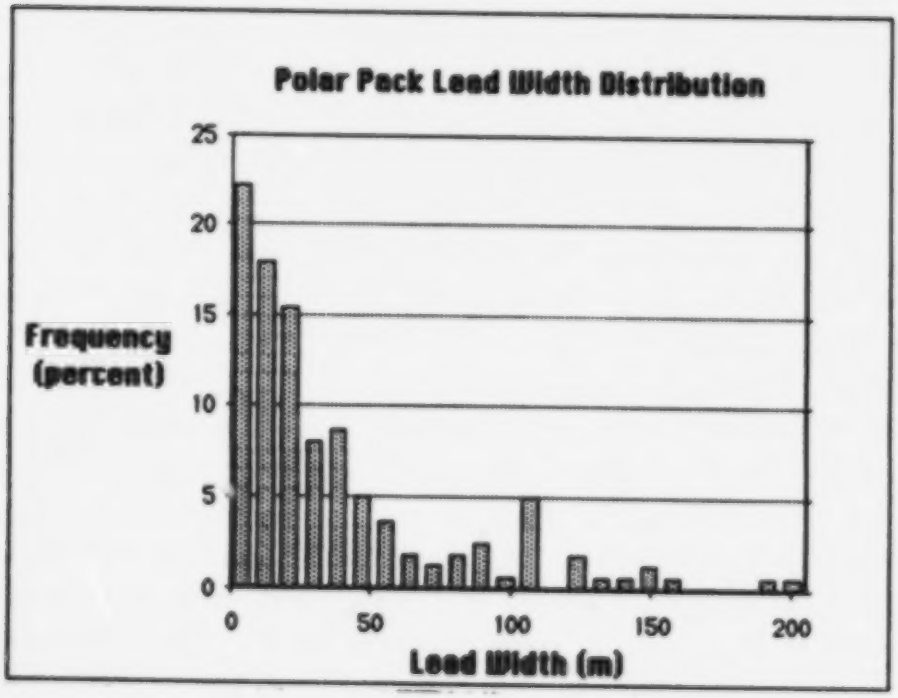

Figure 3.10 Distribution of Lead Widths in the Polar Pack from Aerial Photography (Hall, 1977)

Wadhams (1975) showed that in flying the polar pack into the seasonal pack (south of 72°N), the total number of leads per kilometre increased from a mean of 0.18/km to 0.72/km.

Corresponding U.S. Navy values show winter lead frequencies in the Beaufort Sea of about 0.8/km.

From the available March Landsat imagery showing leads in the Beaufort Sea, a limited set of 25 observations was made of lead aerial density in #/hectare (Figure 3.11).

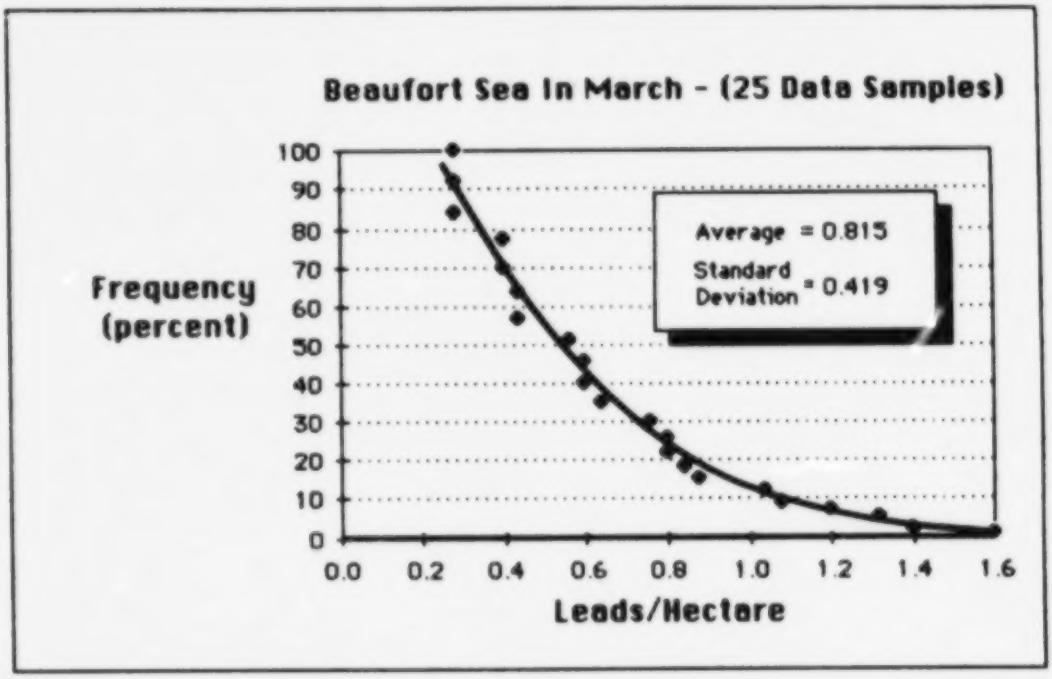

Figure 3.11 Cumulative Probability of Lead Density Derived from March Landsat Imagery

Hartwell (1972) describes the detailed deformation history of a triangular section of pack ice approximately 11 km on the longest leg. Measurements were made from sequential aerial photography over a twelve day period (March 11-23, 1971). The study area in the vicinity of 73°45'N, 130°15'W falls within region PP indicated in the Beaufort Sea location map (Figure 2.1).

Hartwell's study is of particular interest for oil spill fate and behaviour predictions because it demonstrates the magnitude timing and spatial extent of small scale deformation events within a winter pack ice environment.

The results of Hartwell's interpretation are included as a series of detailed ice maps derived from the aerial photography (Appendix E). These maps show the magnitude of shear, compression and extension events occurring between photo flights. Individual leads can be followed as they open and close.

Air photo resolution allows the identification of leads down to several metres in width. Figure 3.12 shows a typical photograph of young pack ice with fresh leads and recently refrozen openings. The dominant lead in this image is 40 m in width.

Scale: 1 mm = 5.1 m

Reference: AIDJEX Bulletin #13

Figure 3.12 Aerial Photography of Pack Ice in the Vicinity of 73°45'N, 130°15'W, March 11, 1971. (Taken by the NASA 990 Research Aircraft Galileo, with a Wild RC-8 Mapping Camera.)

Of particular interest to this study is Hartwell's photographic evidence of lead closures creating new pressure ridges by crushing the ice along the lead edge.

Figure 3.13 shows an example of one of these closing events photographed during the 1971 AIDJEX study (Hartwell, 1972).

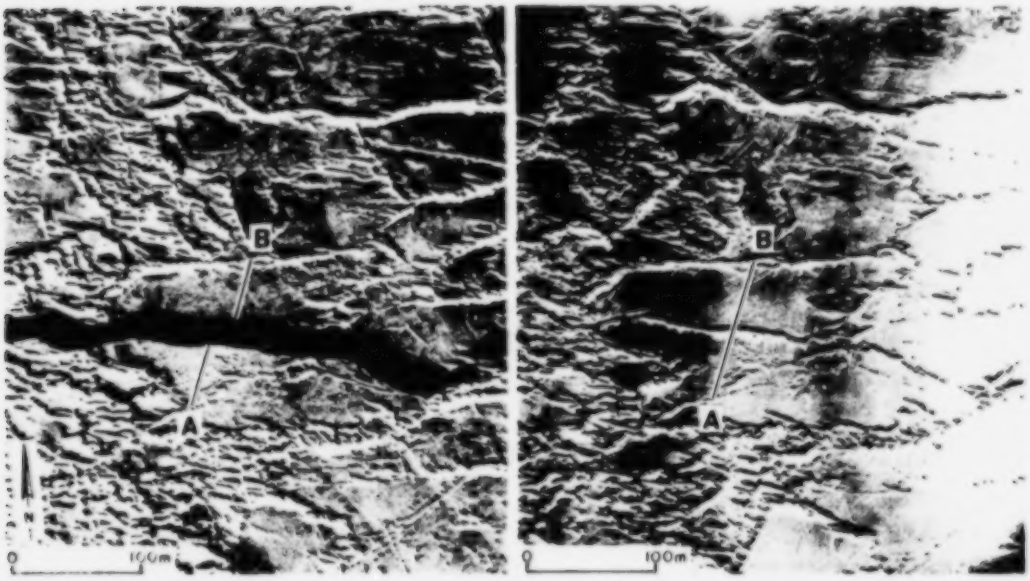

March 11, 1971 March 23, 1971

Figure 3.13 Example of Lead Closure Leading to a Pressure Ridge

3.2.3 Lead Orientation

The bearings of leads measured in the Beaufort Sea and Lancaster Sound are plotted in Figure 3.14. There are no strongly preferred lead orientations, but trends agree with the overall directional motions of the pack ice relative to the local shorelines and fast ice boundaries. In the Beaufort Sea, leads tend to parallel the shore. Region B off the Tuktoyaktuk Peninsula shows a bias towards NE/SW leads, while Region A off Mackenzie Bay favours an E/W orientation.

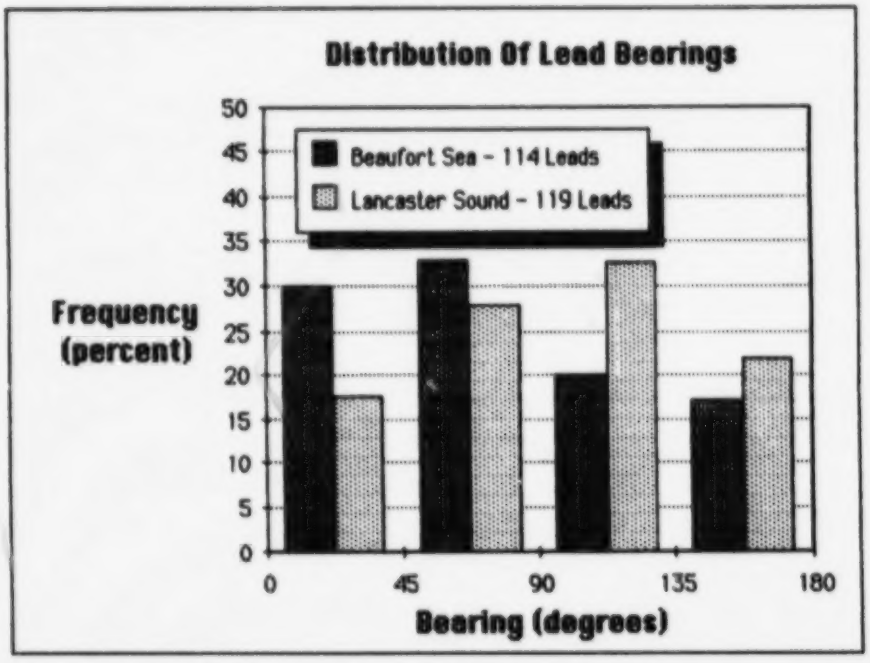

Figure 3.14 Lead Orientation

In Lancaster Sound, there is a slight trend to NW/SE oriented leads in the most westerly Region A. The other two regions lack any preferred lead orientations, but tend more to an E/W alignment paralleling the coastlines. Intuitively, as the ice is

funnelled away from the stable ice edge, leads would be expected to change from a cross channel to a long channel orientation (see example Landsat image shown in Figure 3.8).

3.2.4 Lead Opening and Closing Rates

The distribution of lead opening and closing rates is probably of most interest in terms of modelling lead pumping mechanisms. Figures 3.15 and 3.16 show percent frequency of occurrence of measured rates of change in lead width. Positive rates signify opening and negative rates indicate closing. Both Lancaster Sound and the Beaufort Sea appear as expanding ice environments, that is, openings are favoured over closing by a ratio of 5:1. Peak movement rates encountered during opening events tend to be two to five times higher than rates measured during closings. Lancaster Sound experiences lead opening rates as high as 17 km/day, compared to a peak value of less than 10 km/day measured in the Beaufort Sea. The percent occurrence of closure events is similar for the two regions, but closure rates tend to be higher and more evenly distributed in the Beaufort Sea.

Regional differences in lead dynamics within the study areas are not clear. Few lead closures were observed in Lancaster Sound Region C, which is to be expected in an area where the sound is opening out into Baffin Bay.

The Beaufort Sea seems to be divided into expanding and contracting regions. Amundsen Gulf, and the offshore Mackenzie Bay regions showed only opening leads. Amundsen Gulf is a known area of ice arching between Banks Island and the Parry Peninsula. Ice drifts to the west away from this arch for much of the winter. Limited data for the polar pack showed only closing leads.

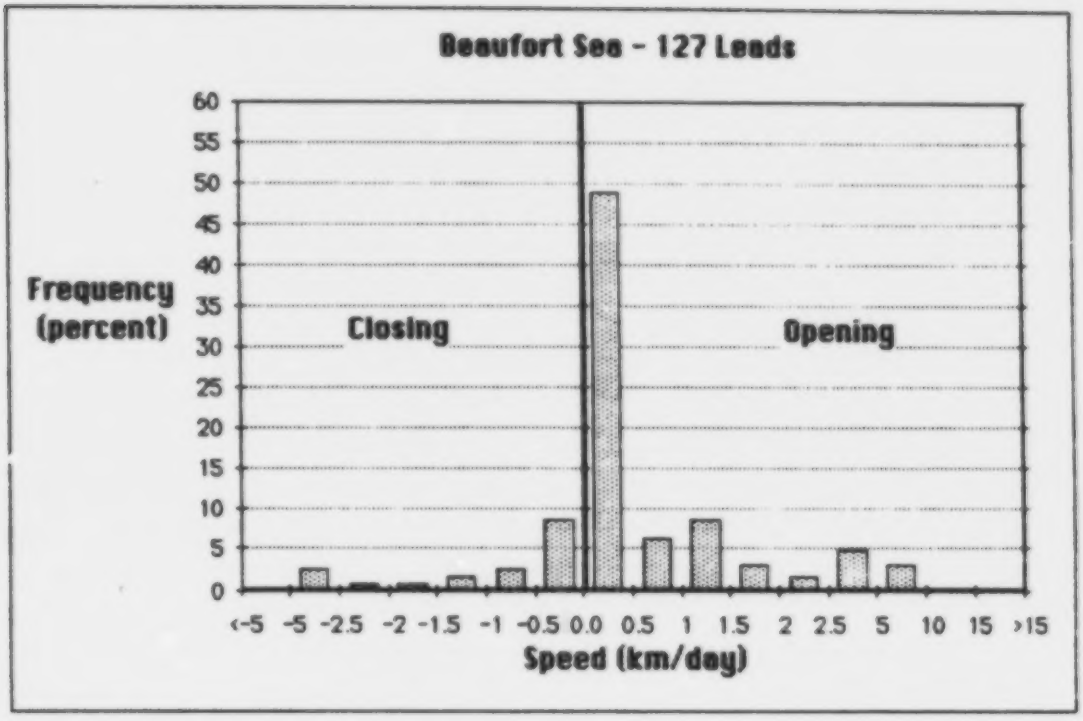

Figure 3.15 Lead Opening and Closing Rates - Beaufort Sea

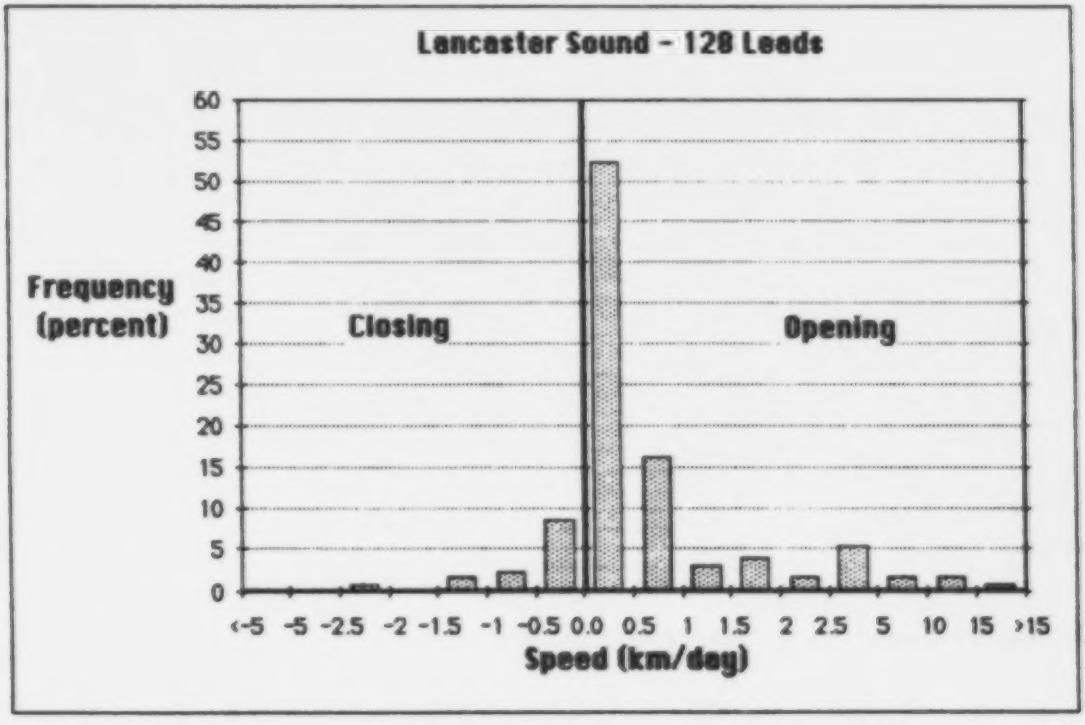

Figure 3.16 Lead Opening and Closing Rates - Lancaster Sound

Region A offshore of Mackenzie Bay showed a strong trend to very slow movement rates, opening at between 0 and 0.5 km/day. This region tends to mark the point where the seasonal pack ice begins to be squeezed between the northerly trending Yukon/Alaskan coast, and the polar pack in its winter journey westward into Soviet waters.

Figures 3.15 and 3.16 clearly show that over 50% of lead motions occur at rates less than 0.5 km/day. Measurements of lead dynamics from aerial photography show maximum motions of approximately 150 m/day (Hartwell, 1972). Caution should be exercised in drawing conclusions about instantaneous lead motions, from 24 hour displacements. As a first approximation, the average rates of lead openings and closings are less than 20 m/hour.

A unique data set on maximum potential short term lead closure rates is contained in personal observations of ice track closure behind icebreakers. Table 3.3 summarizes findings provided by J.D. Bradford (pers. comm.).

Table 3.3 Icebreaker Track Closure Observations
(Source: Bradford, Personal Communication)

Location	Date	Ice Thickness cm	Closure Rate m min^{-1}
Barrow Strait	Oct/73	28	30
Baffin Bay	Apr/70	121	0.8
N.W. Baffin	May/70	38	4.6
Lancaster Sound	May/70	46	15.2
Lancaster Sound	May/70	152	6.1
Grand Banks	Mar/71	23	2.1
Lancaster Sound - Maximum found in this study			1.73

3.3 Floes

Leads are the dominant pack ice characteristic affecting oil distribution in the Beaufort Sea and Lancaster Sound. Thick first year floes in these areas are only present for 4 to 6 weeks during break-up offshore. Ice concentrations quickly reduce to the point where there are only scattered floes, which will have limited impact on oil spill behaviour.

The Labrador Sea is a very different ice environment in that the pack is a mixture of older first year floes from Baffin Bay and Davis Strait, and younger ice forming in-situ between the floes. The Beaufort Sea and Lancaster Sound are areas of ice efflux, while the Labrador Sea is an area of significant ice influx. Floes are the dominant feature in the Labrador Sea. Leads only occur temporarily when large floes divide.

Figure 3.8 showed a mixture of thicker ice floes and leads in young ice in Lancaster Sound on March 30/31, 1981. Figure 3.17 shows an example of floes moving away from the stable ice edge in Lancaster Sound on April 25, 1977. The larger floe "C" is actually a conglomerate of thicker first year floes within a grey-white ice matrix. New ice is forming at the ice edge and gradually thickening as it moves east.

Figure 3.18 shows a pair of images north of Kugmalit Bay in the Beaufort Sea, separated by 24 hours (June 28 to June 29, 1980). Break-up is well advanced, and large floes tens of kilometres across are breaking off the remaining landfast ice in the lower right. Offshore, the pack ice is being compressed from a concentration of about 6/10 on June 28 to over 8/10 on June 29. The dynamics of pack ice in conditions such as shown here would play a major part in controlling the physical process of oil spreading, weathering and dispersion into the water column.

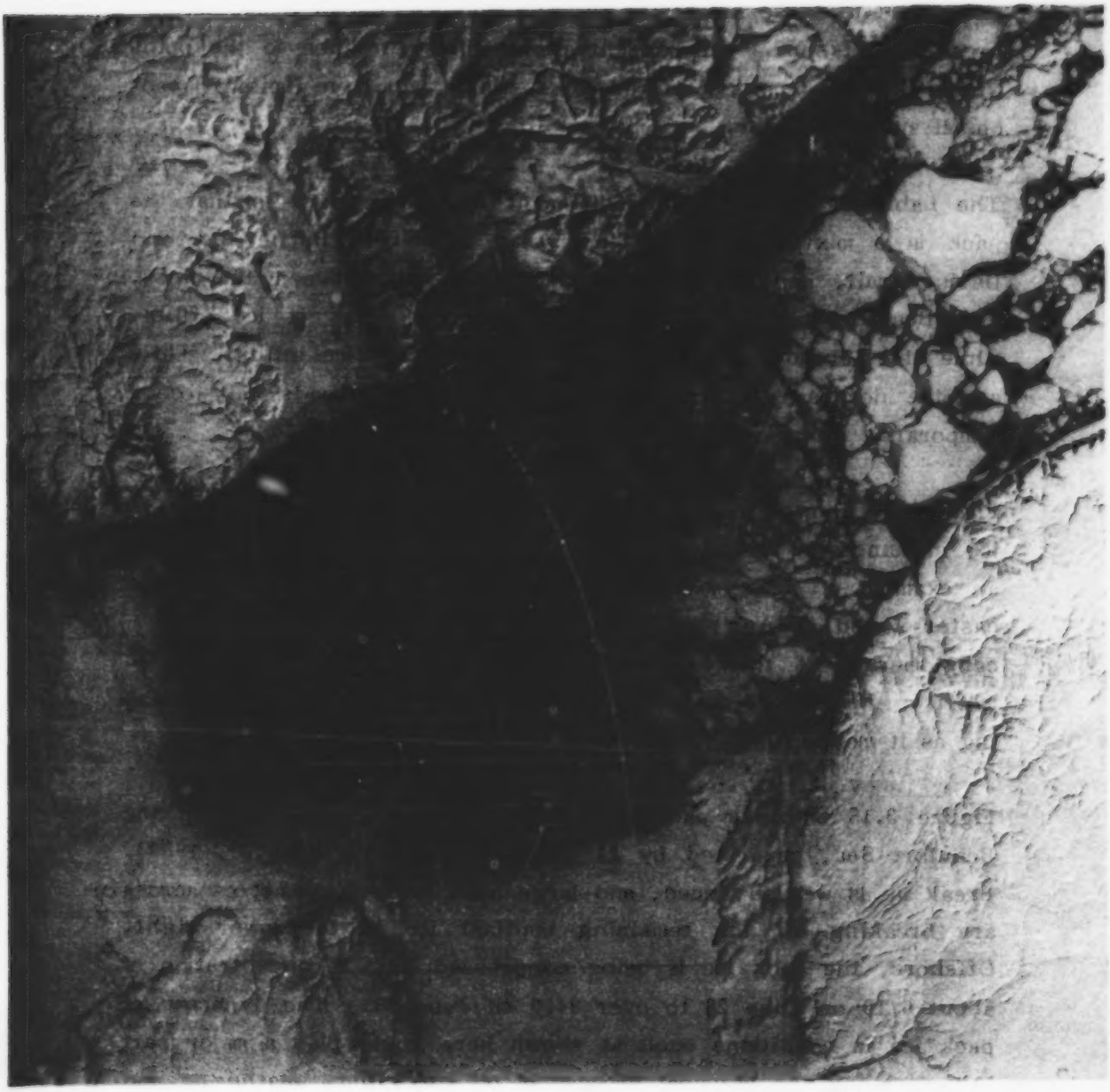

Scale 1:1,000,000

Figure 3.17 Lancaster Sound Landsat Image, April 25, 1977

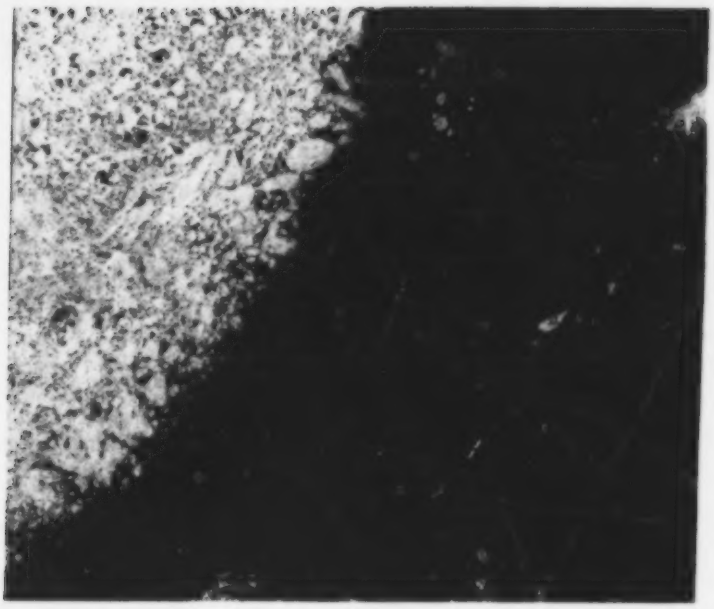

June 28, 1980

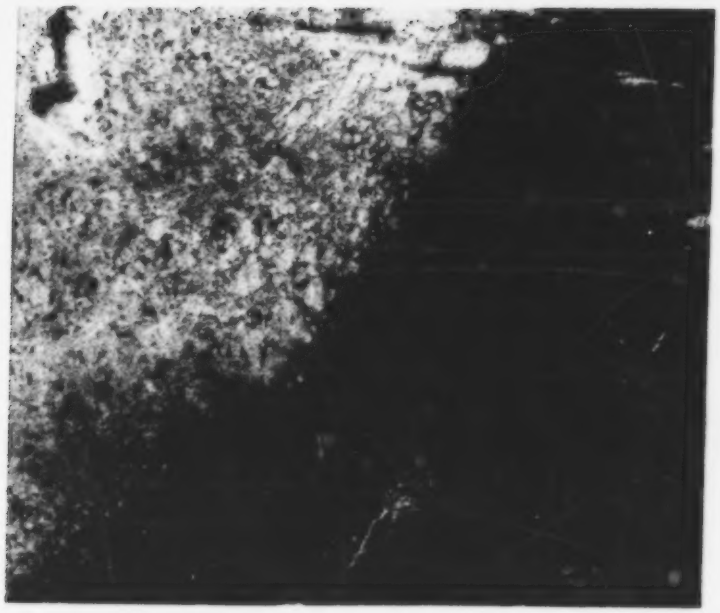

June 29, 1980

Figure 3.18 Landsat Images Showing 24 Hour Changes in Pack Ice Concentration in the Beaufort Sea North of Kugmallit Bay

Scale 1:1,000,000

Figure 3.19 Landsat Image Showing Labrador Sea Pack Ice, February 22, 1979

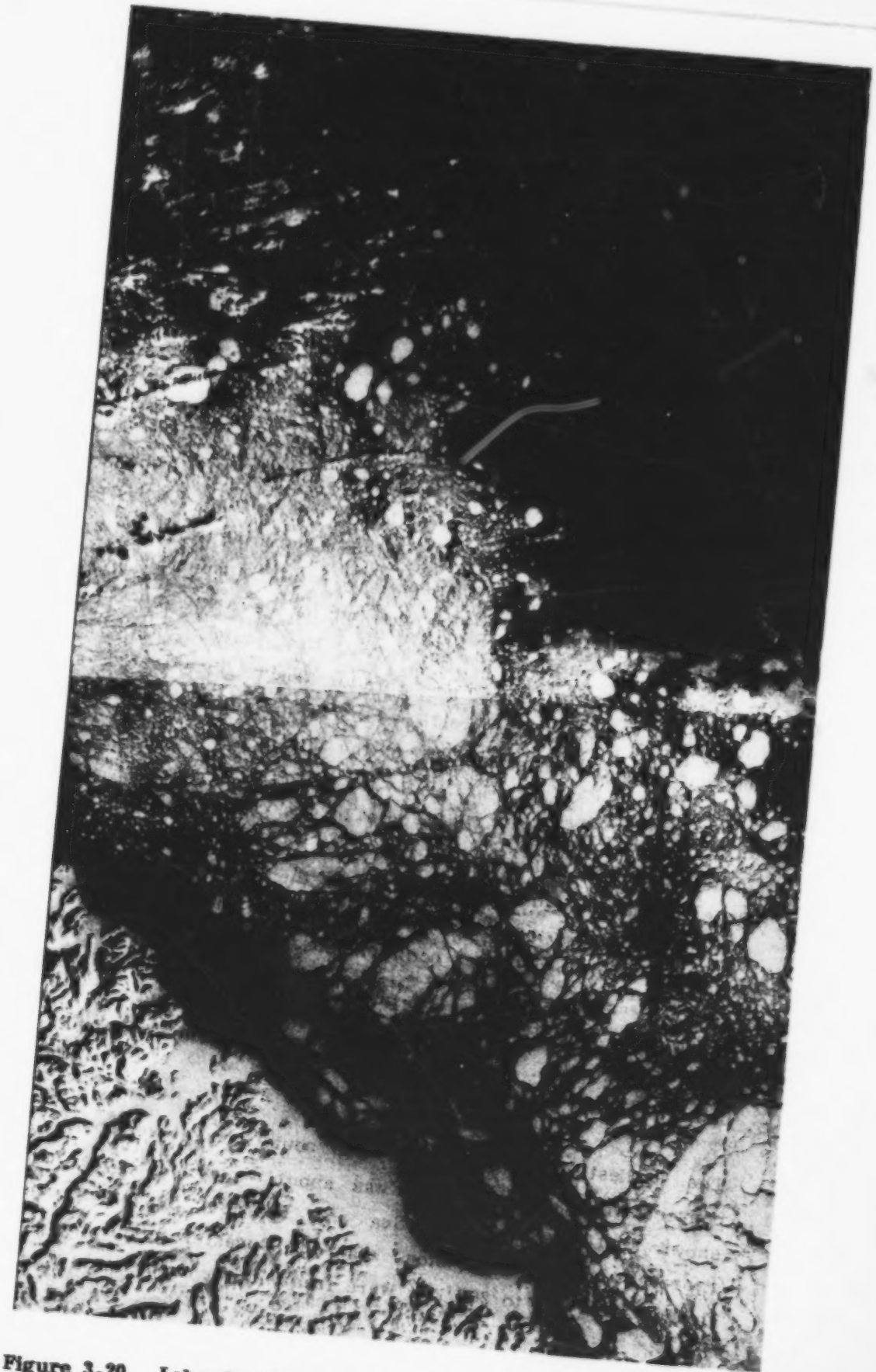

Figure 3.20 Labrador Sea Pack Ice Conditions, April 1, 1979 Scale 1:1,000,000

Labrador Sea pack ice can take on an infinite number of extremely complex formations, from large areas of grey to grey-white ice less than 1 foot thick, to conglomerates of thicker first year floes. This mixture of young ice sheets and older floes is in a constant state of flux. Figures 3.19 and 3.20 show examples of the appearance of changing Labrador Sea pack ice conditions between February and April 1979.

3.3.1 Distribution of Floe Data Sets

Figures 3.21 to 3.23 show the distribution of floe data collected in the three geographic areas according to month, ice concentration, and floe area. Floes examined in Lancaster Sound after June probably originated in surrounding waterways leading into Parry Channel. A small number of floes (10% of the total number) were tracked in the Amundsen Gulf region of the Beaufort Sea in March, May, June, and July. The data set of floes off the Labrador Coast concentrated on the month of April, with smaller subsets in February, March, May and June (all less than 20% of the total).

In terms of grouping the floe data by ice concentration, most information was collected in the 7/10 to 8/10 range, where floes are largely in contact. This is the concentration range considered most important in terms of oil/ice interaction. The Lancaster Sound data set contains the most uniform distribution of measurements over a wide range of ice concentrations. In all, data from 1245 floes was used during this study, 718 in the Beaufort Sea, 382 in Lancaster Sound, and 145 in the Labrador Sea.

The smallest observable floe which could be followed between consecutive statellite images was about 1 km^2. Figure 3.23 shows that the Labrador Sea and Beaufort Sea data sets represent much smaller floes than in Lancaster Sound, where floe areas of 150 to 200 km^2 were frequently encountered.

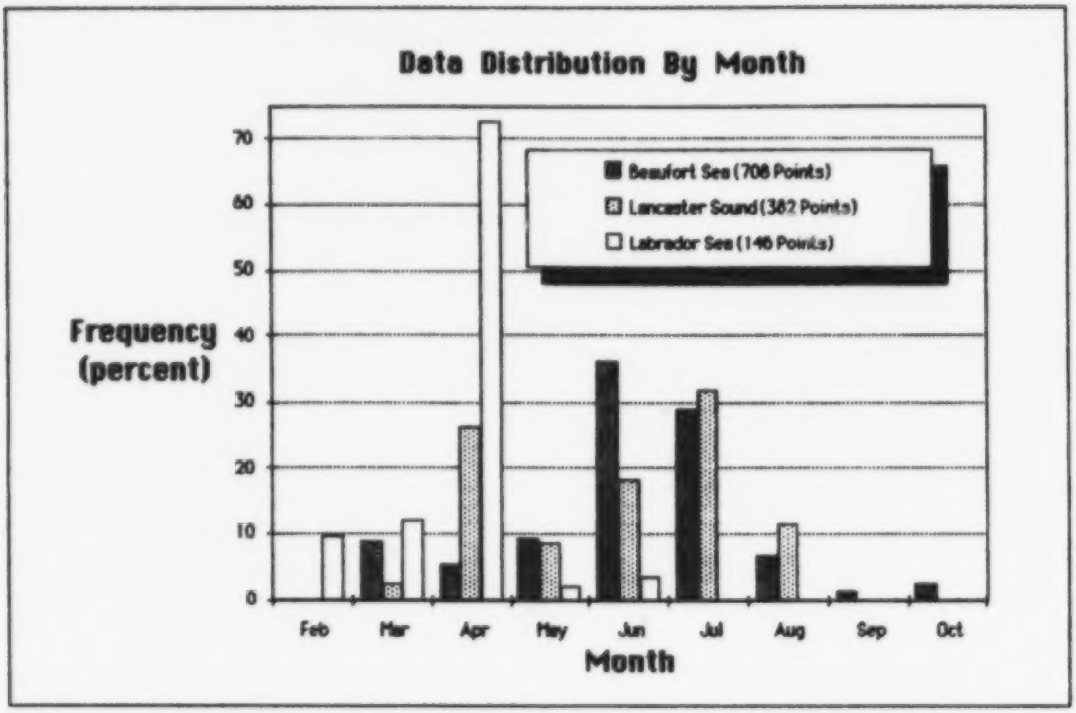

Figure 3.21 Distribution of Floe Data According to Month

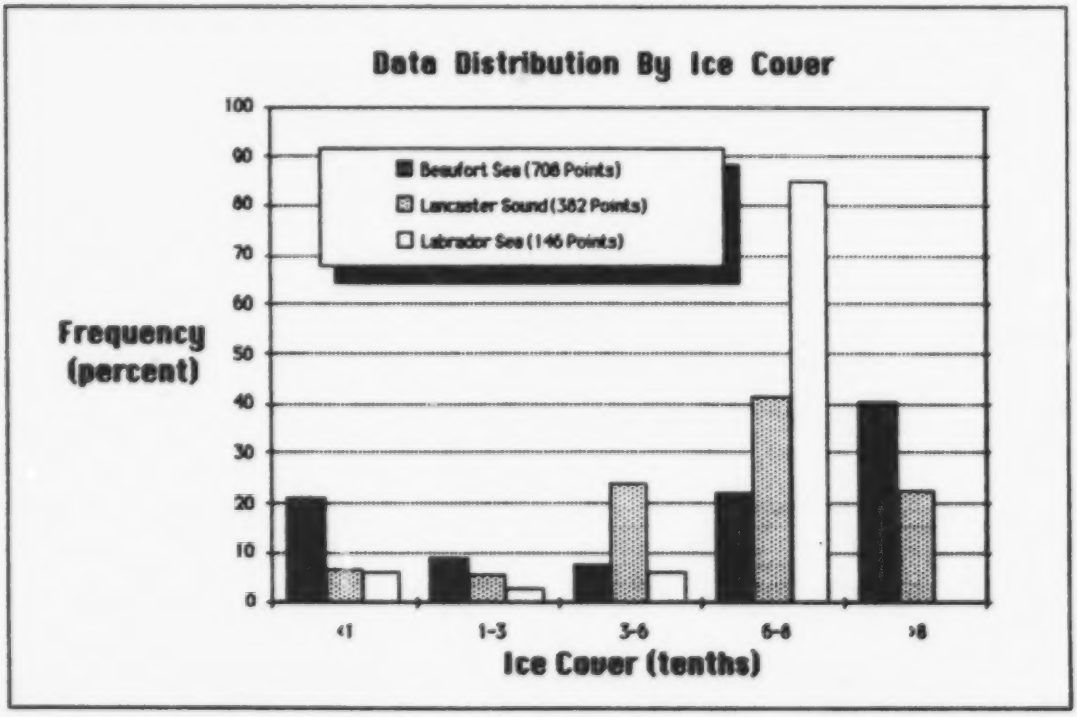

Figure 3.22 Distribution of Floe Data According to Ice Concentration

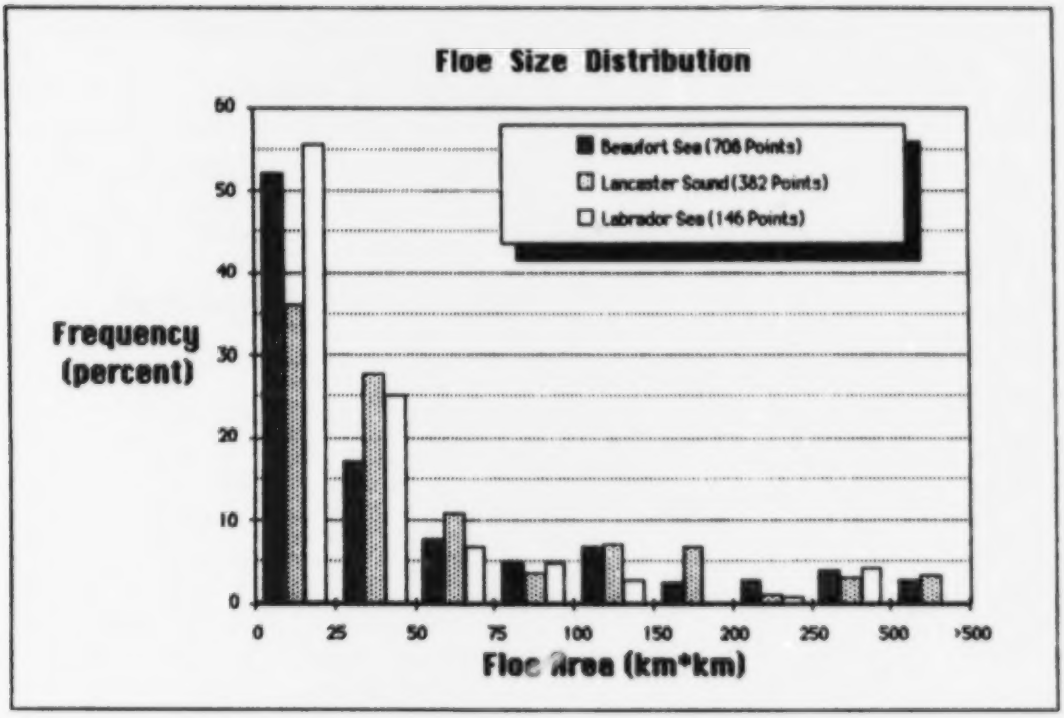

Figure 3.23 Distribution of Floe Data According to Floe Area

3.3.2 Floe Velocities

Floe velocity analysis is presented in seven groups of graphs listed as follows:

1. Frequency Distribution of Floe Speeds
2. Direction of Floe Movements
3. Relationship Between Average Ice Floe Speed and Ice Concentration
4. Relationship Between Average Ice Floe Speed and Floe Area
5. Comparisons Between Other Data Sources
6. Effect of Measurement Interval on Ice Velocity
7. Seasonal Variations in Ice Velocity

1. Floe Speed (Figure 3.24)

Labrador Sea data shows a significantly different ice speed distribution from the other two regions. (Detailed histograms for each region are included in Appendix C.) There is a slight shift towards higher speeds in Lancaster Sound than in the Beaufort Sea. Fewer than 38% of the floes measured in the Beaufort Sea moved at speeds greater than 10 km/d, compared to roughly 45% in Lancaster Sound and 75% off Labrador. The upper decile velocities ranged from about 20 km/d in the two arctic areas to 30 km/d in the Labrador Sea.

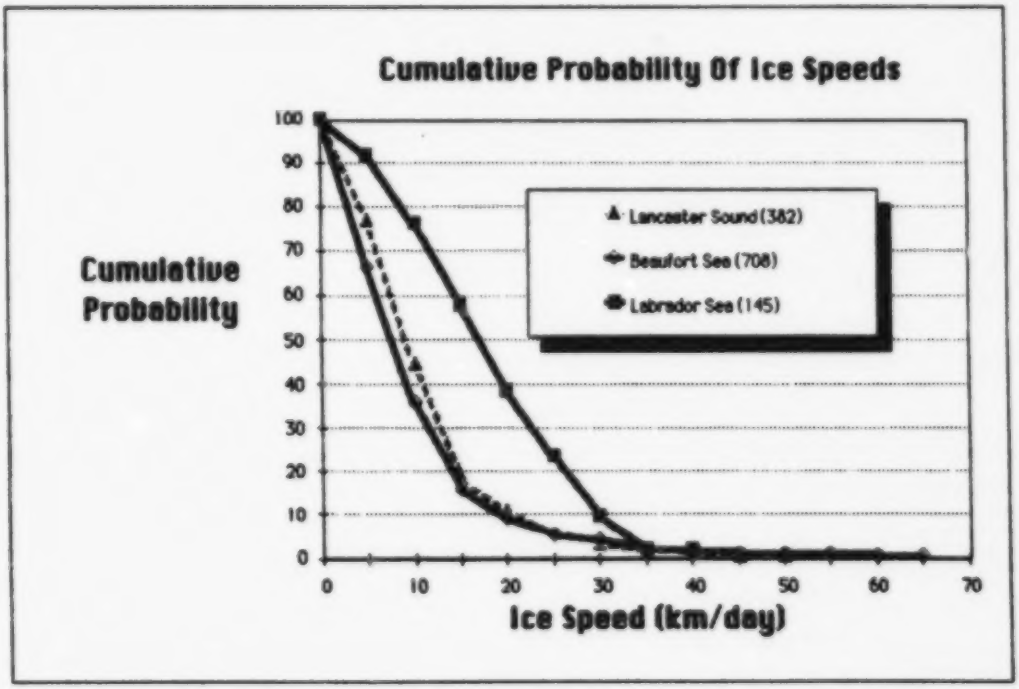

Figure 3.24 Geographic Differences in Floe Speed Distributions

2. Direction of Floe Movements (Figure 3.25)

Floe motions show a stronger trend to preferred directions in the two arctic areas than did lead orientations (Figure 3.14).

In the Beaufort Sea, floe movements tend to be towards the west in agreement with satellite buoy drift data. In Lancaster Sound, floes move predominantly from west to east into Baffin Bay. Labrador Sea floe movements are highly variable in direction, but tend in a southerly direction, or parallel to the coastline. Almost no northerly movements were recorded.

3. Ice Floe Speed vs Concentration

One reasonable hypothesis is that floe motions should decrease as pack ice concentration increases. Surrounding floes tend to oppose very rapid short term movements. Unfortunately only limited hourly or finer time scale measurements are available for comparison with satellite data.

The Landsat analysis in this study uses floe displacements over a 24 hour period. Figure 3.26 indicates that this period is too long to detect a statistically significant variation in floe speed with ice concentration. In spite of the limitations of the available data, both graphs show a trend to larger fluctuations in speed at lower ice concentrations, as well as a reduction of approximately 30% in average speed between 1/10 and 8/10 ice cover.

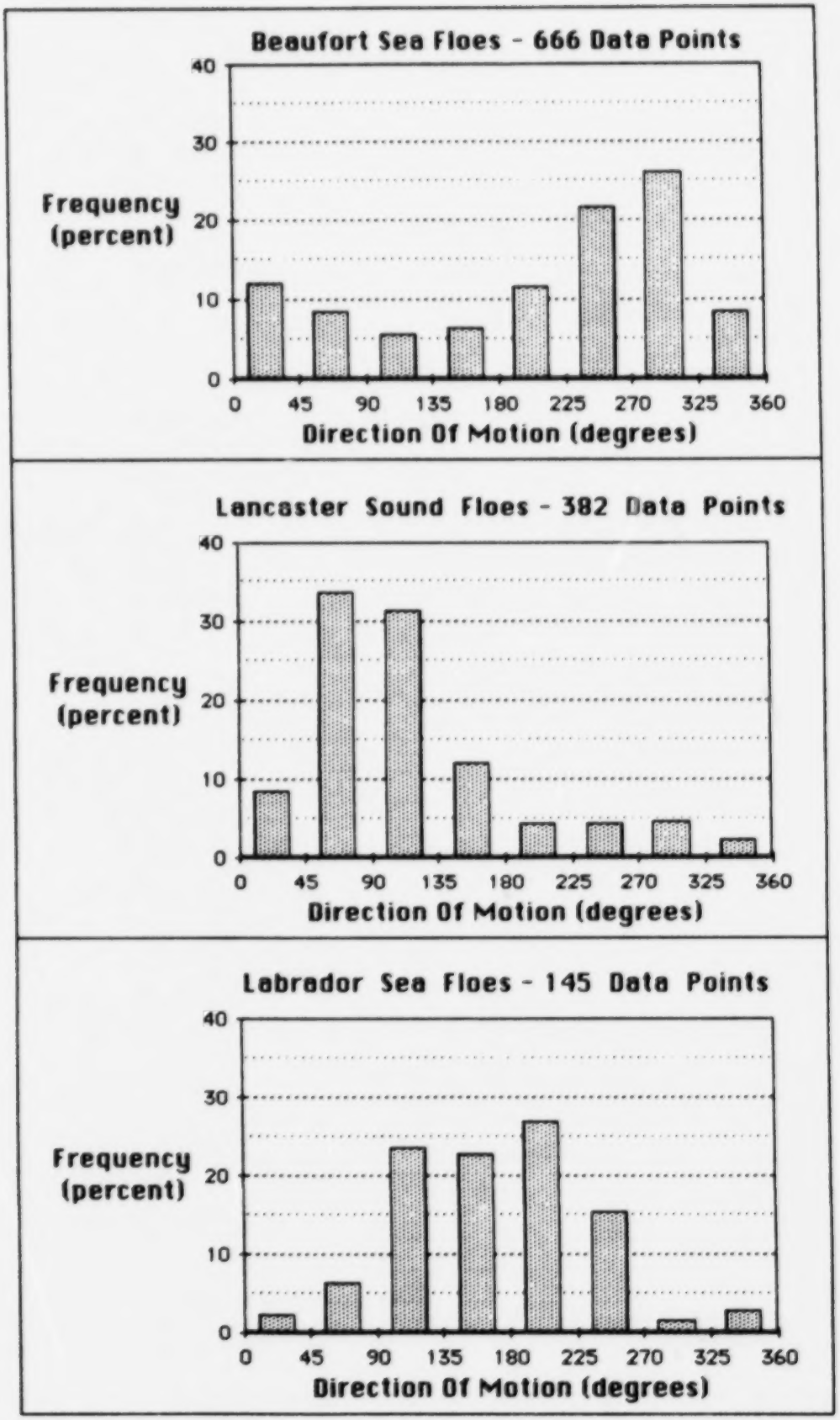

Figure 3.25 Direction of Floe Movements

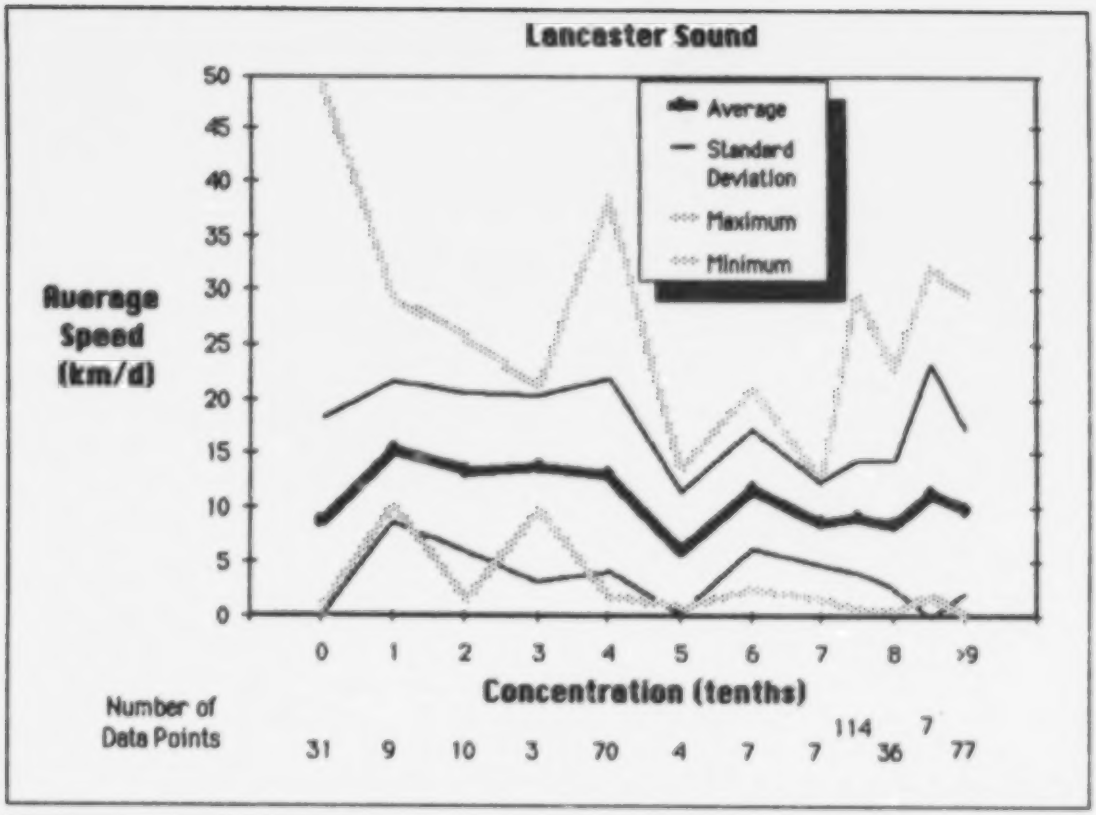

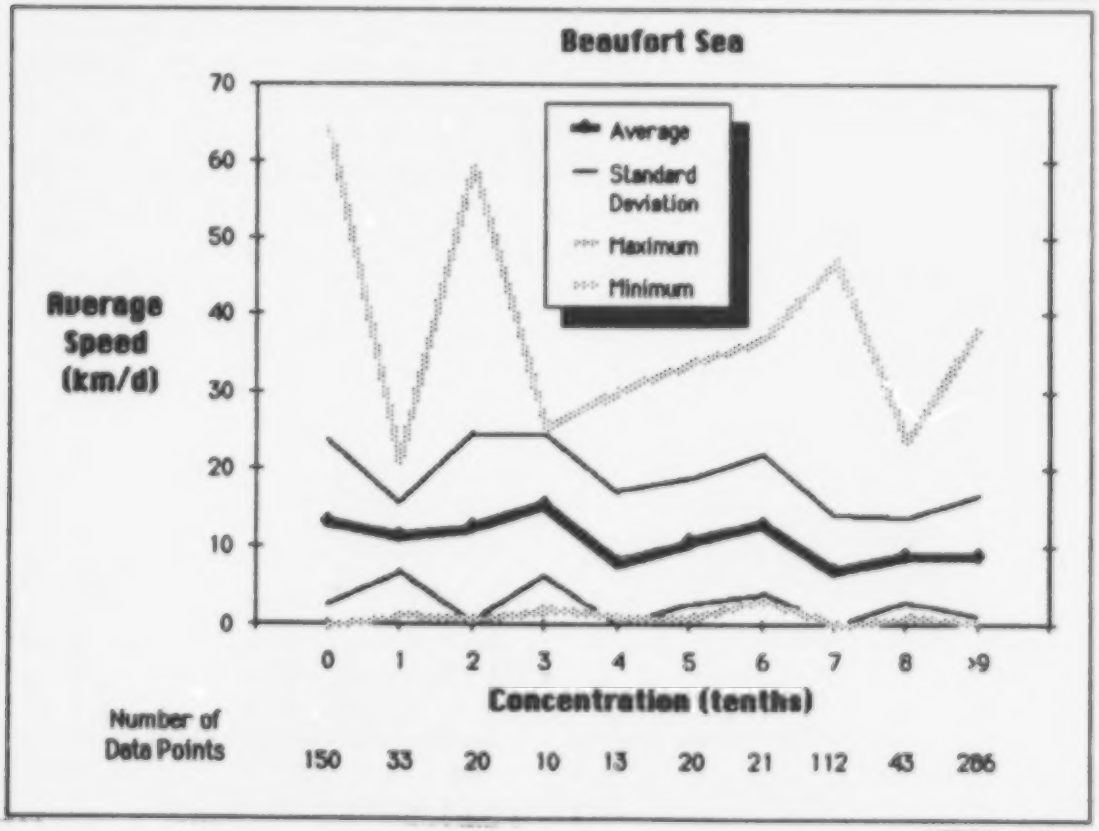

Figure 3.26 Variation in Ice Speed with Concentration

4. Variation in Floe Speed with Floe Size

Floe movements in an open pack situation (<7/10) are governed by wind and current stresses acting on an individual floe. The balance between hydrodynamic resistance and environmental driving forces will not necessarily be achieved at the same speed for all floe sizes. To test this hypothesis, the Beaufort Sea and Lancaster Sound data was sorted by floe area and speed. Figure 3.27 shows that there is no clear trend in daily motion with respect to floe area, for floes 0.01 km^2 to 500 km^2. Marginal ice zone research has shown a definite trend to clustering of different floe sizes near the open ocean boundary in response to an imbalance in short time period acceleration rates of different floe sizes.

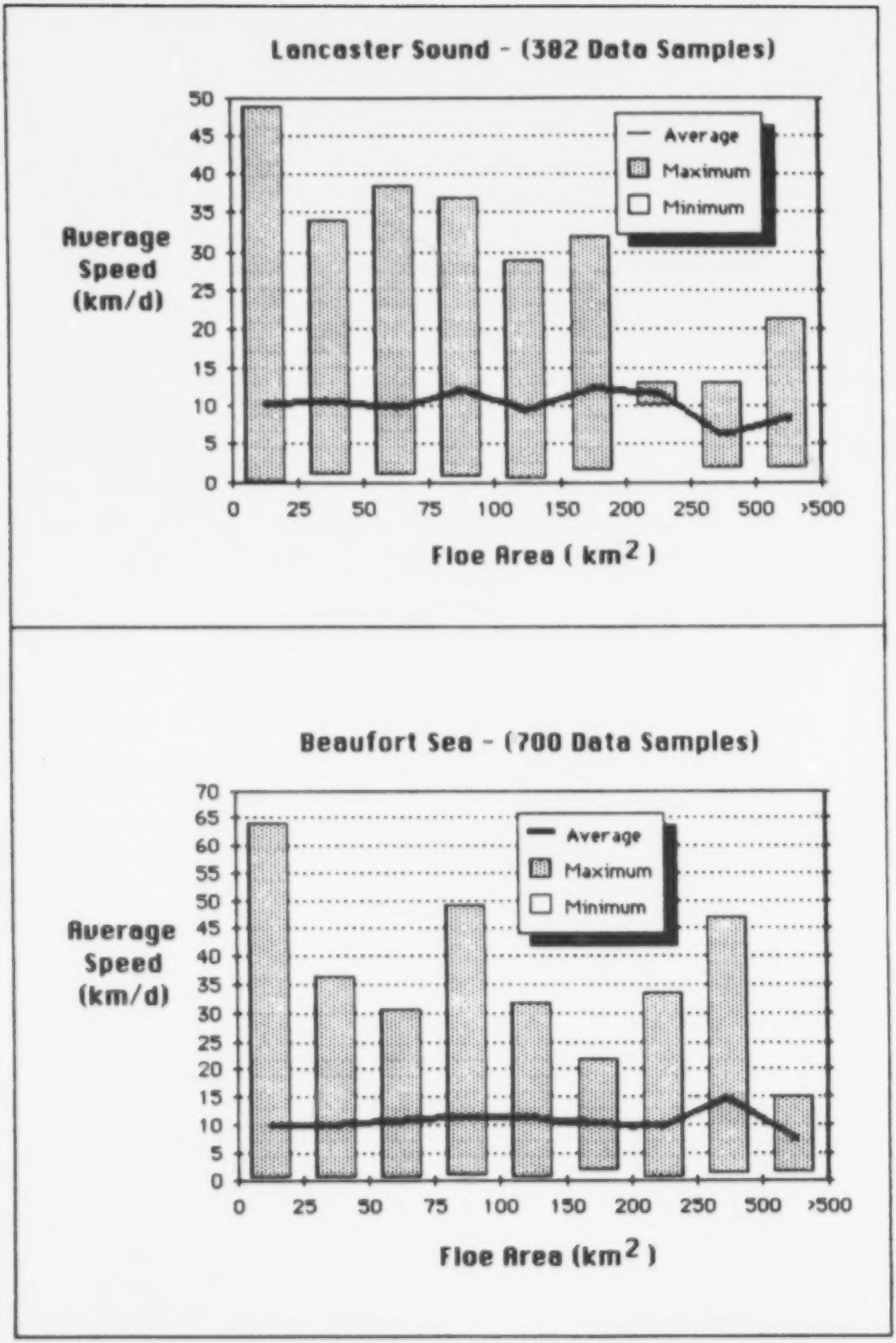

Figure 3.27 Variation in Ice Speed with Floe Area

5. Comparison with Other Data Sources

Figure 3.28 compares July data analyzed by Schwab (1978) and results from new analysis in this study. These two data groups are not significantly different. Therefore, the combination of the two data groups should not distort either data set.

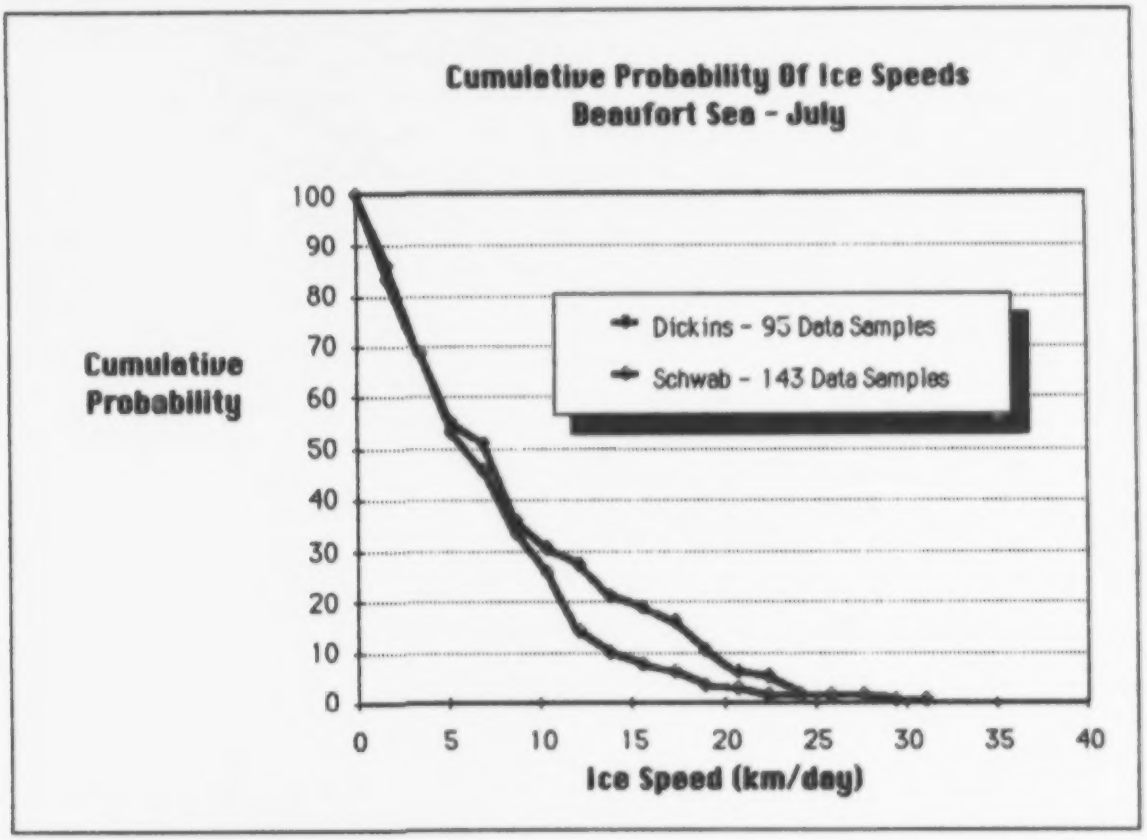

Figure 3.28 Cumulative Probability of Ice Speed - Comparison of Dickins et al. (1985) with Schwab (1978)

Figure 3.29 compares monthly average floe speeds reported by different authors for the Beaufort Sea and Lancaster Sound. Although these are large variations in individual measurements the overall trend of previous work agrees well with results of this study.

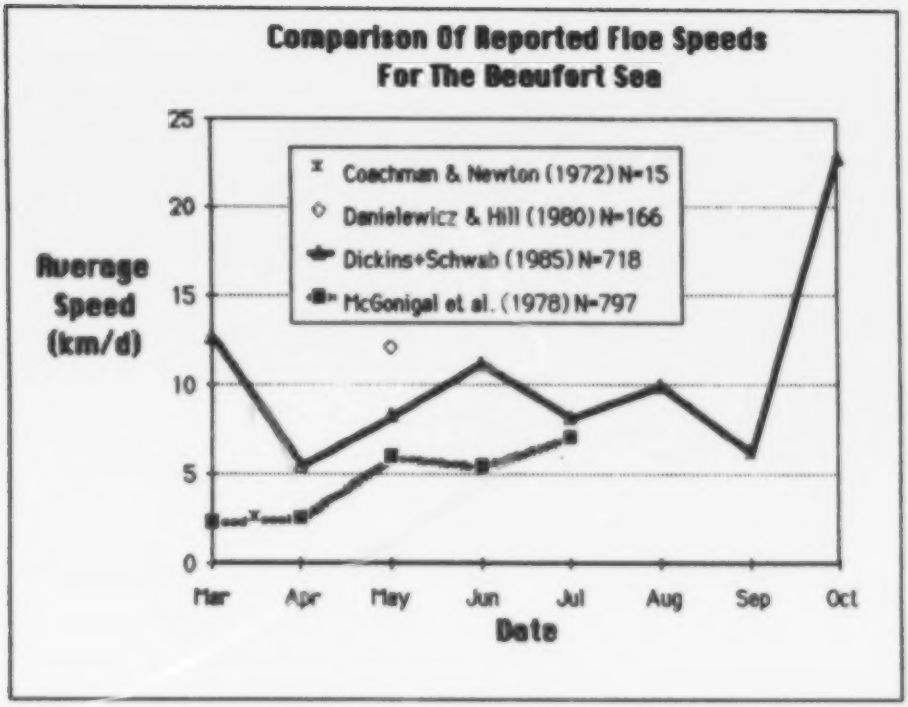

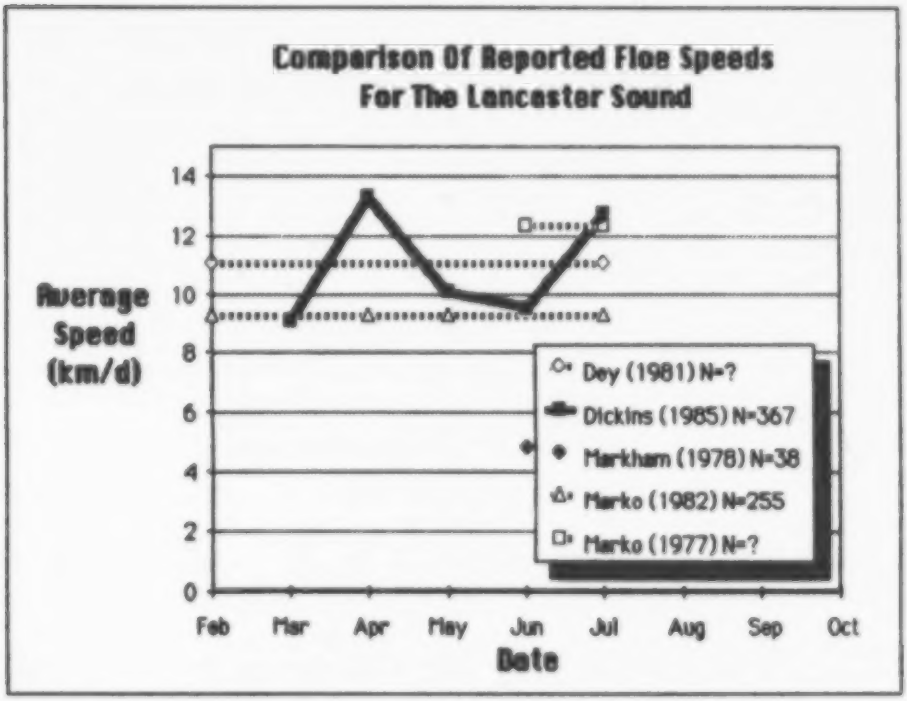

Figure 3.29 Comparison of Monthly Average Floe Speeds from Different Sources

Two other data sets are plotted in Figure 3.30: 12,548 measurements taken at hourly intervals during the summers of 1979 and 1980 by Dome Petroleum Limited in the Beaufort Sea (Marcellus and Morrison, 1982), and 171 hourly measurements taken off Labrador (LeDrew et al., 1977; FENCO, 1977).

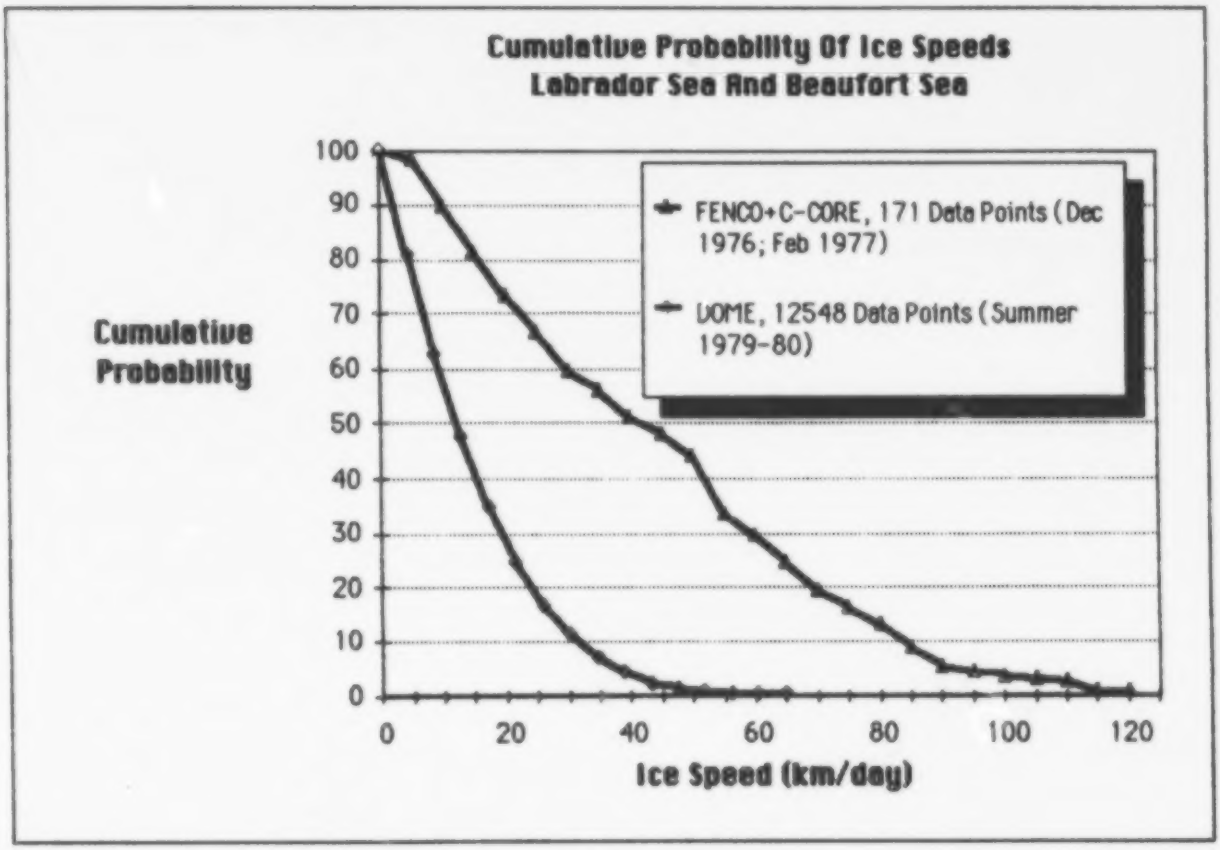

Figure 3.30 Comparison of Reported Ice Speed Distributions for the Beaufort and Labrador Seas

6. Effect of Time Interval on Ice Velocity Distributions

The majority of ice movement data published in previous reports and measured on satellite images in this study is based on a time interval of 24 hours. At shorter time intervals, extreme velocities are likely to be much higher than indicated by the daily average. In an effort to determine the quantitative effect of time interval on measured velocity, a short term data set was acquired for comparison with the 24 hour measurements.

Figure 3.31 shows the differences in summer floe speed distributions between hourly and daily records. The hourly values are up to 70% faster at a given probability level.

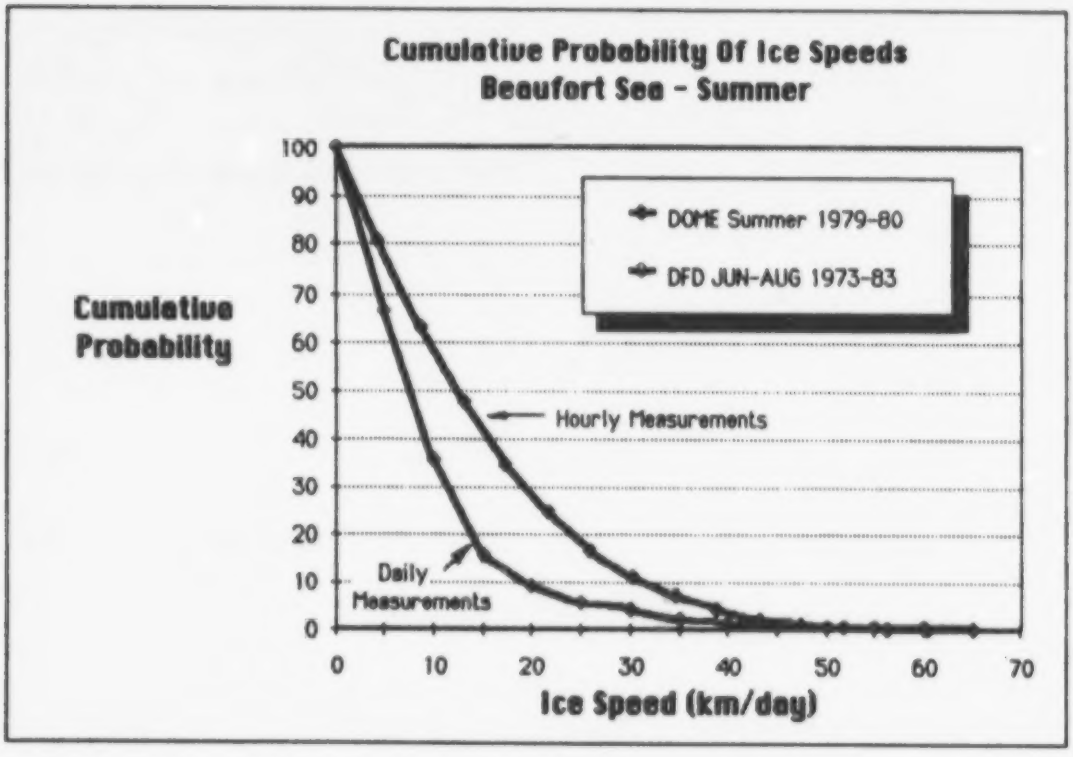

Figure 3.31 Comparison of Daily and Hourly Speed Distributions - Beaufort Sea Summer

Figure 3.32 shows that in the case of winter ice drift where individual floes are constrained by the surrounding pack ice, there appears to be no significant difference between short term case six hourly (Thorndike and Cheung, 1977) and daily (McGonigal and Wright, 1978/ 1979).

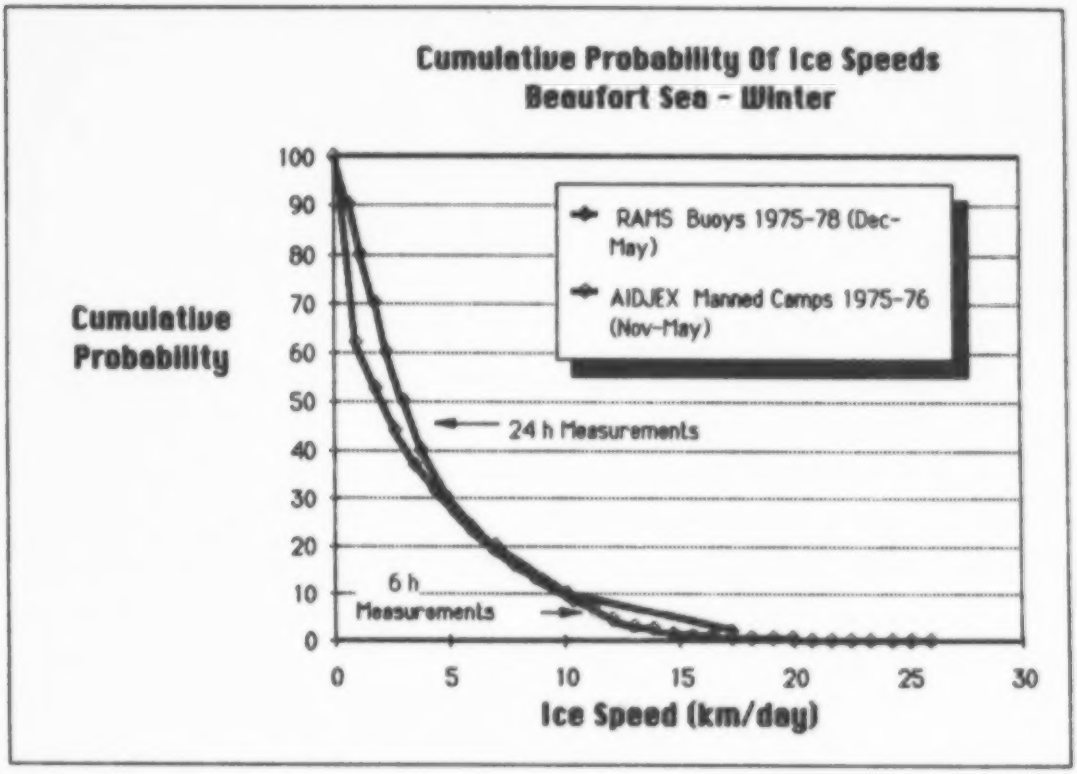

Figure 3.32 Comparison of Six Hourly and Daily Speed Distributions - Beaufort Sea Winter

On a still finer time scale, Figure 3.33 shows the results when the data from three individual floe trajectories is plotted on time scales of 15 minutes and 60 minutes (after Timokhov, 1970).

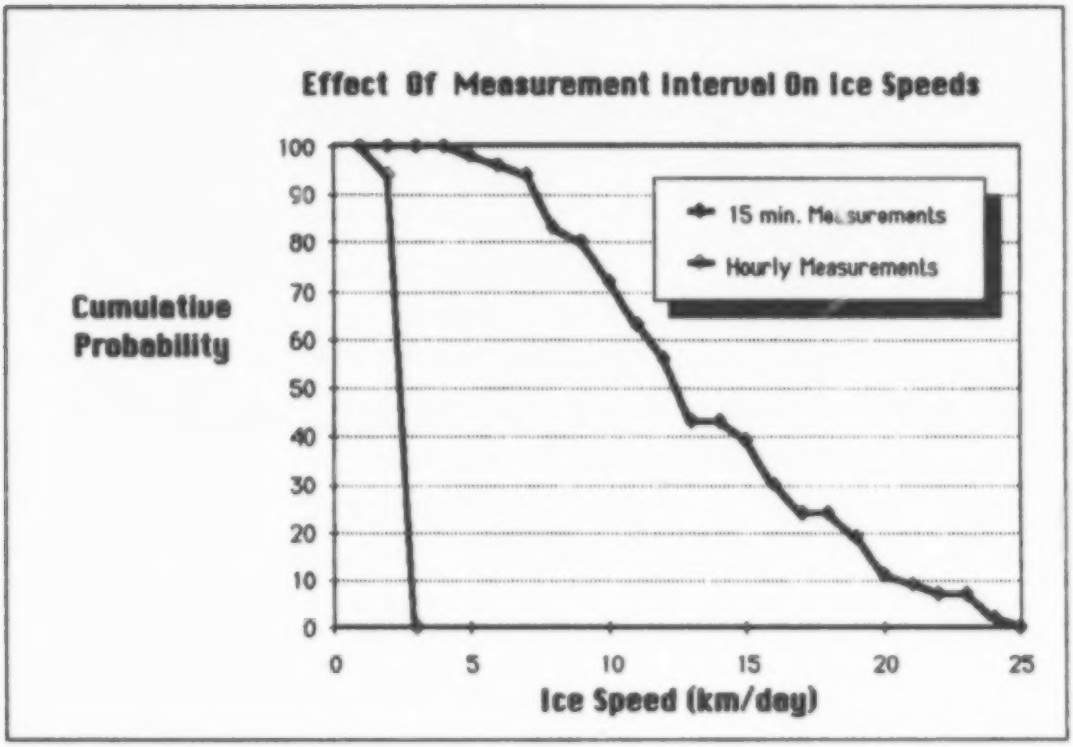

Figure 3.33 **Comparison of 15 Minute and 60 Minute Ice Movements (Three Individual Floes in Open Water)**

7. Seasonal Variability in Ice Velocity Distributions

AIDJEX data (Thorndike and Cheung, 1977) plotted in Figure 3.34 shows a large difference in ice speed distributions between summer and winter months in the polar pack (73 to 75°N). The same trend was not observed when comparing summer and winter data in more southerly areas of active oil exploration. This observation can be explained by considering that the polnyas and leads which are common throughout the winter in the so-called seasonal pack ice zone allow ice to move rapidly during both winter and summer.

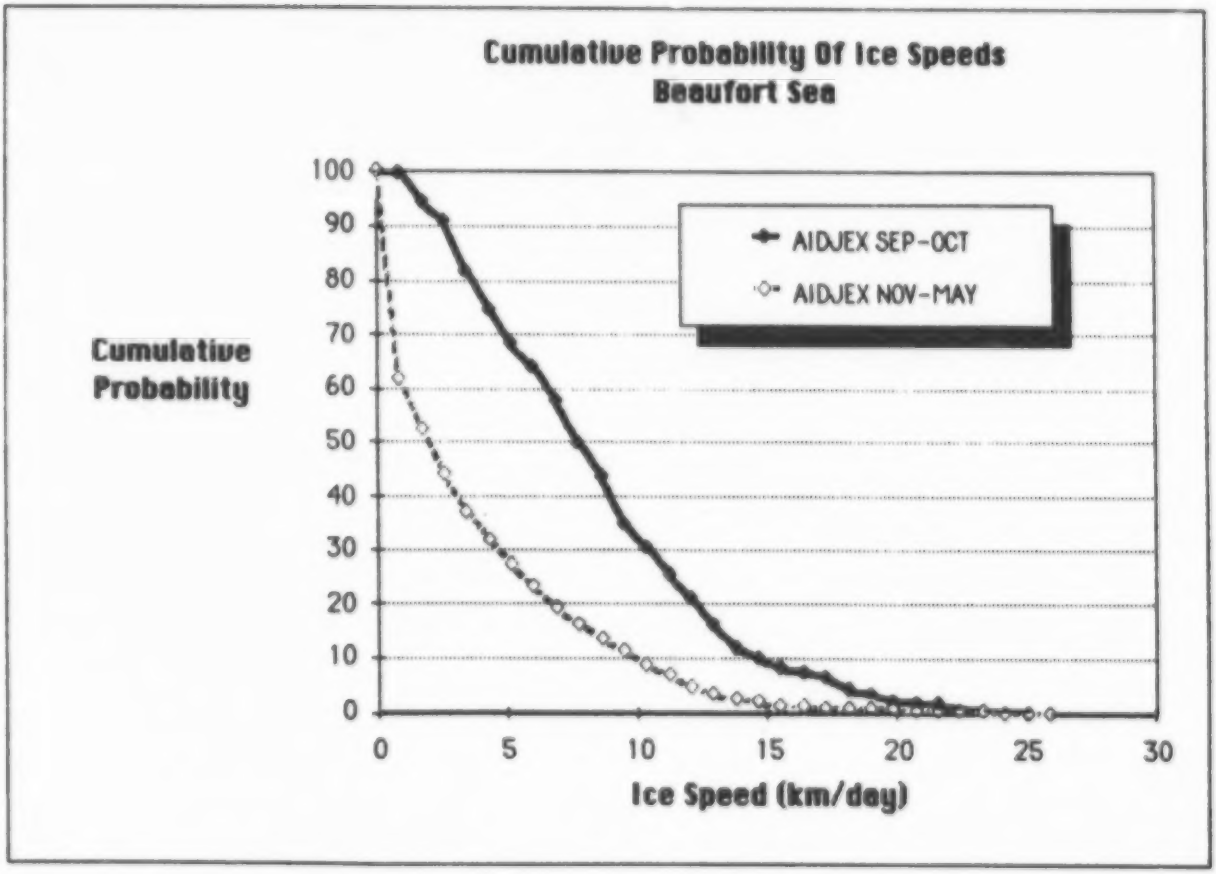

Figure 3.34 Comparison of Summer and Winter Ice Speeds in the Beaufort Sea

3.3.3 Ice Floe Size

Three floe size distributions were developed through the course of this study, one using 1:500,000 SLAR imagery in the Beaufort Sea for May (Figure 3.35), one using 1:20,000 aerial photography in the Labrador Sea in March, and one using a very small scale 1:2,600 aerial photo mosaic in the Labrador Sea on the same date. Figure 3.35 shows that half of the visible floes were less than about 2 km^2.

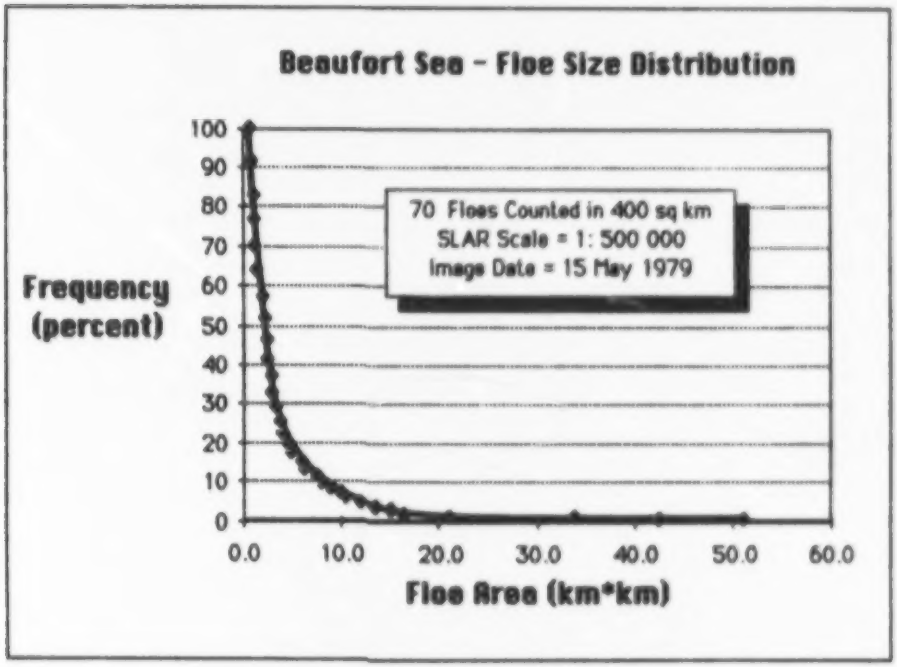

Figure 3.35 Beaufort Sea Floe Size Distribution from SLAR

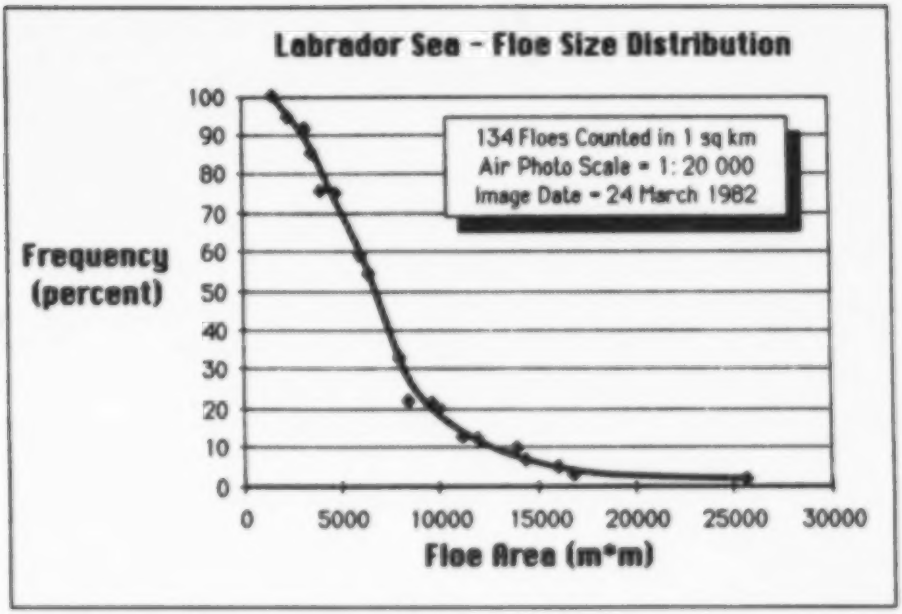

Figure 3.36 Labrador Sea Floe Size Distribution from 1:20,000 Scale Photography

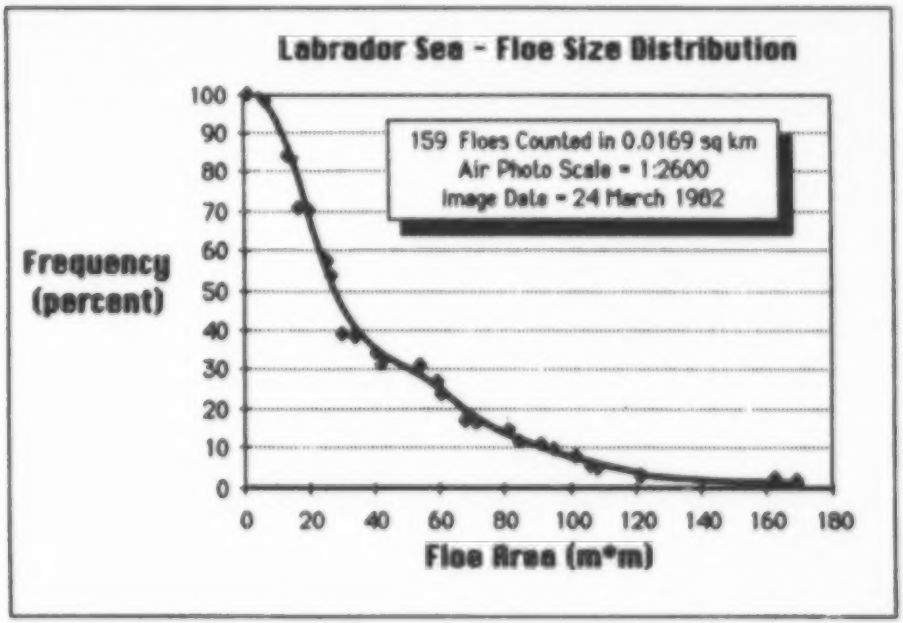

Figure 3.37 Labrador Sea Floe Size Distribution from 1:2,600 Scale Photography

Floe size distributions are highly dependent on the scale and resolution of the remote sensing imagery. This fact is clearly demonstrated by Figures 3.36 and 3.37. At a scale of 1:20,000 the median floe area is approximately 7,000 m^2. With a scale of 1:2,600 the median area becomes 30 m^2, which is of the same order as floe sizes recorded in surface surveys of the Labrador Sea ice pack (FENCO, 1977).

3.4 Ice Freeboard

The freeboard of ice is defined here as the height of the ice surface above sea level at the ice edge. For landfast ice, the freeboard can be accurately calculated from the total ice thickness, by assuming densities of seawater and ice. The main problem in using this approach offshore, is that there is a wide range of ice ages and ice roughness, which leads to significant variations in ice freeboard.

Leads tend to be sharply delineated features with level ice of approximately the same thickness on each side of the lead. The distribution of freeboards at lead edges is assumed to follow the distributions of ice ages. These distributions will shift to progressively thicker ice forms as the winter progresses. Actual measured distributions of level ice thickness offshore are almost non-existent. One data set is available for the Canadian Beaufort Sea using a bottom mounted sonar device recording ice drafts moving over a fixed point (Hoare et al, 1980). This data showed that average first year ice thickness offshore was about 40 cm less than the adjacent landfast ice along the Beaufort coast.

The only offshore measurements of ice thickness in Lancaster Sound were taken during the Manhattan tests in May 1970 (reported in Milnes and Smiley, 1978).

Descriptions of the Labrador Sea pack indicate that freeboard will not be related to level ice thickness. Floes are extremely irregular in cross section and commonly have a raised lip at the edge, as a result of the grinding action within the pack (Appendix D contains sample Labrador Sea floe cross-sections).

Monthly average freeboards, representative of lead edges, are tabulated for the Beaufort Sea based on offshore ice thickness reported by Hoare et al. (1980), and for Lancaster Sound based on theoretical maximum level ice growth as a function of residence time within the Sound.

Average level ice thicknesses for the offshore regions of Lancaster Sound, will be substantially less than for landfast nearshore ice. For example, first year ice at Resolute reaches an average thickness of 180 cm between October and June. Ice forming at the stable edge and drifting east into Baffin Bay will typically reside in the Sound for about one month. In the coldest part of the winter (December to February) this exposure would result in a maximum ice thickness of about 80 cm. Ridging and ice rubble will create areas of thicker ice and, at break-up, floes broken away from the fast ice can temporarily clog the Sound with much thicker level ice than normal for the winter period.

For the Labrador Sea, freeboards have been measured off individual ice floe profiles carried out by C-CORE and FENCO (Winsor and LeDrew, 1979; FENCO, 1977). Table 3.4 shows monthly freeboard estimates for the Beaufort Sea and Lancaster Sound, and values of Labrador Sea floe measurements made in December 1976 and February 1977.

Table 3.4 Representative Ice Freeboard

	Beaufort Sea		Lancaster Sound*1	Labrador Sea
	Avg	Max	Max	Measured Values
	cm		cm	
October	2	5	6	
November	3	5	9	
December	4	10	11	- Freeboard Min 0.2 m
January	8	13	12	Avg 0.9 m Max 2.3 m
February	11	17	11	
March	15	20	11	- 40 to 80 cm (19 floes)
April	18	21	9	
May	20	23	5	Freeboard Min 0.6 m Avg 1.4 m
June	20	-	24*2	Max 2.8 m
July	5-15	-	18*2	
August	-	-	-	
	from Hoare et al. (1980)			from Winsor and LeDrew, 1979; FENCO, 1977

*1 Based on assumed 10 km/day ice drift for 26 days Prince Leopold to Navy Board Inlet. Ice Growth from Resolute Bay records related to freezing degree day accumulations (monthly) after Milne and Smiley (1978).

*2 Reflects thicker first year floes breaking away from the fast ice edge (from Resolute June/July records - Richardson and Burns (1975)).

Note: Ice freeboard has been calculated as 0.126 x Ice Thickness based on Ice s.g. 0.9, Water s.g. 1.03

3.5 Wind Effects on Ice Dynamics

3.5.1 Modification of Measured Ice Speeds to Reflect Cloud Cover Wind Speed Bias

Ice movement statistics collected in this study depended almost entirely on Landsat imagery obtained in the visible spectrum on nearly cloudless days (maximum 15%). As described in 2.4.1 a correlation was requested from AES to ensure that our fair weather data accurately represented the complete distribution of wind speeds in all cloud covers.

Results shown in Figure 3.38 show that for the onshore stations analyzed, higher wind speeds are associated predominantly with increased cloud cover. Skies with cloud cover in excess of 20% (i.e. no Landsat imagery used) occur about 90% of occasions when winds exceed 60 km h^{-1} at all three stations.

This correlation indicates that random sampling of ice motions from Landsat imagery will be biased toward slower movement rates and will likely miss extreme motions associated with storm events. Table 3.5 compares the frequency of a given wind speed occurring in <20% cloud cover to the equivalent frequency for all cloud covers. Above 30 km h^{-1} there are significant differences in frequency, the fair weather case typically seeing less than half the strong wind events that actually occurred.

The average wind speed for all cloud covers is between 13% and 24% higher than the average wind speed associated with clear sky (<20% cover) conditions. Assuming that a similar correlation holds true for offshore areas, it is concluded that average ice speeds sampled from Landsat imagery in this and other studies are underestimated by about 20%.

Correcting for extreme ice movements associated with severe storm events is not possible given the uncertainties in the tails of the wind speed distributions and lack of direct cloud cover/speed correlations offshore.

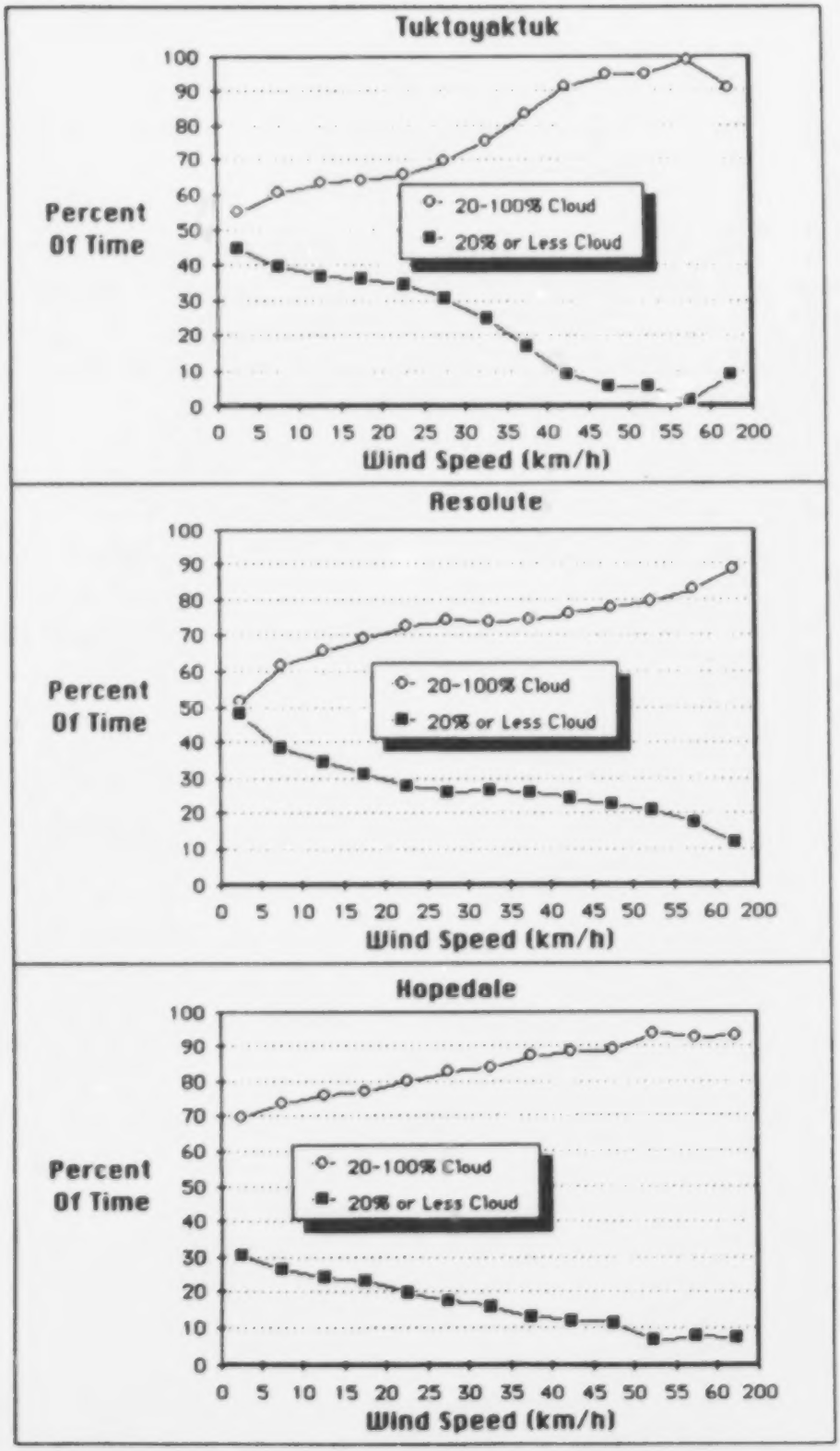

Figure 3.38 Correlation of Cloud Cover with Wind Speed

Table 3.5 Comparison of Relative Frequency of Wind Speeds in Cloud Cover <20% to all Cloud Covers

Wind Speed	Cloud Cover and Location					
	Resolute A		Hopedale		Tuktoyaktuk	
(km/h)	0-20%	0-100%	0-20%	0-100%	0-20%	0-100%
0- 5	21.71	14.39	15.23	10.58	11.52	8.94
5- 10	14.64	12.31	16.50	13.24	15.38	13.52
10- 15	14.66	13.71	14.29	12.58	24.08	22.76
15- 20	12.95	13.45	17.95	16.58	21.42	20.68
20- 25	9.29	10.79	10.13	10.76	12.93	13.23
25- 30	7.90	9.71	12.79	15.32	8.88	10.16
30- 35	7.08	8.51	7.44	9.86	3.82	5.39
35- 40	4.23	5.24	2.40	3.99	1.59	3.35
40- 45	3.15	4.14	1.42	2.57	0.21	0.86
45- 50	1.96	2.82	1.01	1.89	0.10	0.64
50- 55	1.14	1.78	0.24	0.74	0.04	0.24
55- 60	0.76	1.40	0.29	0.80	0.01	0.17
60-200	0.51	1.74	0.36	1.09	0.02	0.08
	100	100	100	100	100	100
Average x =	17.3	21.4	17.1	20.8	15.6	17.7
Standard s =	13.2	15.4	11.0	13.4	8.6	10.0
Deviation						
$(x_{100} - x_{20})/x_{20}$	24%		23%		13%	

3.5.2 Comparison of Average Winds and Ice Velocity

A rigorous correlation of floe velocity and wind velocity is not possible owing to the lack of coordination between ice and wind observations in time and space. Nevertheless, a trend is observed between the average regional speeds of wind and ice. No trend was found for directions.

Table 3.6 summarizes the average speeds. It can be seen that the average daily floe speeds amount to about 2 to 3% of the wind speeds. The ice to wind speed ratio in the last column of Table 3.6 has been adjusted by a 20% reduction of the wind

speed to reflect the bias of our Landsat sample towards slower winds (see previous Section 3.5.1).

The adjusted ratio obtained in this study compares well with estimates by others, ranging from 2 to 5% for ice to wind speed ratios. Markham (1976) reported a median ratio of about 2.5% for floe drifts in June-July 1973, in Amundsen Gulf and off Western Banks Island. His floe direction/wind direction correlation was not conclusive, but the data trend indicated between 20 and 30 degrees deflection to the right of the wind vector.

Table 3.6 Wind Speed/Ice Floe Speed Comparison

Region	Average Speed		V_i/V_w	Modified* V_i/V_w
	Ice Floe km/day	Wind km/h		V_w reduced 20%
Beaufort Sea	9.44 (A+B+BN)	25.7 (July only)	0.015	0.019
Lancaster Sound	9.48 (A+B+C)	28.3 (July only)	0.014	0.017
Labrador Coast	17.51 (A/D+A+B)	28.5 (April only)	0.026	0.032

*According to Section 3.5.1

3.6 Refreezing of Pack Ice Leads

The analysis of lead refreezing rates described in Section 2.5 has been applied to climatic data for four weather stations in the three areas. The results are presented in the following tables. Tables 3.7 to 3.9 include the data used to calculate the refreezing parameters. The data are from the "Canadian Climate Normals 1951-1981." Gaps in the tables are caused by data which results in ice melt rather than refreezing. During certain months, no lead refreezing would be expected.

Table 3.7 Beaufort Sea Climate

Tw = Water Temp (°C)

Ta = Air Temp (°C)

Wind Chill Units (m sec^{-1} °C)

Nicholson Peninsula

Month	Mild ΔT	Mean ΔT	Max ΔT	Wind Chill Mean	Wind Chill Max
January	23.9	27.5	30.9	137	455
February	25.2	29.2	31.4	144	410
March	21.4	24.9	29.0	123	443
April	12.4	16.2	20.0	81	306
May	0.5	4.1	7.5	29	121
June					
July					
August					
September					
October	4.0	6.3	8.7	39	164
November	14.8	18.1	21.3	100	391
December	20.7	24.1	27.7	109	485

ΔT = Tw - Tc

Tuktoyaktuk

Month	Mild ΔT	Mean ΔT	Max ΔT	Wind Chill Mean	Wind Chill Max
January	23.4	26.8	30.0	122	292
February	24.1	27.5	30.7	125	290
March	21.1	24.9	28.6	103	294
April	11.2	15.6	19.9	66	177
May	-0.7	3.1	6.8	16	66
June					
July					
August					
September					
October	3.4	6.1	8.6	31	93
November	14.6	18.1	21.6	87	210
December	20.5	23.6	26.9	113	239

ΔT = Tw = Tc

Table 3.8 Lancaster Area Climate

Resolute Airport

Month	Mild ΔT	Mean ΔT	Max ΔT	Wind Chill Mean	Wind Chill Max
January	26.8	30.5	34.1	182	824
February	28.0	31.6	35.2	174	909
March	26.2	29.8	33.4	152	779
April	17.6	21.5	25.4	118	706
May	6.1	9.3	12.5	49	274
June					
July					
August					
September	1.3	3.5	5.6	21	135
October	10.4	13.5	16.7	79	390
November	19.3	22.9	26.4	120	711
December	24.1	27.7	31.3	151	661

$\Delta T = Tw - Ta$

Table 3.9 Labrador Area Climate

Hopedale

Month	Mild ΔT	Mean ΔT	Max ΔT	Wind Chill Mean	Wind Chill Max
January	10.5	14.3	18.1	91	427
February	9.4	13.8	18.1	86	422
March	5.1	9.4	13.6	59	366
April		3.3	7.0	19	200
May			0.3		7
June					
July					
August					
September					
October					
November		1.8	4.4	12	104
December	6.3	9.7	13.1	67	444

$\Delta T = Tw - Ta$

Tables 3.10 to 3.12 include the calculated grease ice thicknesses, grease ice coverage times, and times to achieve 20 cm of new ice growth under still conditions. Again, gaps in the tables are caused by melting conditions.

Table 3.10 Beaufort Sea Lead Refreezing

Nicholson Peninsula

	With Wind Chill				Still Conditions		
	Grease Ice Thickness		Coverage Time		0.2 m Growth		
Month	Mean	Max	Mean	Max	Min ΔT	Mean ΔT	Max ΔT
	m	m	hr	hr	hr	hr	hr
January	0.3	0.9	48	63	29	26	23
February	0.3	0.8	45	60	28	24	22
March	0.3	0.9	51	66	33	28	24
April	0.3	0.9	70	86	56	43	35
May	0.4	1.0	175	154	1390	170	93
June							
July							
August							
September							
October	0.4	1.1	134	155	174	111	80
November	0.3	1.1	67	87	47	39	33
December	0.3	1.1	51	71	34	29	25

$\Delta T = Tw - Ta$

Tuktoyaktuk

	With Wind Chill				Still Conditions		
	Grease Ice Thickness		Coverage Time		0.2 m Growth		
Month	Mean	Max	Mean	Max	Min ΔT	Mean ΔT	Max ΔT
	m	m	hr	hr	hr	hr	hr
January	0.3	0.6	48	57	30	26	23
February	0.3	0.6	47	55	29	26	23
March	0.2	0.6	49	60	33	23	25
April	0.3	0.5	68	70	62	45	35
May	0.3	0.6	161	117		224	102
June							
July							
August							
September							
October	0.3	0.7	123	115	205	114	81
November	0.3	0.6	64	70	48	39	32
December	0.3	0.5	53	59	34	30	26

$\Delta T = Tw - Ta$

Table 3.11 Lancaster Sound Lead Refreezing

Resolute Airport

Month	With Wind Chill: Grease Ice Thickness Mean (m)	With Wind Chill: Grease Ice Thickness Max (m)	With Wind Chill: Coverage Time Mean (hr)	With Wind Chill: Coverage Time Max (hr)	Still Conditions: 0.2 m Growth Min ΔT (hr)	Still Conditions: 0.2 m Growth Mean ΔT (hr)	Still Conditions: 0.2 m Growth Max ΔT (hr)
January	0.4	1.5	45	64	26	23	21
February	0.3	1.6	43	63	25	22	20
March	0.3	1.4	45	64	27	24	21
April	0.3	1.7	59	83	40	33	28
May	0.3	1.3	100	133	114	75	56
June							
July							
August							
September	0.4	1.5	170	219	535	149	124
October	0.4	1.4	83	111	67	52	42
November	0.3	1.6	55	80	36	31	27
December	0.3	1.3	48	67	29	25	22

$\Delta T = Tw - Ta$

Table 3.12 Labrador Sea Refreezing Rates (Interstices Between Floes)

Hopedale

Month	With Wind Chill: Grease Ice Thickness Mean (m)	With Wind Chill: Grease Ice Thickness Max (m)	With Wind Chill: Coverage Time Mean (hr)	With Wind Chill: Coverage Time Max (hr)	Still Conditions: 0.2 m Growth Min ΔT (hr)	Still Conditions: 0.2 m Growth Mean ΔT (hr)	Still Conditions: 0.2 m Growth Max ΔT (hr)
January	0.4	1.4	82	105	66	49	39
February	0.4	1.4	84	105	74	51	39
March	0.4	1.6	107	134	136	74	51
April	0.3	1.7	210	211		212	100
May		1.5		401			
June							
July							
August							
September							
October							
November	0.4	1.4	222	241		386	158
December	0.4	2.0	197	147	110	72	53

$\Delta T = Tw - Ta$

It is clear from the tables, that predicted coverage times for leads in winter months are relatively constant, and that the differences which would be observed are predicted to be primarily differences in thickness. For the grease ice coverage times, the common result is that the severe environmental conditions extend the coverage time. This is due to the increase in expected ice thickness. As the climate warms, as seen by comparing spring months to winter months, or by comparing the Lancaster area to the Labrador area, refreezing times become larger.

When the results of calculations using the equations used in this analysis are compared to the results of other workers, they are consistent. The calculated heat fluxes and ice production rates correspond to Bauer and Martin (1983), to Andreas et al. (1979), to Schaas and Galt (1972), and to den Hartog et al. (1983).

Three problems are associated with the grease ice coverage determinations.

First, the thickness of the ice cover is only crudely estimated. No experimental or field data were found to give a better estimate than the equation used. Field data is critical in determining coverage times, as an underestimate will also underestimate coverage times.

Second, the coverage time is independent of lead size, because in the integration, all lead dimensions cancel except for ice thickness. This mathematical result is limited to fairly large leads. A comparison of the results of the present analysis to the analysis of Bauer and Martin (1983), shows good correlation down to leads with 50 m width. However, leads smaller than this will probably not have the mature wind and wave conditions of the larger lead, and may be expected to behave more like leads subject to still conditions.

Third, the transition from grease ice to consolidated ice is not well defined. After piling up at the lee edge of the lead, the grease ice has been shown to form a dense dead zone, where it behaves as a

solid. It is likely that in the time taken for the lead to cover, most of this ice will consolidate to solid ice. This assumption is not documented.

The still condition ice growth calculations are standard, and compare well with other research (e.g. Burns, 1975).

4.0 CONCLUSIONS AND RECOMMENDATIONS

Leads are a much more common pack ice characteristic than individual floes in the Beaufort Sea and Lancaster Sound. When ice concentrations are between 4 and 8/10, as in spring break-up, floe motions will control the behaviour of oil spills. In these regions, break-up lasts less than six weeks in a typical ice year. However, the Labrador Sea is an environment where individual floe interactions will be the major factor controlling oil spill behaviour and fate, rather than lead dynamics. An ESRF study in progress will provide new information on oil behaviour in a broken ice environment (S.L. Ross/D.F. Dickins - in preparation).

Where leads are common, they appear to be expanding more often than contracting. Based on 24 hour ice displacement records, this trend to a diverging ice cover would indicate that lead pumping will not be an important factor affecting oil spill distribution within a pack ice environment in the Beaufort Sea or Lancaster Sound. This preliminary conclusion requires verification using more short term ice movement records.

Leads closing in a Beaufort Sea pack ice environment invariably lead to the formation of pressure ridges. These ridges are composed of deformed ice from crushing of the lead edges, as well as broken fragments from any new ice which formed in the lead while it was open. Any oil which may be pumped up onto the lead edges will be incorporated in the complex block structure of the ridge. Lead pumping effects will then become secondary to the more significant matter of oil incorporation within a deformed ice field.

Satellite remote sensing imagery is not satisfactory to derive actual distributions of lead width. Although relative displacements of large leads can be measured accurately, the numerous small leads less than 100 m wide are not detected.

Based on this study's results the following recommendations are made:

1. That future Beaufort Sea floe movement analysis concentrate on the spring break-up period where high quality industry SAR imagery is

available on a daily basis along the entire coast. The break-up period is critical for oil spill behaviour. Oil still incorporated in landfast ice can be rapidly carried offshore in vast floes, and then dispersed over a wide area as these floes break down.

2. That lead pumping be discounted as a significant factor in altering the overall distribution of a large oil spill under moving pack ice. Lead pumping may still be an important factor in governing the behaviour and fate of a surface batch spill in a lead or ship track.

3. That consideration be given to conducting a study of pack ice dynamics in a other offshore areas not covered by this study, e.g. Baffin Bay, Gulf of St. Lawrence.

4. That consideration be given to designing a field project to measure small scale lead and floe dynamics within the interior of a pack ice field.

5. That research be conducted to determine whether there is a critical measurement time interval below which ice speed distributions are constant. A useful outcome of such an investigation would be to identify convenient factors which would allow conversion of daily ice speeds into distributions at shorter time scales of more interest to oil spill modelling.

6. That the results of this study be used as a basis to predict the behaviour and fate of oil spilled in pack ice in different offshore areas. Such predictions should be associated with specific release scenarios, e.g. pipeline, vessel damage and blowout.

ACKNOWLEDGEMENTS

The success of this study depended to a large part on gaining access to a variety of remote sensing data sources. The authors wish to express their appreciation for the time and effort expended by a number of individuals who provided assistance with data acquisition, particularly:

- John Miller of Petro Canada
- Chris Hill of Dome Petroleum
- Bob Frederking of NRC
- Fred Geddes of the Atmospheric Environment Service
- Doug Bradford of Fisheries and Oceans
- Lynn Arsenault of Cold Region Remote Sensing

Many painstaking measurements of pack ice characteristics were carried out by Ingrid Bjerkelund, Peter Bein, and Michael Cassidy. Sections on correlation of ice movements and wind statistics were prepared by Peter Bein. Material on refreezing the pack ice leads was developed by Blair Humphrey.

The authors appreciate the cooperation of Gulf Canada Corporation in releasing data on floe movements by Don Schwab.

REFERENCES AND BIBLIOGRAPHY

Agerton, D.J. and J.R. Kreider. 1979. Correlation of Storms and Major Ice Movements in the Nearshore Alaskan Beaufort Sea. in Proceedings POAC 1979, Trondheim.

Andreas, E.E., C.A. Paulson, R.M. Williams, R.W. Lindsay and J.A. Businger. 1979. Boundary Layer Meteorology 17:57-91.

Atmospheric Environment Service. 1979, 1980. Beaufort Weather and Ice Office Annual Reports, Edmonton.

Atmospheric Environment Service. 1982. Canadian Climate Normals 1951-1980. Volume 1: Radiation. Volume 2: Temperature. Volume 4: Degree Days. Volume 5: Winds. Environment Canada, Ottawa.

Bauer, J. and S. Martin. 1983. J. Geophys. Res. 88:2917-2925.

Buckley, J.R., T. Gammelsrod, J.A. Johannessen, O.M. Johannessen and L.P. Roed. 1979. Science 203:165-167.

Burns, B.M. 1974. The Climate of the Mackenzie Valley-Beaufort Sea. Volume II. Environment Canada, Ottawa.

Coachman, L.K. and J.L. Newton. February 1972. Water and Ice Motion in the Beaufort Sea, Spring 1970. AIDJEX Bulletin No. 12, pp. 61-77.

Convey, A.D. 1972. Engineering Memorandum 1972 Grand Banks Aerial Reconnaissance. Amoco Canada Petroleum Co., Calgary, Alberta. Project #59-EC-40-72-9.

Croasdale, K.R. and L.G. Spedding. 1972. Landfast Ice Movement - Mackenzie Delta 1972. Imperial Oil Ltd., Production Research and Technology Service Laboratory Report. APOA-33-1, IPRT-5ME-72.

Culshaw, S.T. and B.R. LeDrew. 1977. Labrador Sea Ship in the Ice - A Pilot Study. In the Proceedings of the Port and Ocean Engineering for the Arctic Conference. St. John's, Vol. II, pp. 1122-1131.

Danielewicz, B.W. and G.R. Pilkington. 1981. Selected Environmental Characteristics of Beaufort Sea Ice. Dome/Canmar Technical Report, Calgary.

den Hartog, G., S.D. Smith, R.J. Anderson, D.R. Topham and R.G. Perkin. 1983. J. Geophys. Res. 88:2911-2916.

Denner, W.W. and T.E. Keliner. 1981. Numerical Modelling Labrador Pack Ice Dynamics. In Proceedings of the Port and Ocean Engineering in the Arctic Conference, Quebec, Vol. III, pp. 1330-1347.

Dey, B. April 20, 1981. Monitoring Winter Sea Ice Dynamics in the Canadian Arctic with NOAA-TIR Images. J. Geophysical Research, Vol. 86, No. C4, pp. 3223-3235.

Dickins, D.F. et al. 1985. Statistical Description of Pack Ice in the Beaufort Sea, Lancaster Sound and the Labrador Sea. Unpublished report by Environment Canada (E62) used as basis for current study, Ottawa.

Dunbar, M.J. 1981. Polynyas in the Canadian Arctic. Occasional Papers 45. Canadian Wildlife Service. Environment Canada. pp. 29-44.

FENCO. December 1976. Davis Strait Ice and Oceanographic Investigation Winter (76/77) for Imperial Oil Ltd. APOA 128-1, Calgary.

Foster, T.D. 1972. J. Phys. Ocean. 2:462-469.

Frederking, R., M. Sayed, E. Wessels, A.J. Child and D. Bradford. 1984. Ice Interaction with Adams Island, Winter 1982-1983. IAHR Ice Symposium, Hamburg.

Hall, R.T. 1977. AIDJEX Modelling Group Studies Involving the Use of Remote Sensing Data. In preprints, Symposium on Sea Ice Processes and Models, Seattle.

Hartwell, A.D. May, 1972. Airphoto Analysis of Ice Deformation in the Beaufort Sea. AIDJEX Bulletin No. 13, pp. 1-34.

Hibler, W.D., W.F. Weeks, S. Ackley, A. Kovacs and W.J. Campbell. May, 1972. Mesoscale Strain Measurements on the Beaufort Sea Pack Ice (AIDJEX 1971). AIDJEX Bulletin No. 13, pp. 35-76.

Hibler, W.D., III, W.B. Tucker and W.F. Weeks. March 1976. Techniques for Using Landsat Imagery without Land References to Study Sea Ice Drift and Deformation. AIDJEX Bulletin No. 31, pp. 115-136.

Hoare, R.D.; B.W. Danielewicz; G.R. Pilkington and J.C. O'Rourke. January 1980. Seasonal Pack Ice Characteristics in the Shear Zone of the Beaufort Sea Based on Data From an Upward Looking Sonic Profiler (1978-1979) APOA 147.

Kozo, T.L. 1983. J. Geophys. Res. 88:2926-2934.

Kupetski, V.N. 1962. Gos i Oceanogr. Inst. Moskva 70:47-60. Quoted in Dunbar, 1981.

Lachapelle, A. 1981. Wind and Waves - Lancaster Sound. In Proceedings of the Port and Ocean Engineering in the Arctic Conference. Quebec, Canada, Vol. II, pp. 830-842.

LeDrew, B.R. and K.A. Gustajtis. November 1979. Oil Spill Scenario for the Labrador Sea. C-CORE EPS 3-EC-79-4.

Marcellus, R.W. and T.B. Morrison. 1982. Ice Design Statistics for the Canadian Beaufort Sea. Canada Marine Engineering Limited, Calgary.

Markham, W.E. October 1978. Ice Climatology of the Beaufort Sea. Technical Report No. 26. Reprinted.

Markham, W.E. 1980. Ice Atlas, Eastern Canadian Seaboard. Environment Canada. AES, Toronto.

Marko, J.R. September 1976. Satellite Observations of the Beaufort Sea Ice Cover. Technical Report No. 34. Reprinted.

Marko, J.R. July 1977. A Satellite-Based Study of Sea Ice Dynamics in the Central Canadian Arctic Archipelago. Institute of Ocean Sciences, 205-C-77-4.

Marko, J.R. 1982. The Ice Environment of Eastern Lancaster Sound and Northern Baffin Bay. Environmental Studies No. 26. Indian and Northern Affairs Canada, Ottawa.

Marko, J.R. and R.E. Thomson. February 20, 1977. Rectilinear Leads and Internal Motions in the Ice Pack of the Western Arctic Ocean. J. Geophysical Research, Vol. 82, No. 6. 468.

Marko, J.R. and S. Bannerman. July 1982. Comparison of Observed and Simulated Ice Floe Drift and Relevence to Oil Spill Modeling Accuracy. Arctic Sciences Limited for Institute of Ocean Sciences, Sidney.

Martin, S. and P. Kauffman. 1981. J. of Glaciology 27:283-313.

McGonigal, D. and B.D. Wright. 1978 and 1979. Beaufort Sea Ice Movement. RAMS Buoy Data Analysis. Vol. I and II, Gulf Canada Ltd., Frontier Research Division, Calgary.

Milne, A.R. and B.D. Smiley. February 1978. Offshore Drilling in Lancaster Sound. Possible Environmental Hazards. Institute of Ocean Sciences, Sidney.

MIZ Bulletin Series. 1984-Current. Issued by CRREL, Hanover, N.H. (Hibler, W.E. and P. Wadhams, Editors).

Murphy, D.L., I.M. Lissauer and J.C. Myers. 1983. Movement of Satellite Tracked Buoys in the Beaufort Sea. USCG Avery Point, Groton, Conn.

Murphy, D.L., P.A. Tebeau and I.M. Lissauer. 1981. Long-Term Movement of Satellite-Tracked Buoys in the Beaufort Sea - An Interim Report. USCG Avery Point, Groton, Conn.

NORCOR. August 1977. Probable Behaviour and Fate of a Winter Oil Spill in the Beaufort Sea. Environmental Protection Service. EPS-4-EC-77-5.

Pritchard, R.S., M.D. Coon, M.G. McPhee and E. Leavitt. September 1977. Winter Ice Dynamics in the Nearshore Beaufort Sea. AIDJEX Bulletin No. 37, pp. 37-94.

Richardson, F.A. and B.M. Burns. 1975. Ice Thickness Climatology for Canadian Stations. Atmospheric Environment Service, Toronto.

Robe, R.Q., I.M. Lissauer and J.C. Myers. 1983. Beaufort Sea Drifting Buoys, USCG, Groton, Conn.

Rothrock, D.A. 1979. Modeling Sea-Ice Features and Processes. J. Glaciology, Vol. 24, No. 90.

Schaas, R.H. and J.A. Galt. 1973. Arctic 26:208-221.

Seasat SAR Data Over Canada. Coverage and Sources. May 1982. The Radarsat Project Office, Ottawa.

Smith, S.D., R.J. Anderson, G. den Hertog, D.R. Topham and R.G. Perkin. 1983. J. Geophys. Res. 88:2900-2910.

Sowden. 1980. Selected Physical Characteristics - Background Report 1 - Lancaster Sound Regional Study. Indian and Northern Affairs Canada. Ottawa.

Spedding, L.G., P. McLellan and C. Soares. 1978. Summer Ice Floe Size and Distribution in the Southern Beaufort Sea. Imperial Oil Ltd., Calgary.

Spedding, L.G. 1973-77. Landfast Ice Movement - Mackenzie Delta 1972-77. Imperial Oil Ltd., Reports APOA-51-1, 67-1, 83-1, 105-4, Calgary.

Spedding, L.G. 1983. A Large Landfast Ice Movement. in Proceedings POAC 83, Helsinki.

Thorndike, A.S. and J.Y. Cheung. 1977. AIDJEX Measurements of Sea Ice Motion 11 April 1975 to 14 May 1976. AIDJEX Bulletin No. 35.

Timokhov, L.A. 1970. Dynamics of the Ice Cover and Changes in its Compactness. AIDJEX Bulletin 3.

Topham, D.R., R.G. Perkin, S.D. Smith and R.J. Anderson. 1983. J. Geophys. Res. 88:2888-2899.

Wadhams, P. 1975. Sea Ice Morphology in the Beaufort Sea. Beaufort Sea Project Technical Report No. 36, Institute of Ocean Sciences, Sidney, B.C.

Wadhams, P. 1979. Field Experiments on Wave-Ice Interaction in the Labrador and East Greenland Currents, Polar Record, Vol. 19, No. 121.

Wadhams, P. 1980. Ice Characteristics in the Seasonal Ice Zone. Cold Regions Science & Technology Vol. 2.

Wadhams, P. 1984. Arctic Sea Ice Morphology and its Measurement. Arctic Technology and Policy Proceedings of the Second Annual MIT Sea Grant College Program and Lecture Seminar. Eds: I. Dyer and C. Chryssostomidis.

Wadhams, P. and R.J. Horne. 1980. An Analysis of Ice Profiles Obtained by Submarine Sonar in the Beaufort Sea. J. Glaciology Vol. 25, pp. 401-424. GG-14.

Welch, J.P., I.M. Lissauer, G.L. Hufford, T.S. Ellis, B.D. Thompson, L.D. Farmer and R.R. Hiltabrand. 1977. Some Dynamics of Spilled Oil in a Fractured Ice Field in Buzzards Bay, Massachusetts. J. Ocean Engineering, Vol. 4, pp. 197-203.

Winsor, D.W. and B.R. LeDrew. November 1979. Ice Features Characterization - Labrador Offshore. Oil Spill Scenario for the Labrador Sea. Environmental Protection Service EPS 3-EC-79-4.

APPENDIX A

LISTING OF REMOTE SENSING DATA

SLAR IMAGERY USED IN STUDY

Lancaster Sound				Beaufort Sea			
Day	Month	Year	I.D. Number	Day	Month	Year	I.D. Number
21	July	78	NDZ 079	14	May	79	252
22	July	78	080	15	May	79	253
24	Aug	78	107	16	June	81	Dome/Canmar
27	Aug	78	110	17	June	81	Dome/Canmar
28	Aug	78	111	30	June	81	Dome/Canmar
02	Sept	78	115	01	July	81	Dome/Canmar
02	Sept	78	116	14	June	83	Dome/Canmar
26	Aug	79	290	15	June	83	Dome/Canmar
28	Aug	79	291	10	May	84	Dome/Canmar
29	Aug	79	292	11	May	84	Dome/Canmar
31	Aug	79	296				
02	Sept	79	297				
02	July	80	456				
03	July	80	457				
21	July	81	677				
22	July	81	678				
02	July	82	867				
04	July	82	869				
12	July	82	875				
13	July	82	876				
27	July	82	885				
28	July	82	886				
17	July	83	1087				
19	July	83	1089				
23	July	83	1092				
24	July	83	1093				
06	Aug	83	1102				
08	Aug	83	1104				
17	Aug	83	1111				
19	Aug	83	1112				
20	Aug	83	1113				
21	Aug	83	1114				
22	Aug	83	1115				

Landsat Imagery Used in Study

BEAUFORT SEA				
YEAR	DATE	MONTH	TR	FR
1973	16	JUNE	66	10
	18	JUNE	68	10
1974	11	MARCH	64	10
	12	MARCH	65	10
	13	MARCH	66	10
	16	MARCH	69	10
	18	MARCH	71	10
	6	APRIL	72	10
	7	APRIL	73	10
	5	MAY	65	10
	6	MAY	66	10
	16	JULY	65	10
	17	JULY	66	10
	18	JULY	67	9
	18	JULY	67	10
	19	JULY	68	9
"	19	JULY	68	10
1975	10	MARCH	68	9
	10	MARCH	68	10
	11	MARCH	69	9
	11	MARCH	69	10
	14	MARCH	72	10
	16	MARCH	74	10
	25	MARCH	65	10
	27	MARCH	67	10
	28	MARCH	68	10
	30	MARCH	70	10
	22	JUNE	64	10
	24	JUNE	66	10
	26	JUNE	68	10
1976	16	JULY	67	10
"	17	JULY	68	10
"	18	JULY	69	10
	19	JULY	70	10
"	20	JULY	71	10
"	20	JULY	71	11
	21	JULY	72	10
	21	JULY	72	11
1977	5	JUNE	67	10
	6	JUNE	68	10
	8	JUNE	64	10
	9	JUNE	65	10
1978	3	JULY	64	10
	4	JULY	65	10
	5	JULY	66	10
	6	JULY	67	10
	7	JULY	68	10
	8	JULY	69	10
	10	JULY	71	10
1979	7	MARCH	68	10
	8	MARCH	69	10
"	8	MARCH	69	11
"	9	MARCH	70	10
"	9	MARCH	70	11

D F DICKINS ASSOCIATES LTD.

Landsat Imagery Used In Study

BEAUFORT SEA

YEAR	DATE	MONTH	TR	FR
** 1979	12	MARCH	64	10
	13	MARCH	65	10
	4	APRIL	69	10
	6	APRIL	71	10
	7	APRIL	72	10
	1	JULY	67	10
	3	JULY	69	10
1980	24	JUNE	66	10
**	26	JUNE	68	10
	28	JUNE	70	10
	29	JUNE	71	10
	30	JUNE	72	10
1981	19	MARCH	64	10
	20	MARCH	65	10
	21	MARCH	66	10
	22	MARCH	67	10
	24	MARCH	69	10
	28	MARCH	73	10
	29	MARCH	74	10
**	13	MAY	65	10
**	14	MAY	66	10
	7	JUNE	72	10
	7	JUNE	72	11
	9	JUNE	74	10
	9	JUNE	74	11
	20	JUNE	67	10
	21	JUNE	68	10
	23	JUNE	70	9
	23	JUNE	70	10
	23	JUNE	70	11
	24	JUNE	71	9
	24	JUNE	71	10
	24	JUNE	71	11
	25	JUNE	72	10
	25	JUNE	72	11
1982	1	MAY	67	10
	2	MAY	68	10
	7	JUNE	68	10
	9	JUNE	70	10
	23	JUNE	66	10
	25	JUNE	68	10
	26	JUNE	69	10
	27	JUNE	70	10
	27	JUNE	70	11
	28	JUNE	71	10
	28	JUNE	71	11
	29	JUNE	72	10
	30	JUNE	73	10
	30	JUNE	73	11
	10	JULY	65	10
	11	JULY	66	10
	12	JULY	67	10
	13	JULY	68	10
	14	JULY	69	10
1983	1	JUNE	68	10

D F DICKINS ASSOCIATES LTD.

Landsat Imagery Used in Study

BEAUFORT	SEA			
YEAR	DATE	MONTH	TR	FR
1983	1	JUNE	68	11
	3	JUNE	66	11
	3	JUNE	66	10
1984	15	MARCH	68	10
	15	MARCH	68	11
	17	MARCH	66	10
	17	MARCH	66	11

Landsat Imagery Used In Study

LANCASTER SOUND				
YEAR	DATE	MONTH	TR	FR
* 1973	26	MAY	45	7
	27	MAY	46	7
1975	23	JUNE	47	7
	24	JUNE	48	7
1976	1	APRIL	42	7
	2	APRIL	43	7
	3	APRIL	44	7
	4	APRIL	45	7
1977	23	APRIL	42	7
	24	APRIL	43	7
	25	APRIL	44	7
**	26	APRIL	45	7
	24	JUNE	44	7
	25	JUNE	45	7
1981	30	MARCH	39	7
	31	MARCH	40	7
	4	APRIL	44	7
	5	APRIL	45	7
	6	APRIL	46	7
	19	APRIL	41	7
	20	APRIL	42	7
	8	MAY	42	7
	9	MAY	43	7
	24	MAY	40	7
	25	MAY	41	7
	10	JUNE	39	7
	11	JUNE	40	7
	12	JUNE	41	7
	13	JUNE	42	7
	14	JUNE	43	7
	15	JUNE	44	7
	16	JUNE	45	7
	18	JUNE	47	7
	2	JULY	43	7
	3	JULY	44	7
	4	JULY	45	7
	5	JULY	46	7
	6	JULY	47	7
1982	13	JUNE	38	7
	14	JUNE	39	7
1983	19	JULY	36	8
	17	JULY	38	7
	17	JULY	38	8
	15	JULY	40	8
	13	JULY	42	7
	13	JULY	42	8

Landsat Imagery Used in Study

LABRADOR COAST

YEAR	DATE	MONTH	TR	FR
1974	1	APRIL	13	16
	1	APRIL	13	17
	1	APRIL	13	18
	2	APRIL	14	16
	2	APRIL	14	17
	2	APRIL	14	18
1975	19	FEB	13	17
	19	FEB	13	18
	20	FEB	14	17
	20	FEB	14	18
	9	MARCH	13	18
	10	MARCH	14	17
	10	MARCH	14	18
	23	APRIL	13	17
	23	APRIL	13	18
	23	APRIL	13	19
	24	APRIL	14	17
	24	APRIL	14	18
	24	APRIL	14	19
	25	APRIL	15	17
	25	APRIL	15	18
	25	APRIL	15	19
1976	10	MARCH	11	19
	10	MARCH	11	20
	11	MARCH	12	19
	12	MARCH	13	17
	12	MARCH	13	18
	12	MARCH	13	19
	13	MARCH	14	17
	13	MARCH	14	18
	26	APRIL	13	16
	26	APRIL	13	17
	26	APRIL	13	18
	27	APRIL	14	16
	27	APRIL	14	17
	27	APRIL	14	18
1978	19	MAY	10	20
	19	MAY	10	21
	20	MAY	11	20
	20	MAY	11	21
	8	JUNE	12	18
	8	JUNE	12	19
	9	JUNE	13	18
	9	JUNE	13	19

Landsat Imagery Used in Study

LABRADOR	COAST			
YEAR	DATE	MONTH	TR	FR
1979	21	FEB	9	20
	21	FEB	9	21
	22	FEB	10	20
	22	FEB	10	21
	1	APRIL	12	18
	1	APRIL	12	19
	2	APRIL	13	18
	2	APRIL	13	19
1982	29	APRIL	11	19
	29	APRIL	11	20
	30	APRIL	12	19
1984	7	APRIL	13	15
	7	APRIL	13	16
	7	APRIL	13	17
	7	APRIL	13	18
	8	APRIL	12	15
	8	APRIL	12	16
	8	APRIL	12	17
	8	APRIL	12	18

APPENDIX B

EXAMPLES OF FLOE MOVEMENT TRACKS MAPPED FROM SUCCESSIVE SLAR IMAGES

Reference: Atmospheric Environment Service
Beaufort Weather and Ice Office
1979, 1980 Reports

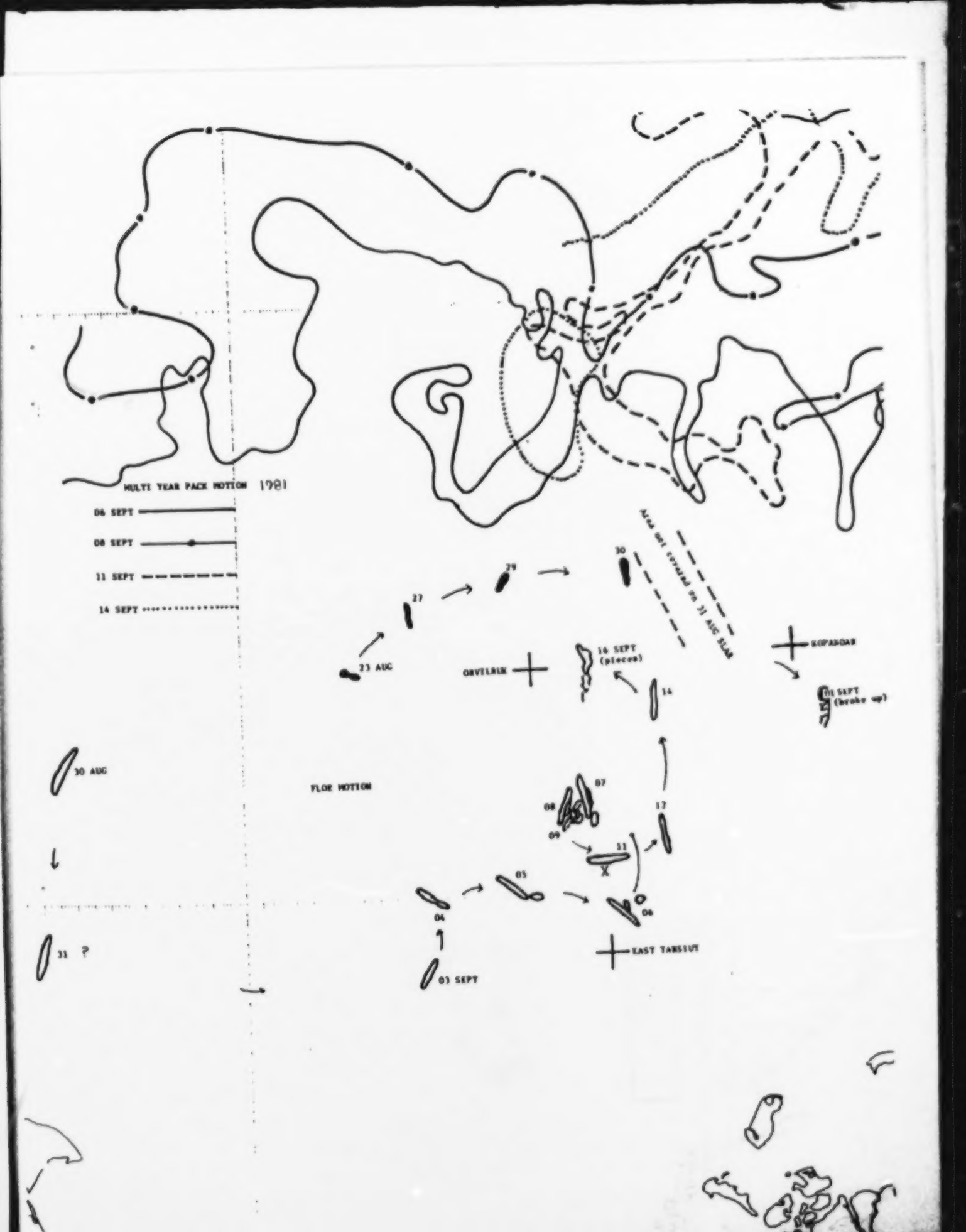
MULTI YEAR PACK MOTION 1981
06 SEPT
08 SEPT
11 SEPT
14 SEPT
AREA NOT COVERED ON 31 AUG SLAR
23 AUG
27
29
30
ORVILAUX
16 SEPT (pieces)
14
KOPASOAR
01 SEPT (broke up)
30 AUG
FLOE MOTION
07
08
09
12
11
05
04
06
31 ?
01 SEPT
EAST TARSIUT

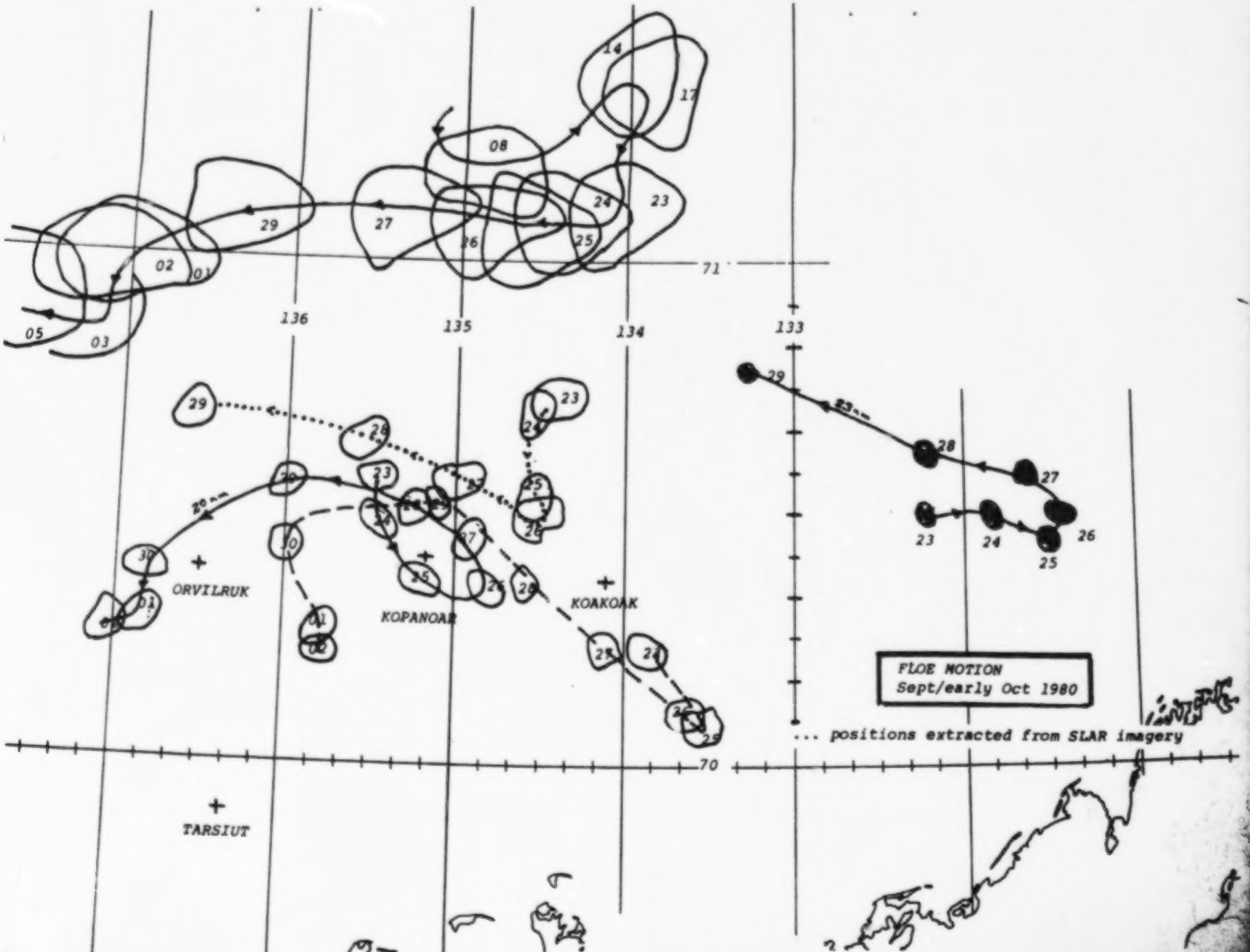
71
70
136
135
134
133
ORVILRUK
KOPANOAR
KOAKOAK
TARSIUT
FLOE MOTION
Sept/early Oct 1980
... positions extracted from SLAR imagery

APPENDIX C

MONTHLY AND REGIONAL FLOE SPEED DISTRIBUTIONS

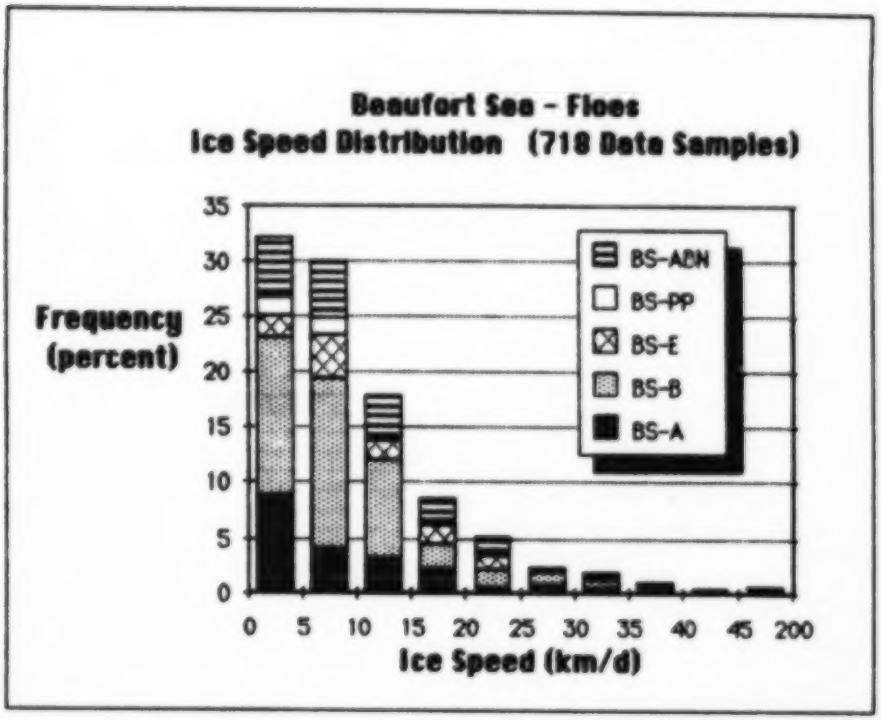
Beaufort Sea - Floes
Ice Speed Distribution (718 Data Samples)
Frequency (percent)
35
30
25
20
15
10
5
0
BS-ADN
BS-PP
BS-E
BS-B
BS-A
0 5 10 15 20 25 30 35 40 45 200
Ice Speed (km/d)

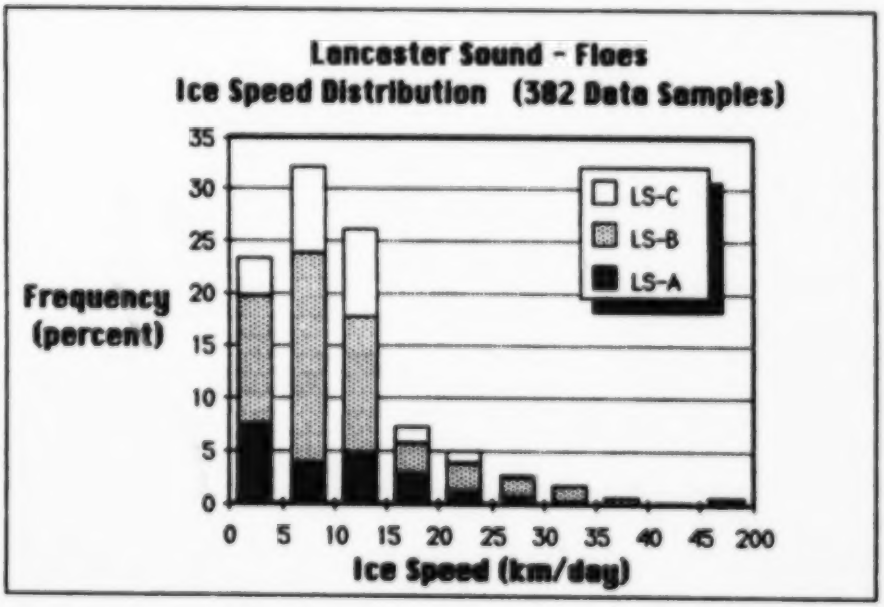
Lancaster Sound - Floes
Ice Speed Distribution (382 Data Samples)
Frequency (percent)
35
30
25
20
15
10
5
0
LS-C
LS-B
LS-A
0 5 10 15 20 25 30 35 40 45 200
Ice Speed (km/day)

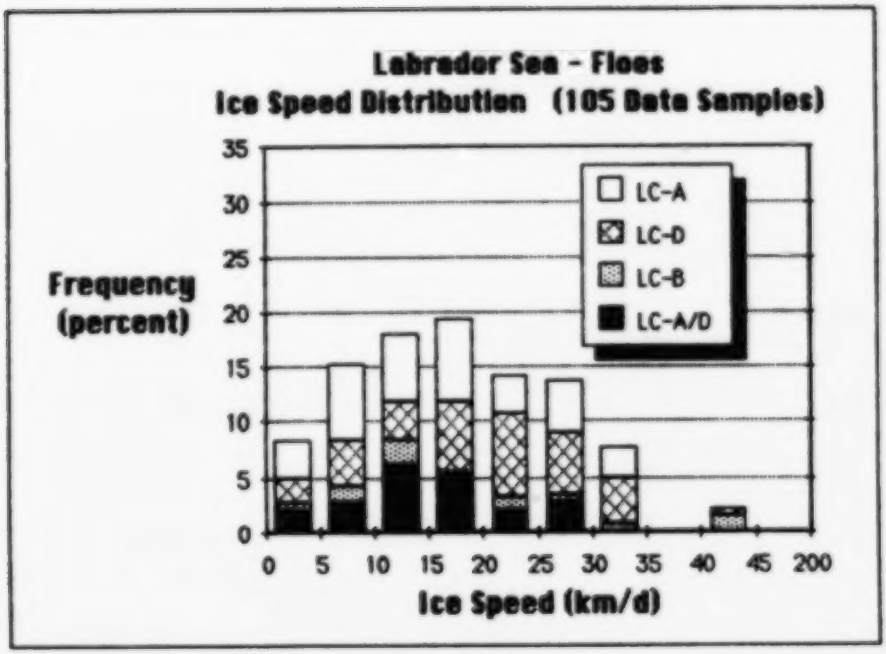
Labrador Sea - Floes
Ice Speed Distribution (105 Data Samples)
Frequency (percent)
35
30
25
20
15
10
5
0
LC-A
LC-D
LC-B
LC-A/D
0 5 10 15 20 25 30 35 40 45 200
Ice Speed (km/d)

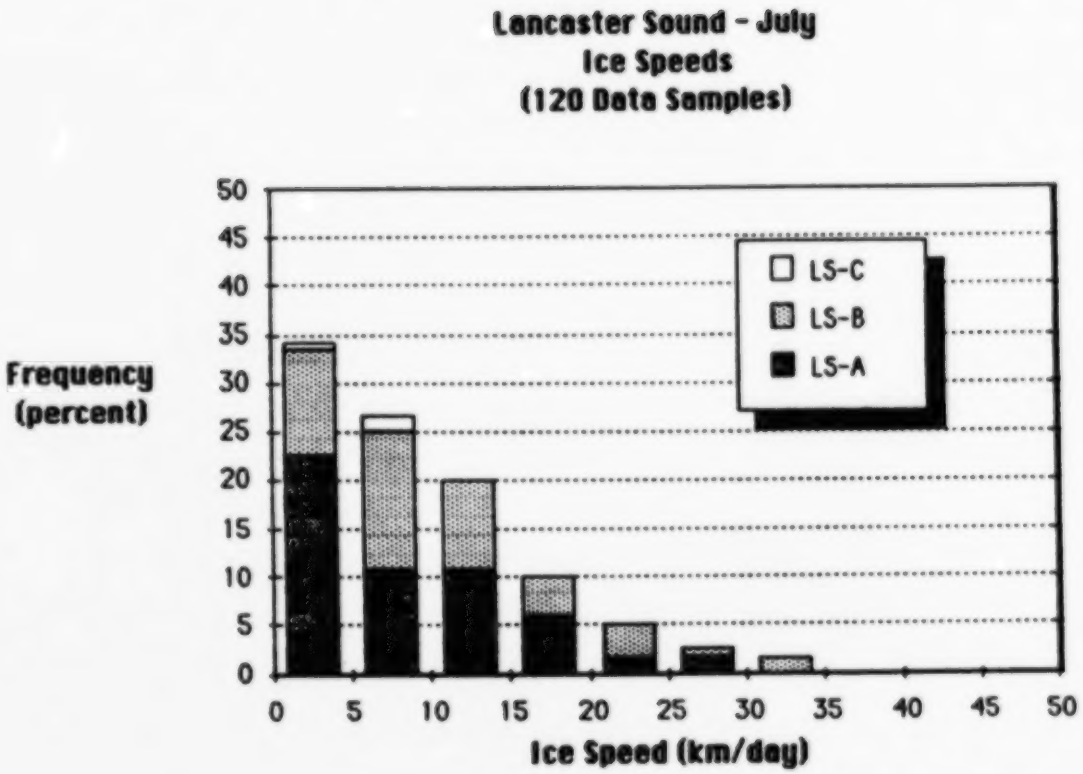
Lancaster Sound - July
Ice Speeds
(120 Data Samples)
Frequency
(percent)
50
45
40
35
30
25
20
15
10
5
0
LS-C
LS-B
LS-A
0
5
10
15
20
25
30
35
40
45
50
Ice Speed (km/day)

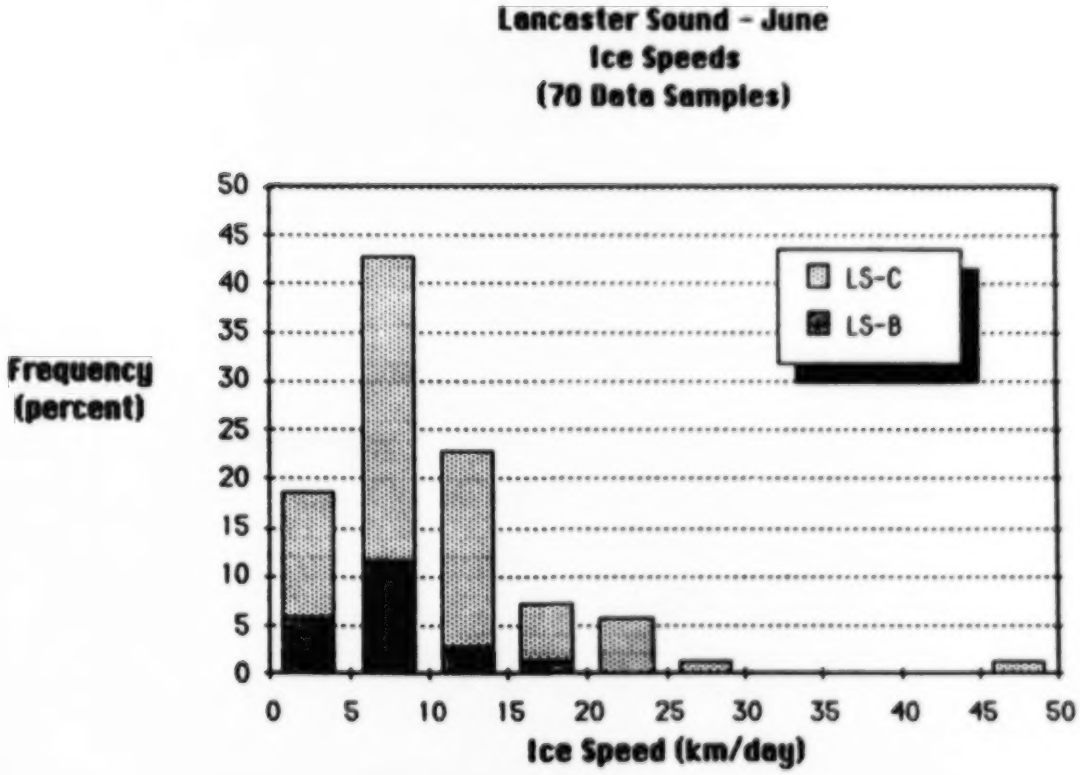
Lancaster Sound - June
Ice Speeds
(70 Data Samples)
Frequency
(percent)
50
45
40
35
30
25
20
15
10
5
0
LS-C
LS-B
0
5
10
15
20
25
30
35
40
45
50
Ice Speed (km/day)

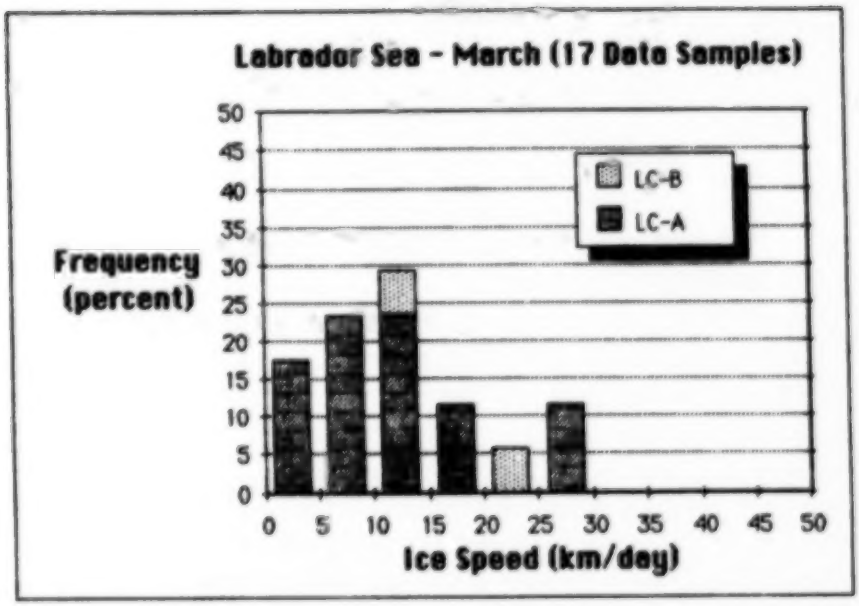
Labrador Sea - March (17 Data Samples)
Frequency (percent)
50
45
40
35
30
25
20
15
10
5
0
LC-B
LC-A
0 5 10 15 20 25 30 35 40 45 50
Ice Speed (km/day)

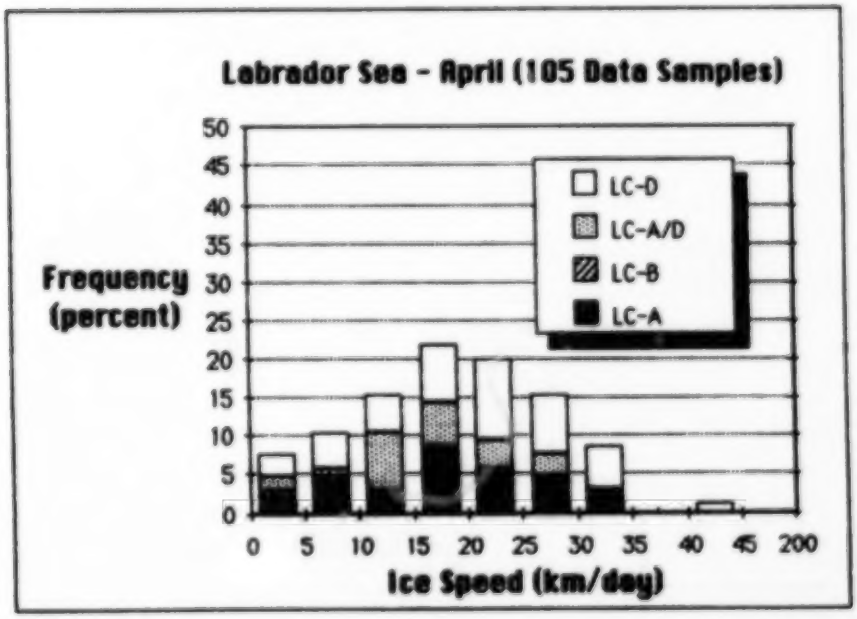
Labrador Sea - April (105 Data Samples)
Frequency (percent)
50
45
40
35
30
25
20
15
10
5
0
LC-D
LC-A/D
LC-B
LC-A
0 5 10 15 20 25 30 35 40 45 200
Ice Speed (km/day)

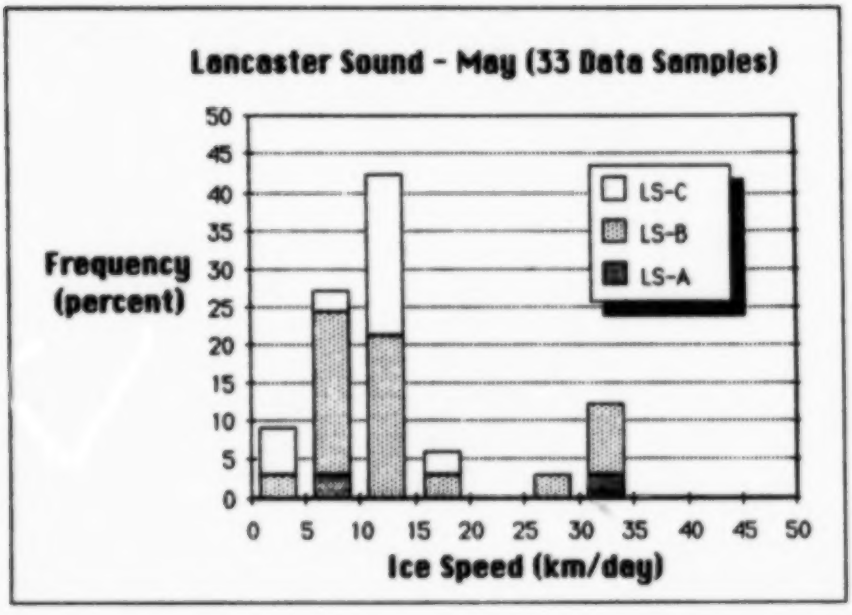
Lancaster Sound - May (33 Data Samples)
Frequency (percent)
50
45
40
35
30
25
20
15
10
5
0
LS-C
LS-B
LS-A
0 5 10 15 20 25 30 35 40 45 50
Ice Speed (km/day)

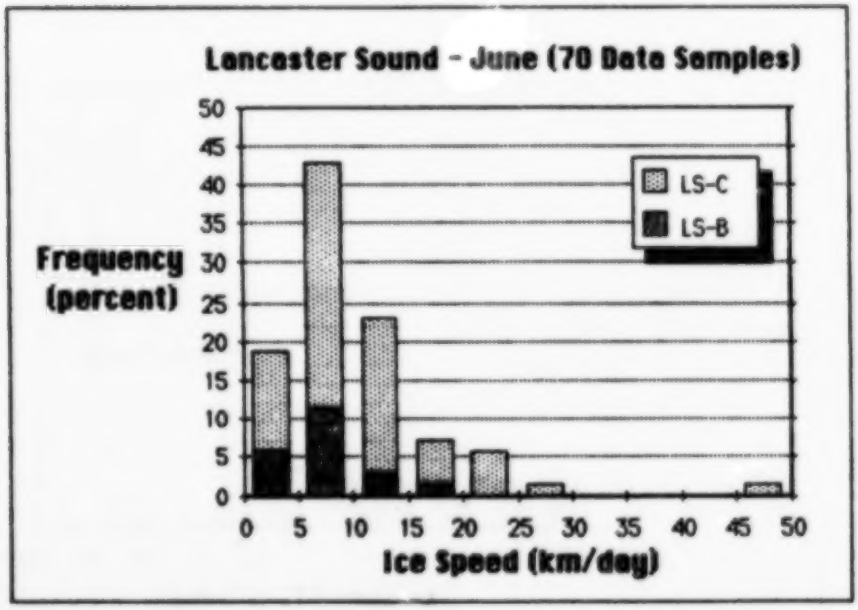
Lancaster Sound - June (70 Data Samples)
Frequency (percent)
50
45
40
35
30
25
20
15
10
5
0
LS-C
LS-B
0 5 10 15 20 25 30 35 40 45 50
Ice Speed (km/day)

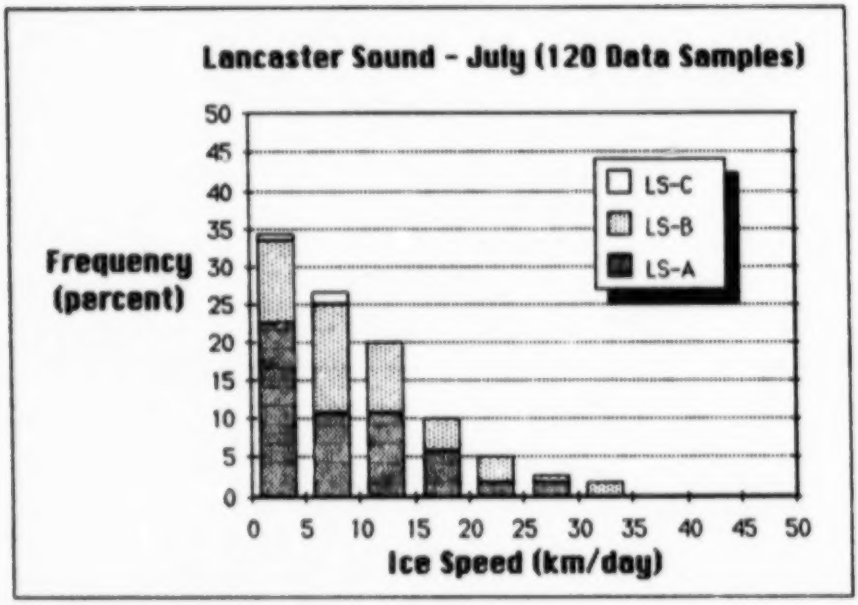
Lancaster Sound - July (120 Data Samples)
Frequency (percent)
50
45
40
35
30
25
20
15
10
5
0
LS-C
LS-B
LS-A
0 5 10 15 20 25 30 35 40 45 50
Ice Speed (km/day)

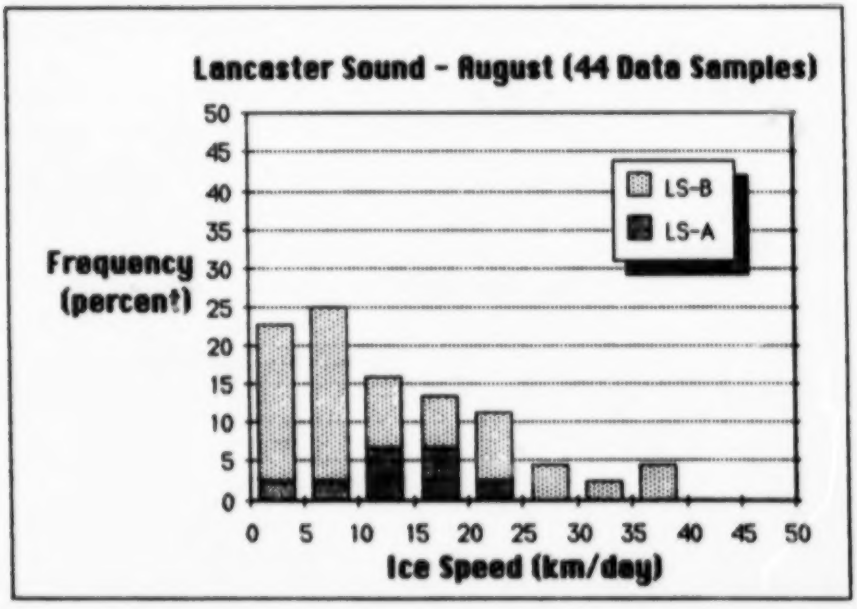
Lancaster Sound - August (44 Data Samples)
Frequency (percent)
50
45
40
35
30
25
20
15
10
5
0
LS-B
LS-A
0 5 10 15 20 25 30 35 40 45 50
Ice Speed (km/day)

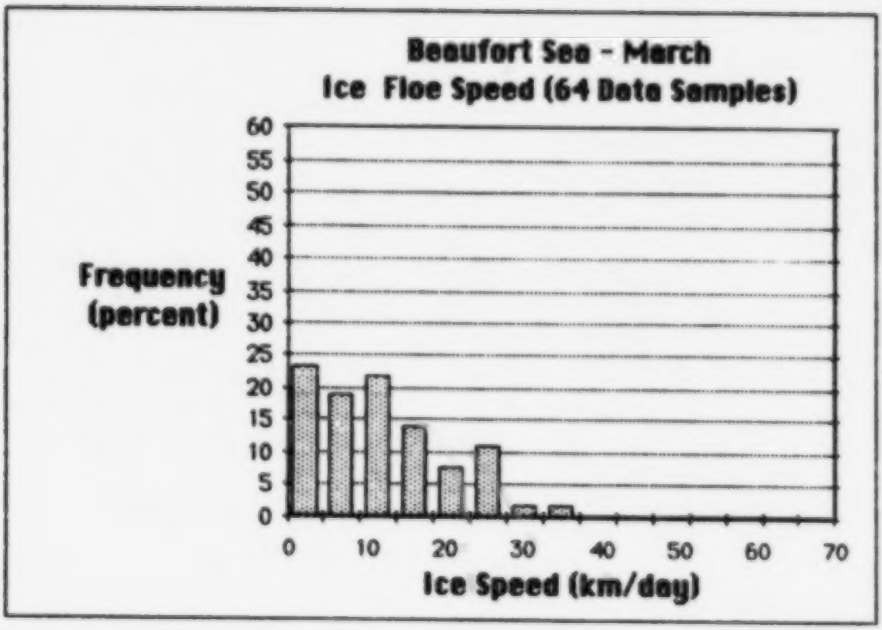
Beaufort Sea - March
Ice Floe Speed (64 Data Samples)
Frequency (percent)
60
55
50
45
40
35
30
25
20
15
10
5
0
0
10
20
30
40
50
60
70
Ice Speed (km/day)

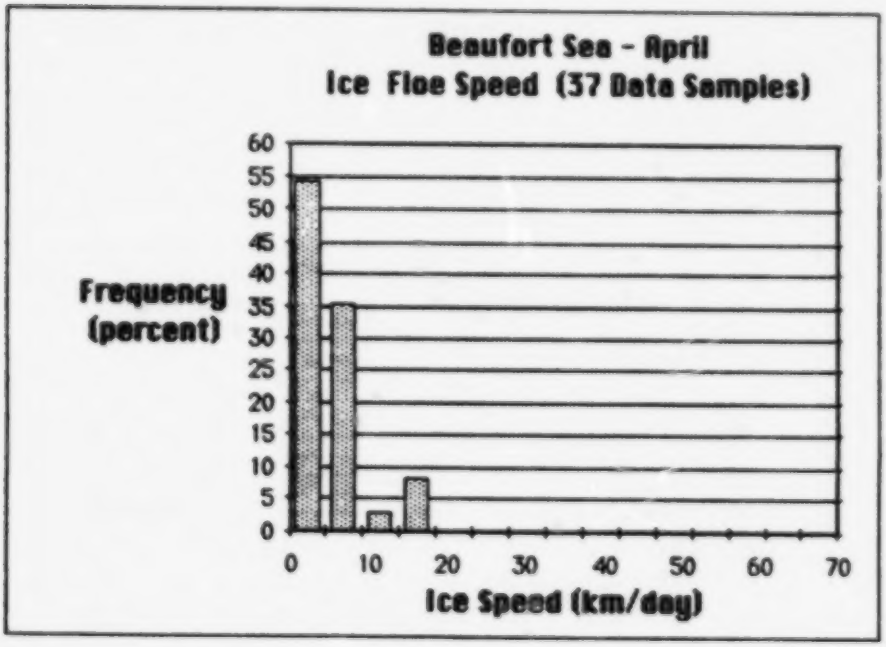
Beaufort Sea - April
Ice Floe Speed (37 Data Samples)
Frequency (percent)
60
55
50
45
40
35
30
25
20
15
10
5
0
0
10
20
30
40
50
60
70
Ice Speed (km/day)

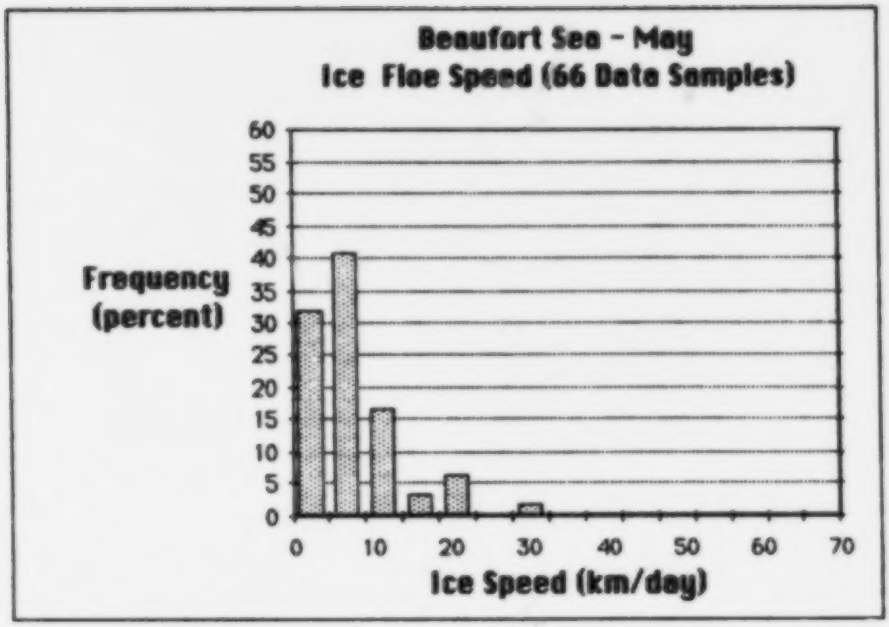
Beaufort Sea - May
Ice Floe Speed (66 Data Samples)
Frequency (percent)
60
55
50
45
40
35
30
25
20
15
10
5
0
0
10
20
30
40
50
60
70
Ice Speed (km/day)

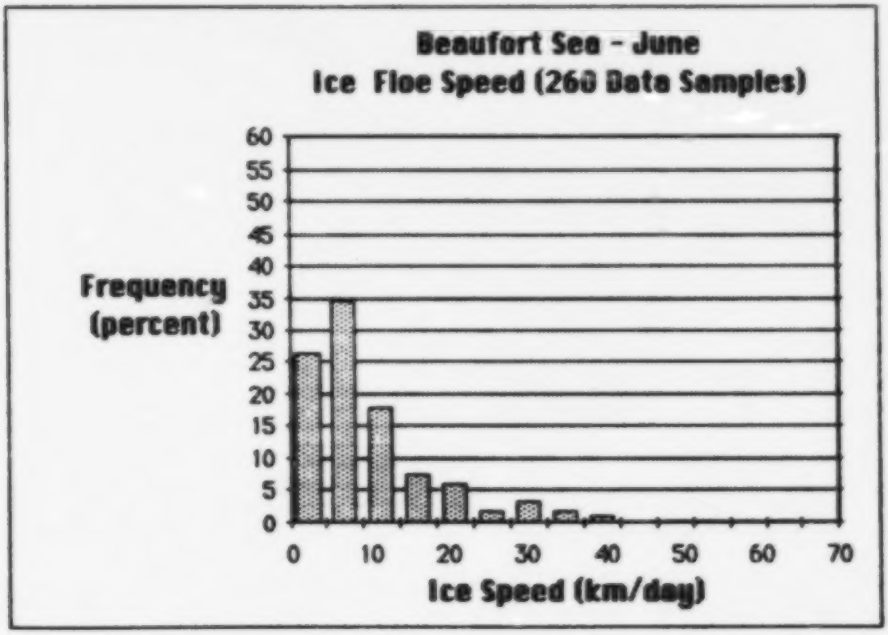
Beaufort Sea - June
Ice Floe Speed (260 Data Samples)
Frequency (percent)
60
55
50
45
40
35
30
25
20
15
10
5
0
0
10
20
30
40
50
60
70
Ice Speed (km/day)

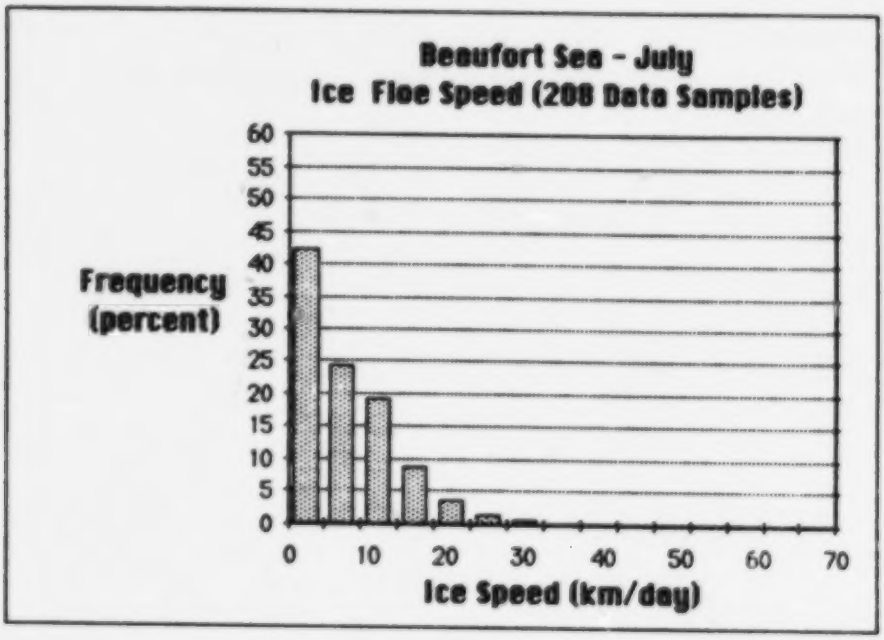
Beaufort Sea - July
Ice Floe Speed (208 Data Samples)
Frequency (percent)
60
55
50
45
40
35
30
25
20
15
10
5
0
0
10
20
30
40
50
60
70
Ice Speed (km/day)

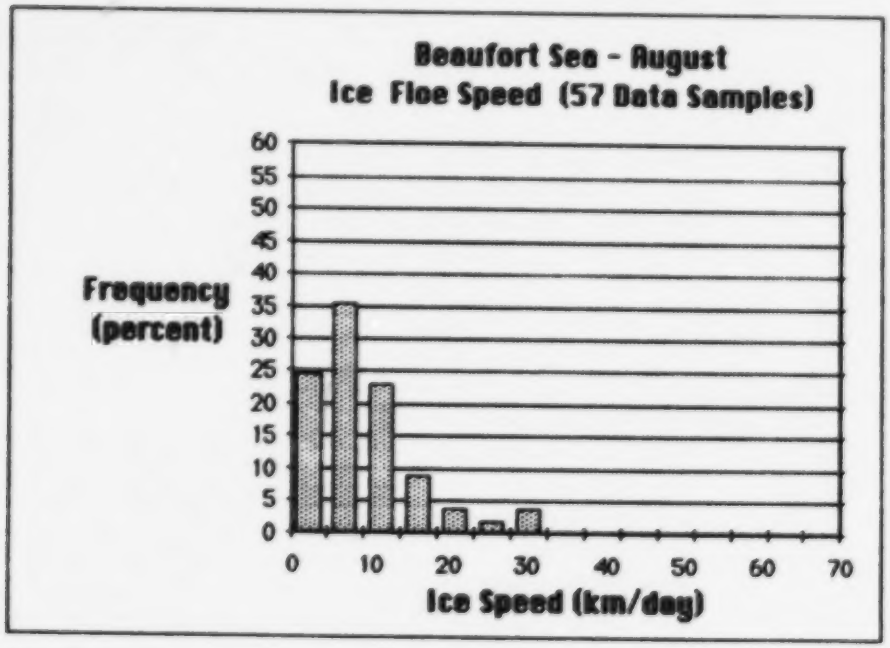
Beaufort Sea - August
Ice Floe Speed (57 Data Samples)
Frequency (percent)
60
55
50
45
40
35
30
25
20
15
10
5
0
0
10
20
30
40
50
60
70
Ice Speed (km/day)

APPENDIX D

REPRESENTATIVE PROFILES OF LABRADOR SEA ICE CAKES

from LeDrew and Gustajtis, 1979

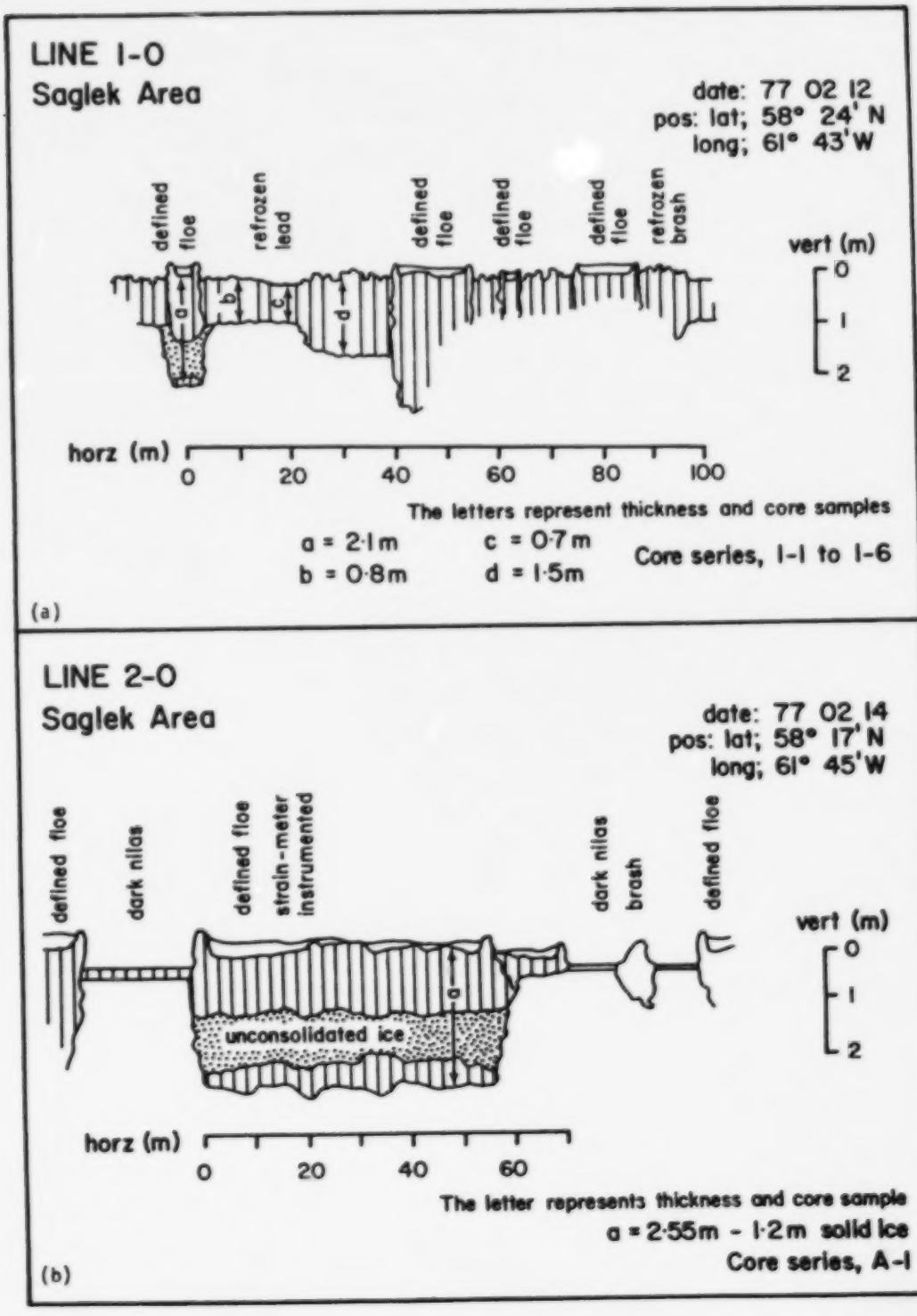
LINE 1-0
Saglek Area
date: 77 02 12
pos: lat; 58° 24' N
long; 61° 43' W
defined floe
refrozen lead
defined floe
defined floe
defined floe
refrozen brash
vert (m)
0
1
2
a
b
c
d
horz (m)
0
20
40
60
80
100
The letters represent thickness and core samples
a = 2·1m
b = 0·8m
c = 0·7m
d = 1·5m
Core series, 1-1 to 1-6
(a)
LINE 2-0
Saglek Area
date: 77 02 14
pos: lat; 58° 17' N
long; 61° 45' W
defined floe
dark nilas
defined floe
strain-meter instrumented
dark nilas
brash
defined floe
vert (m)
0
1
2
a
unconsolidated ice
horz (m)
0
20
40
60
The letter represents thickness and core sample
a = 2·55m - 1·2m solid ice
Core series, A-1
(b)

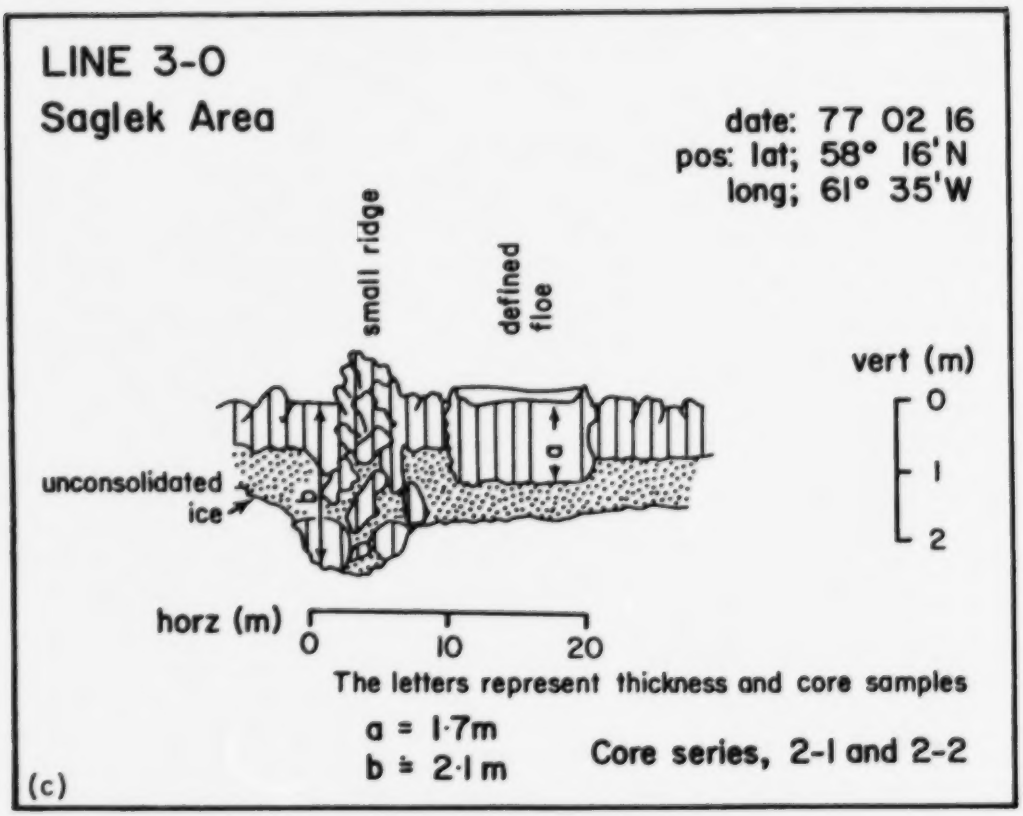
LINE 3-0
Saglek Area
date: 77 02 16
pos: lat; 58° 16'N
long; 61° 35'W
small ridge
defined floe
vert (m)
0
1
2
a
b
unconsolidated ice
horz (m)
0
10
20
The letters represent thickness and core samples
a = 1·7m
b = 2·1 m
Core series, 2-1 and 2-2
(c)

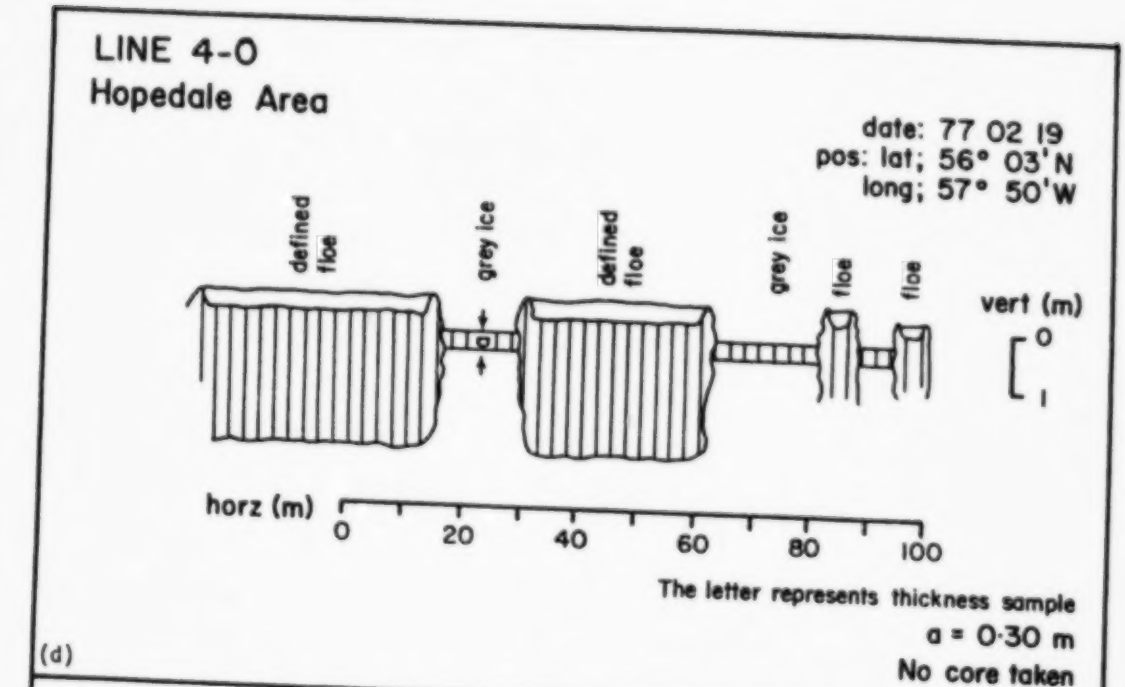
LINE 4-0
Hopedale Area
date: 77 02 19
pos: lat; 56° 03'N
long; 57° 50'W
defined floe
grey ice
defined floe
grey ice
floe
floe
vert (m)
0
1
a
horz (m)
0
20
40
60
80
100
The letter represents thickness sample
a = 0·30 m
No core taken
(d)

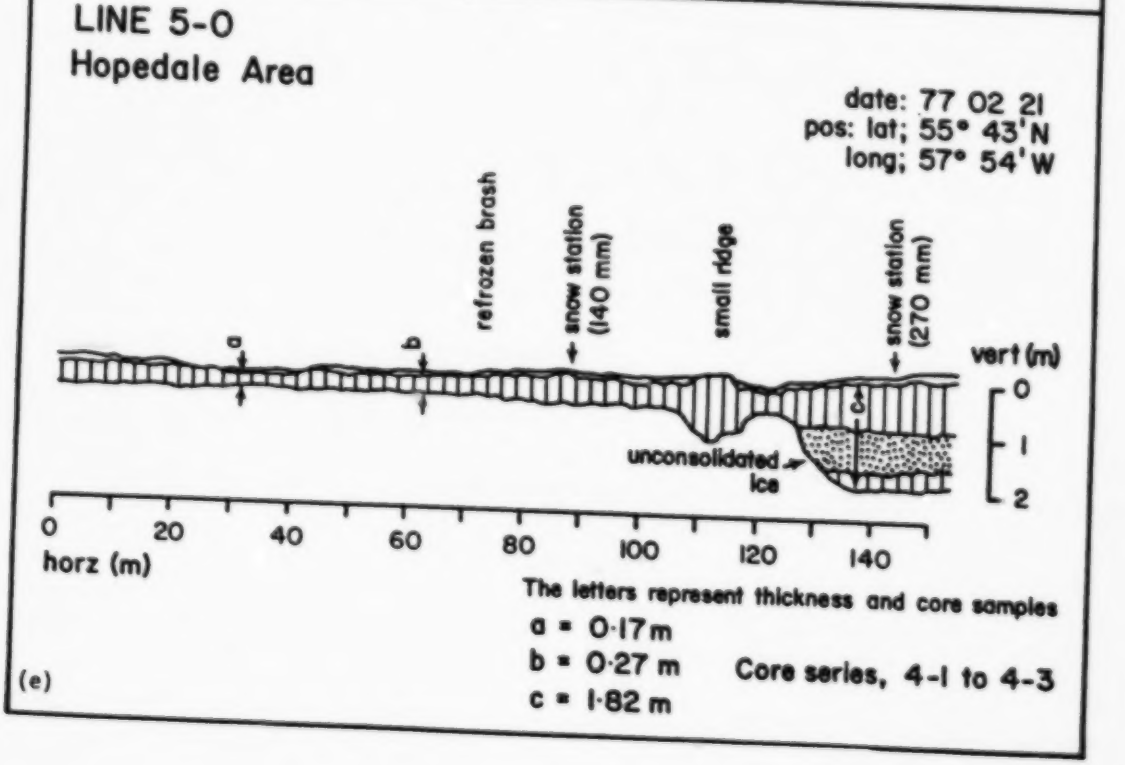
LINE 5-0
Hopedale Area
date: 77 02 21
pos: lat; 55° 43'N
long; 57° 54'W
refrozen brash
snow station (140 mm)
small ridge
snow station (270 mm)
a
b
c
vert (m)
0
1
2
unconsolidated ice
0
20
40
60
80
100
120
140
horz (m)
The letters represent thickness and core samples
a = 0·17 m
b = 0·27 m
c = 1·82 m
Core series, 4-1 to 4-3
(e)

LINE 6·0
Hopedale Area

date: 77 02 20
pos: lat; 55° 44' N
long; 57° 54' W

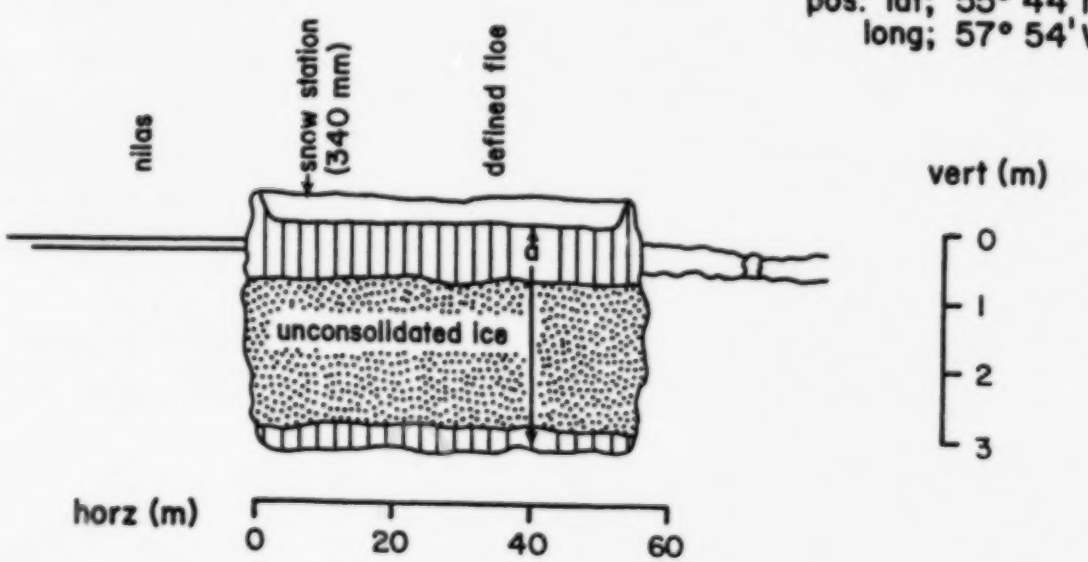

The letter represents thickness and core sample
a = 3·2m - 0·8m solid ice
Core series, A-2

(f)

LINE 7·0
Hopedale Area

date: 77 02 23
pos: lat; 55° 29'N
long; 55° 50'W

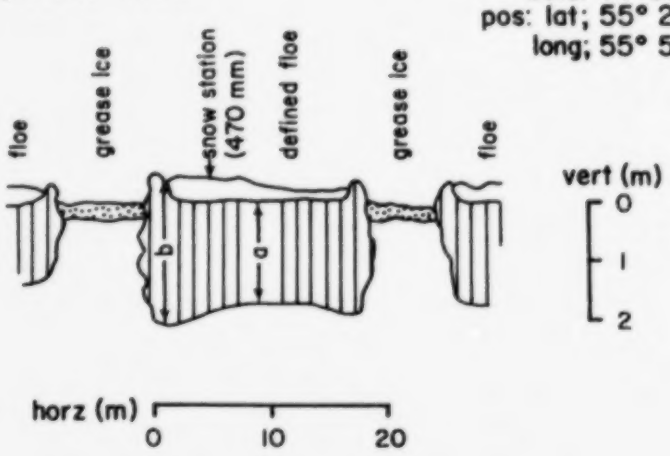

The letters represent thickness and core samples

a = 1·75m Core series, 5-0
b = 2·40

(g)

LINE 8·0
Hopedale Area

date: 77 02 24
pos: lat; 55° 05' N
long; 54° 39'W

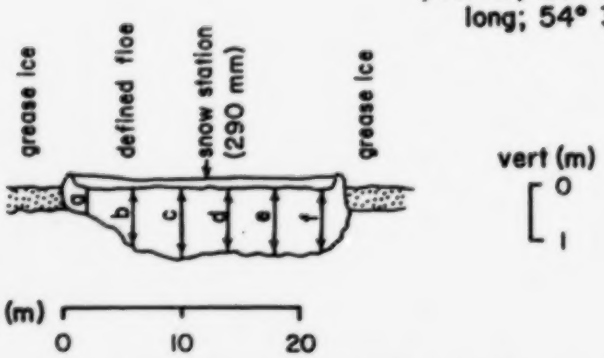

The letters represent thickness and core samples

a = 0·42m d = 1·10m
b = 1·03m e = 1·15m Core series, 6-1 to 6-6
c = 1·20m f = 1·10m

(h)

APPENDIX E

CHANGING LEAD AND FRACTURE SYSTEMS MAPPED FROM AERIAL PHOTOGRAPHY OF WINTER PACK ICE IN THE VICINITY OF 73°45'N, 130°15'W MARCH 11 TO 23, 1971

Reference: Hartwell, 1972

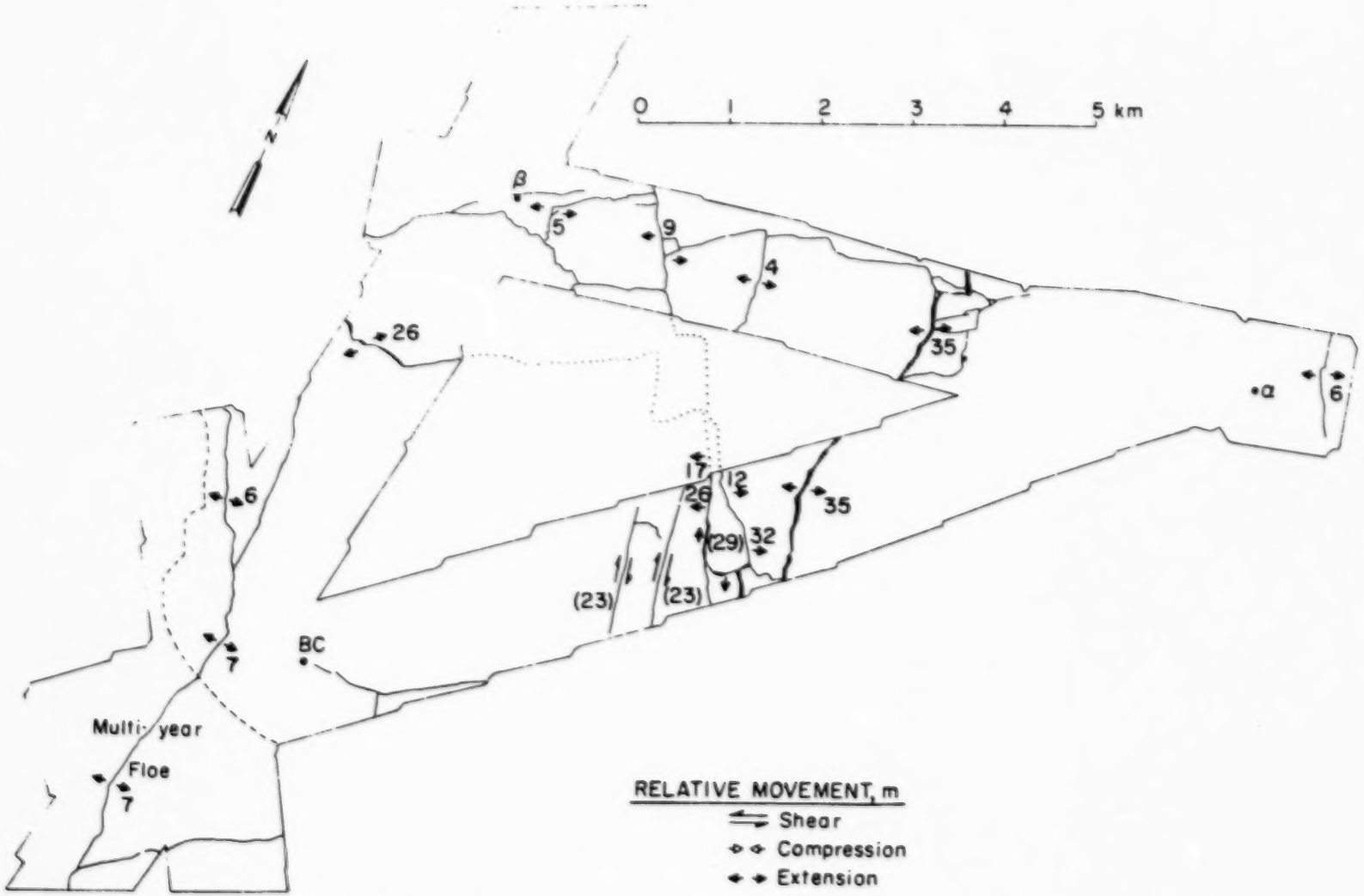

Lead and fracture system on 11 March. Arrows indicate type and direction of relative movement; approximate magnitude given in meters. Earlier movement indicated by parentheses.

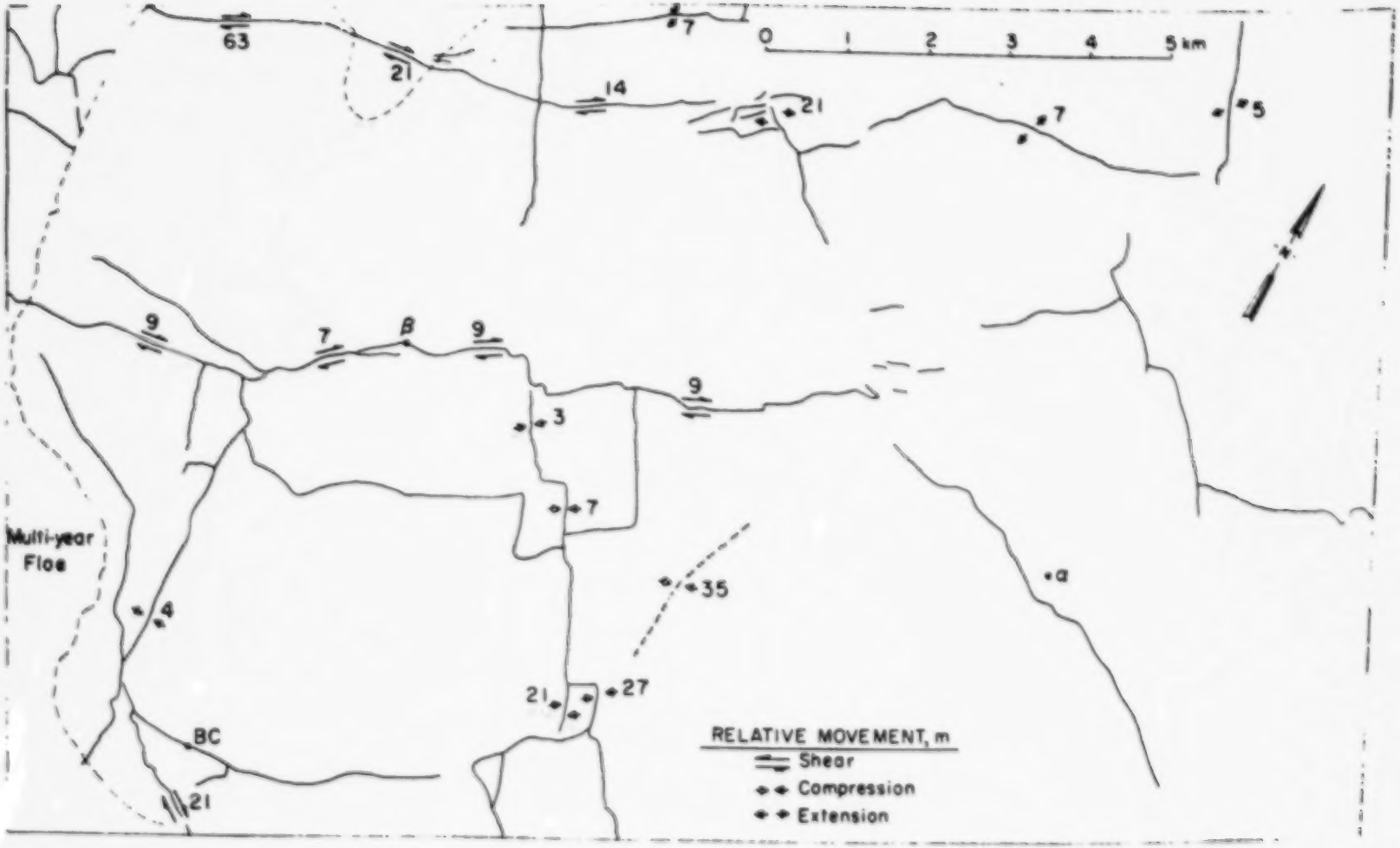

Lead and fracture system between 12 March and 15 March; note NE-SW shear zones.

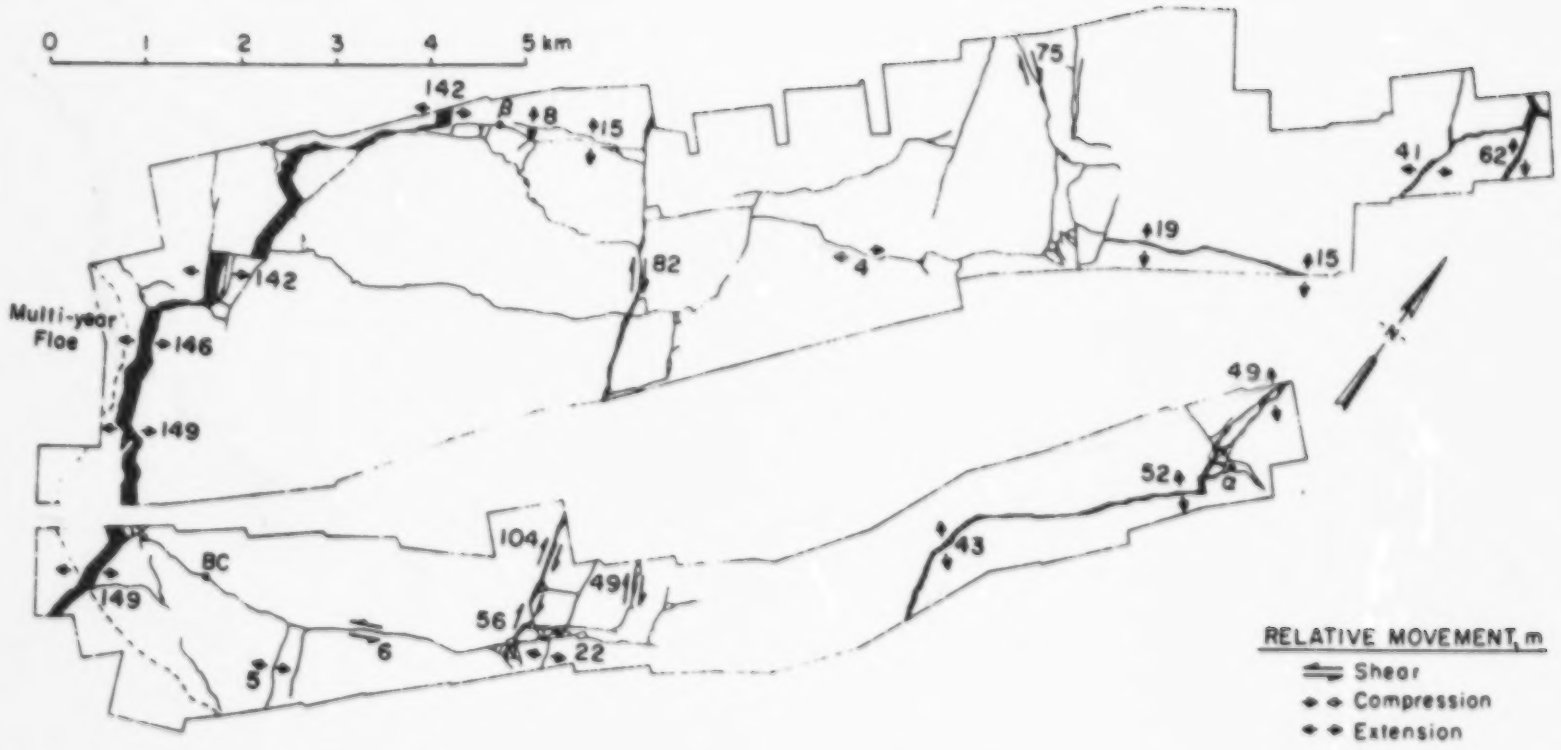

Lead and fracture system between 16 March and 20 March; note large extension to left and shear in center.

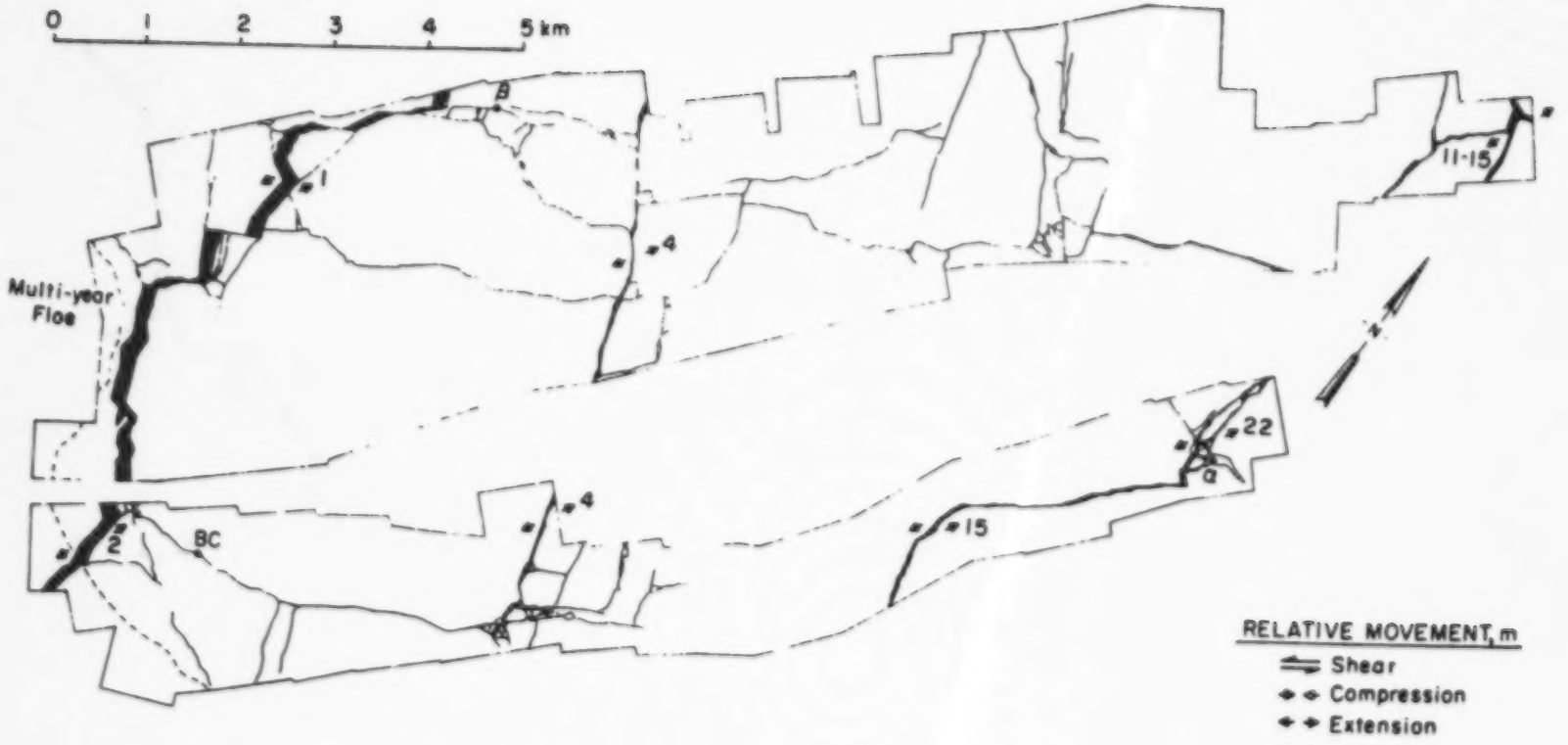

Lead and fracture system on 21 March.

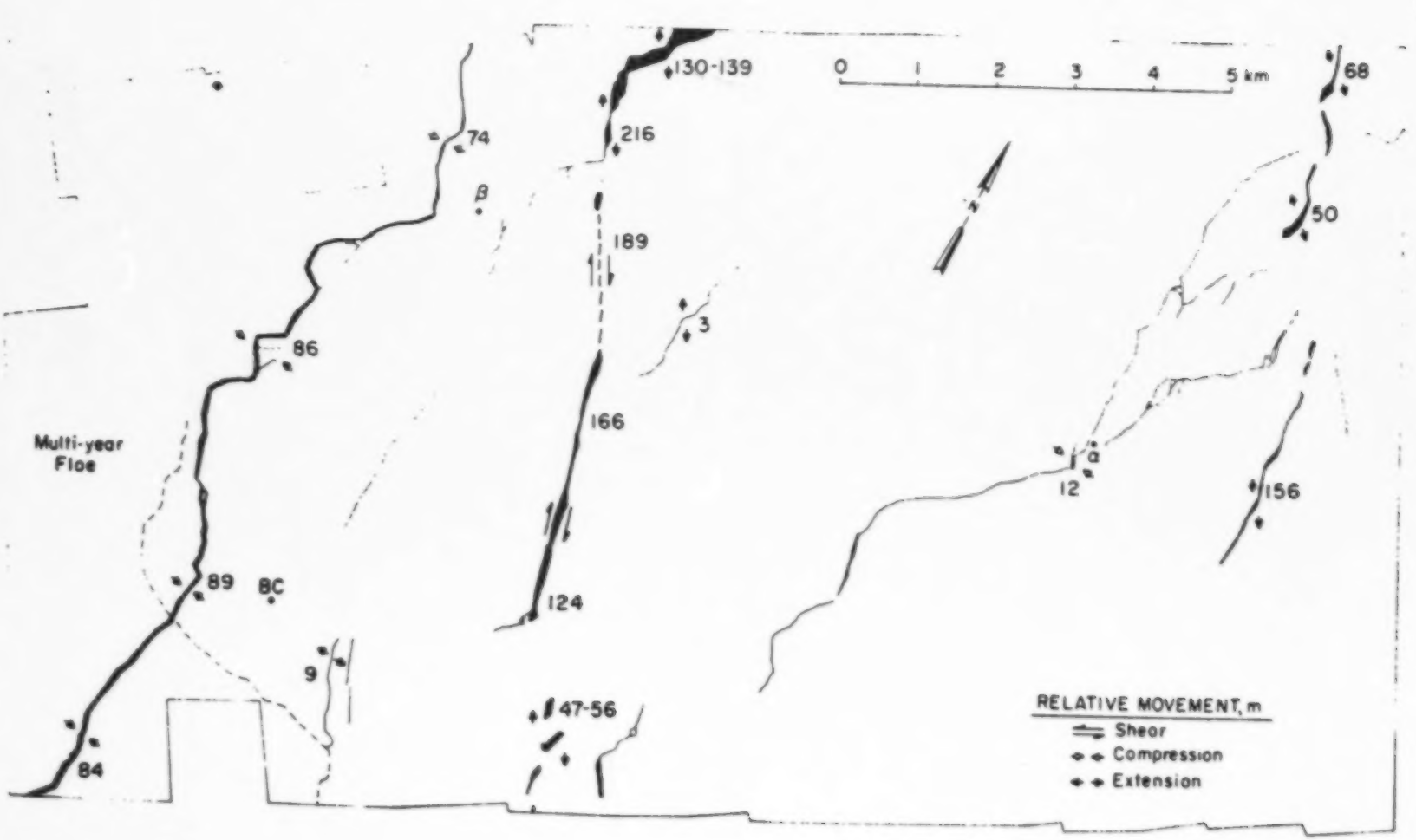

Lead and fracture system on 22 March; note continued shearing in center of strain triangle.

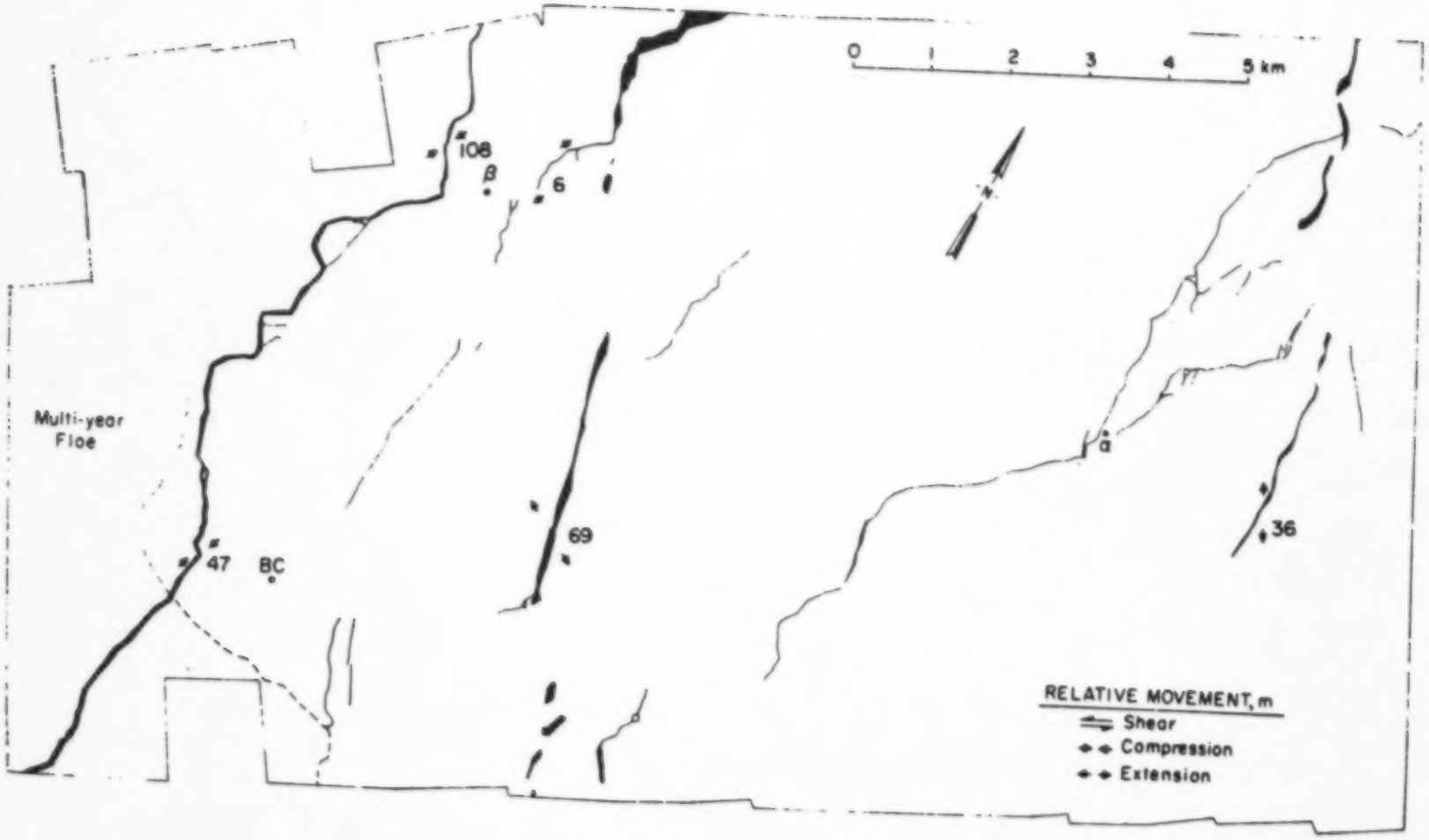

Lead and fracture system on 23 March.